NEW METHODS FOR QUANTIFYING THE SYNCHRONY OF CONTRACTION AND RELAXATION IN THE HEART

A Dissertation
Presented to
The Academic Faculty

by

Brandon K. Fornwalt

In Partial Fulfillment
of the Requirements for the Degree
Doctor of Philosophy in the
School of Biomedical Engineering

Georgia Institute of Technology / Emory University
August 2008

NEW METHODS FOR QUANTIFYING THE SYNCHRONY OF CONTRACTION AND RELAXATION IN THE HEART

Approved by:

John N. Oshinski, PhD, Advisor
School of Biomedical Engineering
Georgia Institute of Technology and Emory University

Oskar Skrinjar, PhD
School of Biomedical Engineering
Georgia Institute of Technology

Derek A. Fyfe, MD, PhD
School of Medicine
Emory University

W. Robert Taylor, MD, PhD
School of Biomedical Engineering
Georgia Institute of Technology and Emory University

Angel R. León, MD
School of Medicine
Emory University

Date Approved: April 21, 2008

ACKNOWLEDGEMENTS

First and foremost I would like to thank my wife for all her support throughout my education, which has sometimes demanded long hours that I would have much rather spent with her (and Jada and June). I would also like to thank my incredibly supportive family that has been there every step of the way.

I would also like to thank:

1. John Oshinski for being such a fun, honest person. I hope that I can some day follow in his footsteps. He is truly the best advisor a graduate student could hope for.
2. Jana Delfino (who unfortunately had to deal with me the most of all these people during graduate school) for her patience, generosity and continual encouragement.
3. Derek Fyfe for sharing with me his energy and passion for life and research. He took the time to introduce me to this incredible field, and working with him convinced me that I should pursue a PhD. Please, never stop tapping your head Dr. Fyfe.
4. Takeshi Arita for all those fun, stimulating discussions about research.
5. The MD/PhD program (Mary, Chuck, Marie, Allen, Barbara, Sabrina) for all their support – especially when times got tough in my first year of graduate school. Thanks for always listening and caring.
6. Angel León for guiding me through the murky waters of clinical research and sharing his excitement and passion with me.
7. Bob Taylor for advising me every step of the way as a person who actually practices medicine and does great research all in a days work. I aspire to be like him.

8. Oskar Skrinjar for exciting me about image processing and spending the time to teach a very high-quality graduate course which played a huge role in my thesis.
9. Pat Frias for introducing me to the world of pediatric EP and guiding me through some great clinical research.
10. All the CHOA people (Alicia, Bill Mahle, Carey, Christine, Cyrus, Dean, Diana, Georgia, Joe, John, Josh, Melinda, Peggy, Pete, Robert Campbell, Rose, Shelley, Tiffany, Tracy, Vince) for welcoming me into their family and putting up with me!
11. Other labmates: Bill, Calvin, Dan, Kevin, Matt, Michelle for acting like my results were cool sometimes even though they really weren't (I needed the encouragement).
12. My fellow MD/PhD classmates (Keisha, Lamar, Lindsey, Rolston, Scott, Steeds and all the others) for the good times with all the free food.
13. Steven Marzec for his ridiculous computer knowledge and answers to every single question I ever asked him.
14. The BME program office for always being helpful (Beth, Leita, Sally, Shannon).
15. The Crawford Long group (Dean Notabartolo, John Merlino, Mo Bhasin, Pat BeDell, and Paige Smith) for helping me collect data.

TABLE OF CONTENTS

LIST OF TABLES

Page

LIST OF FIGURES

Page

LIST OF SYMBOLS AND ABBREVIATIONS

AAI	Right Atrial Appendage Pacing
CMR	Cardiac Magnetic Resonance
CRT	Cardiac Resynchronization Therapy
IFF	Internal Flow as a Fraction of Stroke Volume
LV	Left Ventricular, or Left Ventricle
MaxDiff	Max Difference in time-to-peak in the 2 or 4-chamber images
MRI	Magnetic Resonance Imaging
ms	milliseconds
NSR	Normal Sinus Rhythm
NYHA	New York Heart Association
ROI	Region of Interest
RVA	Right Ventricular Apex
SD	Standard Deviation
SLD	Septal-to-lateral Delay
TDI	Tissue Doppler Imaging
Ts-SD	Standard Deviation of times-to-peak in the 12 LV Segments
XC	Cross-correlation
XCD	Cross-correlation Dyssynchrony

SUMMARY

Synchronous contraction and relaxation of the myocardium is required to optimize cardiac function. Regional timing of contraction and relaxation is dyssynchronous in many patients with heart failure. Cardiac resynchronization therapy (CRT) is a highly successful treatment for dyssynchronous heart failure. Patients are currently selected for CRT using surface electrocardiogram QRS duration as a measure of dyssynchrony. However, up to 30% of patients selected for CRT show no improvement. This poor response rate may in part be explained by the poor correlation between mechanical dyssynchrony and QRS duration. Thus, better methods to quantify mechanical dyssynchrony in the heart may improve the poor CRT response rate.

The overall goal of this project was to develop better methods to diagnose dyssynchrony in the left ventricle (LV). We developed two new methods with different approaches. The first method improved upon existing tissue-Doppler based echocardiographic diagnosis of dyssynchrony by utilizing a cross-correlation (XC) function to quantify dyssynchrony during post-processing as opposed to the quantitatively simplistic "time-to-peak" analysis that is currently utilized. The second method utilized standard cine cardiac magnetic resonance (CMR) images to quantify the dyssynchrony in the flow of blood within the LV, which may represent a more direct, physiologically relevant measure of dyssynchrony.

Specific aim 1 demonstrated that the new XC delay parameters can be quantified accurately with a stationary region of interest and therefore require significantly less post-

processing time to calculate compared to the time-to-peak dyssynchrony parameters. Specific aim 2 showed that XC delays are superior to existing time-to-peak dyssynchrony parameters at discriminating patients with LV dyssynchrony from those with normal function. The time-to-peak parameters showed dyssynchrony in approximately half of the normal, healthy volunteers while the XC delay parameters had nearly perfect diagnostic accuracy. The results of specific aim 3 showed that XC delays could diagnose acute, pacing-induced dyssynchrony in young, healthy children with 79% accuracy while the time-to-peak parameters showed accuracies of 71%, 57% and 57%. Specific aim 4 showed that CMR-based quantification of LV internal flow can be used to discriminate patients with dyssynchronous heart failure from normal controls with 95% accuracy.

In summary, both tissue Doppler-based cross-correlation delay and cardiac magnetic resonance-based internal flow analysis may help improve the poor CRT response rate by improving the accuracy to diagnose left ventricular dyssynchrony. In addition, the superior ability of these methods to diagnose dyssynchrony may prove useful in risk-stratification and monitoring of other disease processes which affect the heart.

CHAPTER 1

PROJECT SPECIFIC AIMS

Introduction

Synchronous contraction and relaxation of the myocardium is required to optimize cardiac function[1]. Regional timing of contraction and relaxation is *dyssynchronous* in many patients with severe congestive heart failure[2, 3]. Cardiac resynchronization therapy (CRT) is a relatively new treatment for dyssynchronous heart failure that results in both acute and long-term benefits[4, 5]. Patients are currently selected for CRT using surface electrocardiogram QRS duration as a measure of dyssynchrony. However, up to 30% of patients selected for CRT show no improvement[5]. This poor response rate may in part be explained by the poor correlation between mechanical dyssynchrony and QRS duration[6]. Thus, better methods to quantify mechanical dyssynchrony in the heart may improve the poor CRT response rate[7].

There are two primary approaches to quantifying mechanical dyssynchrony in the heart: 1) examine the dyssynchrony in the motion or contraction between multiple segments of the heart and 2) examine the dyssynchrony in the flow of blood in the left ventricle (LV) that is caused by dyssynchronous contraction of the myocardium. Each of these methods has its limitations which this project has attempted to improve upon.

The motion of LV myocardium is most often quantified by Tissue Doppler velocity imaging (TDI). Many TDI-based methodologies to quantify dyssynchrony have been proposed, yet no single methodology has emerged as a widespread standard. Most

investigators utilize "time-to-peak" analysis where the time from the electrocardiogram Q-wave to the peak systolic velocity of one ventricular wall is compared to that of an opposing ventricular wall[8, 9]. This analysis may be limited by its quantitative simplicity: it utilizes only 1 data point from the 140 points typically collected per heart beat.

To overcome this limitation, we developed a new mathematical method to calculate a temporal delay between two myocardial velocity curves. Our method utilizes a cross-correlation (XC) function to quantify either *systolic*, *diastolic* or *whole-cycle* cross-correlation delay (XCD) using TDI data collected *throughout* the cardiac cycle (not just peak values).

The second approach to quantify mechanical dyssynchrony in the heart is to examine the dyssynchrony in the flow of blood within the LV. Ventricular dyssynchrony creates abnormal systolic flow patterns in the LV which results in a reduced efficiency of ventricular ejection due to blood flowing *internally* within the LV instead of moving directly through the LV and into the aorta[10]. This internal flow has been quantified by conductance catheter[11] and used to demonstrate the benefit of CRT[12]. However, the clinical utility of this approach is currently limited by the invasive nature of catheterization. It may be possible to quantify internal flow *non-invasively* from regional volume curves of the LV derived from cardiac magnetic resonance (CMR) images. The ability to quantify internal flow non-invasively will greatly improve its potential clinical use and may provide a better physiologic measure of the effect of ventricular dyssynchrony than existing parameters.

Specific Aims

The **objectives** of this project were to 1) evaluate the ability of XC delays to diagnose mechanical dyssynchrony in the heart, and 2) develop a non-invasive method to quantify internal flow within the LV as a measure of dyssynchrony. We **hypothesized** that 1) XC delays are more sensitive and specific in diagnosing dyssynchrony compared to currently utilized methods for quantifying dyssynchrony and 2) internal flow can be quantified with cardiac magnetic resonance imaging and will be increased in patients with LV dyssynchrony compared to normal volunteers.

The specific aims of this project were to:

1) **Quantify the effect of region of interest (ROI) tracking on the diagnosis of LV dyssynchrony from tissue Doppler images.** Analysis was performed on 18 patients who satisfied standard CRT enrollment criteria. *Successful completion of this aim demonstrated that XC delays can be accurately quantified with a stationary region of interest and therefore require minimal post-processing time.*

2) **Evaluate the ability of XC delays to discriminate between positive and negative control groups compared to previously published dyssynchrony parameters.** Analysis was performed on 11 pre-CRT TDI exams from patients who showed a positive response to CRT (greater than 15% reduction in LV end-systolic volume after 3 months of pacing). Negative controls were volunteers with no history of heart disease, normal echocardiogram and normal 12-lead electrocardiography. ROC analysis was performed to quantify each dyssynchrony

3) **Evaluate the ability of XC delays to diagnose acute "pacing-induced dyssynchrony."** Dyssynchrony was created by pacing the right ventricular apex (RVA) of pediatric patients undergoing catheter ablation for non-preexcited supraventricular tachycardia. TDI exams were acquired during this dyssynchronous state and compared to TDI exams acquired during atrial pacing at the same rate as a negative control. ROC analysis was performed to quantify each dyssynchrony parameter's ability to discriminate between atrial pacing and RVA pacing. *Successful completion of this aim demonstrated that systolic XC delay showed the greatest ability to diagnose acute pacing-induced dyssynchrony.*

4) **Develop and evaluate a new method for quantifying left ventricular internal flow from standard cine cardiac magnetic resonance images.** Regional volume curves were generated for the LV using a semi-automated border detection and segmentation algorithm. Internal flow was calculated as the sum of the absolute changes in regional volume minus the absolute change in global LV volume. As a preliminary study, internal flow was quantified in patients with severely dyssynchronous (QRS>150 ms) class III/IV heart failure and a group of healthy, normal controls. *Successful completion of this aim demonstrated that patients with dyssynchronous heart failure had nearly 6 times the internal flow present in healthy controls.*

CHAPTER 2

BACKGROUND AND INTRODUCTION TO NEW METHODOLOGY

Background

Cardiac Resynchronization Therapy

Cardiac resynchronization therapy (CRT) utilizing biventricular pacemakers is a relatively new treatment for patients with end-stage, drug-refractory heart failure[4, 5]. CRT results in an acute hemodynamic benefit[13-16], reverse ventricular remodeling,[17-20] and improved quality of life[4, 21, 22]. This positive response to CRT was initially thought to derive from the resolution of inter-ventricular dyssynchrony (discoordinate contraction between the left and right ventricles). Therefore, patients with *inter*-ventricular dyssynchrony were chosen to receive CRT. It was shown that QRS duration measured on a surface electrocardiogram was a good marker for inter-ventricular dyssynchrony[23]. Consequently, patients with a wide QRS complex (> 120 ms) were enrolled in the initial randomized clinical trials of CRT[5]. Current selection criteria also require an ejection fraction <35%, New York Heart Association (NYHA) class III or IV heart failure[5] and stable clinical condition despite optimal medical therapy for at least 3 months.

However, specificity of current selection criteria is low, as 20 to 30% of selected patients do not respond to CRT[5]. Sensitivity is also low as some patients with heart failure have benefited from CRT despite the fact that they do not satisfy current selection criteria[24]. This becomes a critical issue as CRT is an invasive and expensive therapy with

each device costing from $25 – $40,000 and total per patient hospital charges approaching $100,000[25, 26]. These factors mandate the need for the development of more specific and sensitive patient selection criteria for CRT[26, 27].

Left ventricular (LV) dyssynchrony (dyssynchrony *within* the left ventricle) may better predict response to CRT[27]. Approximately 30% of patients with wide QRS lack LV dyssynchrony[28]. This may partially explain the low response rates in the initial CRT trials. In fact, the majority of recent evidence suggests that LV dyssynchrony is important in predicting response to CRT whereas *inter*-ventricular dyssynchrony is not useful[7].

Quantification of Left Ventricular Dyssynchrony

Numerous techniques have been used to assess LV dyssynchrony[27]. However, no single method has emerged as a widespread standard. Conventional echocardiographic methods for measuring LV dyssynchrony include M-mode measurement of the septal-to-posterior wall motion delay[29], Fourier phase angle analysis of wall displacement[30], and calculation of regional fractional area changes using contrast imaging[31]. As noted by Bax *et al*[27], these techniques are restricted by the use of a single imaging plane and, therefore, do not quantify *global* LV dyssynchrony. Three-dimensional echocardiography and modeling can overcome this limitation[32], but limited availability and prolonged time required for image processing has, up to now, limited its clinical applicability.

Tissue Doppler velocity imaging (TDI) of the myocardium has recently emerged as a powerful tool to quantify LV mechanical dyssynchrony[27]. Using TDI, it is possible to obtain a time-varying velocity curve for a single ventricular wall at frame rates

approaching 300 Hertz (corresponding to one data point every 3.3 milliseconds). TDI assessment of the LV may represent the best method to diagnose dyssynchrony[7].

Quantification of Left Ventricular Dyssynchrony Using Tissue Doppler Imaging

TDI has most often been used to quantify dyssynchrony as the simple difference in time-to-peak systolic myocardial velocity between the septum and lateral wall of the LV[8, 33]. This parameter is referred to as the septal-to-lateral delay (SLD). SLD greater than 60 ms predicted response to CRT with a sensitivity and specificity of 76 and 88%, respectively[8]. The maximal difference in time-to-peak velocity in any 2 of the 4 basal septal, lateral, anterior and inferior ventricular segments (MaxDiff) has also been used to quantify dyssynchrony[34]. A MaxDiff greater than 65 ms predicted response to CRT with a sensitivity and specificity of 92%[34].

Yu *et al* extended this "time-to-peak" analysis by using the standard deviation of times-to-peak systolic myocardial velocity of the 12 standardized LV mid-wall and basal segments (Ts-SD) as a measure of dyssynchrony[19]. This method has provided a global measure of LV dyssynchrony that can be calculated with moderate post-processing time. By quantifying Ts-SD in 88 normal subjects and taking the mean (17 ms) plus two standard deviations (2 * 7.8 = 15.6 ms) of Ts-SD in these normals, Yu *et al* determined a threshold value of 32.6 ms to diagnose LV dyssynchrony[6]. However, multiple threshold values for Ts-SD dyssynchrony have been reported by Yu *et al*. For instance, the authors used a threshold of 31.4 ms to predict response to CRT with a sensitivity and specificity of 96 and 78%, respectively[35]. In a different population of patients, Yu *et al* reported a

threshold of 34.4 ms to predict response to CRT with a sensitivity and specificity of 87 and 81%, respectively[36].

Refinement of CRT Selection Criteria

In a recent CRT review article, Bax *et al* suggested that it is mandatory to expand current guidelines for patient selection for CRT to include TDI assessment of LV dyssynchrony[7]. However, a recent study showed that the most commonly used TDI dyssynchrony parameters agree on the diagnosis of dyssynchrony only half the time[37]. In addition, the first multi-center trial to prospectively determine the ability of echocardiographic parameters (including tissue Doppler parameters) to predict response to CRT (PROSPECT)[38] recently completed enrollment. The initial results showed that no parameter predicted response to CRT as hypothesized[39].

Thus, despite the success of echocardiographic parameters in predicting response to CRT in small, single-center studies, no parameter predicted response to CRT in the first multicenter trial. In addition, the PROSPECT trial showed poor reproducibility of echocardiographic parameters between the 2 core labs in the study. Therefore, better methods to diagnose mechanical dyssynchrony in the heart are needed.

Limitations of Current Dyssynchrony Parameters

There are three major limitations of existing dyssynchrony parameters which this thesis addresses. First, existing dyssynchrony parameters were all developed solely to

identify patients who will benefit from CRT[7]. There are many causes for a non-response to CRT in addition to the absence of baseline dyssynchrony[7]. Thus, discrimination of responders to CRT from non-responders is *not* equivalent to discrimination of synchronous contraction from dyssynchronous contraction. No dyssynchrony parameter has undergone rigorous scientific evaluation for diagnosis of dyssynchrony using positive and negative controls.

Prior to determining whether CRT selection criteria should be expanded to include assessment of LV dyssynchrony by TDI, it is important to show that the dyssynchrony parameters are normal in negative control subjects and abnormal in positive control subjects with known mechanical dyssynchrony. This rigorous evaluation of dyssynchrony parameters can be performed in a model system of dyssynchrony such as "pacing-induced dyssynchrony." In this model, dyssynchrony is created by pacing the right ventricular apex at a rate that overcomes intrinsic conduction. This "pacing-induced dyssynchrony" can be compared to normal, synchronous contraction at the same rate during atrial pacing as a negative control.

The second limitation of current dyssynchrony parameters is that they are all quantitatively simplistic. For example, 8 TDI-based parameters (including those mentioned above) were compared in the PROSPECT trial[38]. Seven of these 8 parameters are based on a "time-to-peak" analysis where the time from the electrocardiogram Q-wave to the peak velocity of a ventricular wall is compared to that of a different ventricular wall[40]. This "time-to-peak" analysis is quantitatively simplistic in that it utilizes only 1 data point from the 140 points typically collected per heart beat. Furthermore, it makes the assumption that the peak velocity is the most clinically

important component criterion of ventricular synchrony. This peak can also be difficult to identify as there are often two peaks of similar magnitude that occur at different times during systole. "Time-to-peak" analysis also focuses on systolic synchrony and disregards diastolic synchrony.

Using a more advanced signal processing technique called a cross-correlation function, it may be possible to quantify the synchrony of contraction throughout systole *and* the synchrony of relaxation throughout diastole. By utilizing all data points on the velocity curves, cross-correlation analysis *does not rely on peak values* like "time-to-peak" analyses. We hypothesized that cross-correlation analysis will provide a more robust measure of dyssynchrony than methods based on "time-to-peak" analysis and will ultimately assist in the refinement of current CRT selection criteria.

Introduction to Cross-Correlation Analysis of Dyssynchrony

A cross-correlation (XC) function is used in digital signal processing to calculate a temporal delay between two discrete-time signals with a constant time step between data points. Tissue Doppler myocardial velocity data collected from the same image in different locations essentially represents two discrete-time signals with the same time vector and different amplitudes where amplitude is equal to velocity. For example, from an apical 4-chamber tissue Doppler image, we can obtain the velocity curve from the basal septum and compare this to the velocity curve from the basal lateral wall using a cross-correlation function. Figure 2.1 shows two discrete-time signals acquired at 140 frames per second with a time resolution of 7 milliseconds. The temporal delay between

the signals in Figure 2.1 was artificially set to 98 milliseconds in order to illustrate how the XC function works. The solid line signal is identical to the dashed line signal with *half* the amplitude and a 98 millisecond temporal delay.

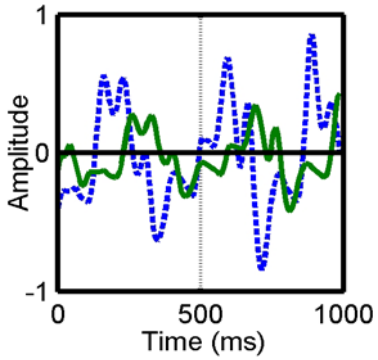

Figure 2.1: Two discrete-time signals with a temporal delay of 98 ms.

Now let x and y be the myocardial velocity vectors of the two curves in Figure 2.1, with N data points**,** and a constant time differential between data points equal to Δt (7 milliseconds in Figure 2.1). Note that the time length of the signals is then equal to $N * \Delta t$ (~1000 milliseconds in Figure 2.1). Then the normalized cross-correlation function $C_{xy}(m)$ can be calculated for any temporal delay, m, where m is an integer multiple of Δt:

$$C_{xy}(m) = \begin{cases} \dfrac{\sum_{n=0}^{N-m-1}\left(x_{n+m}-\bar{x}\right)\cdot\left(y_n-\bar{y}\right)}{\left[\sum_{n=0}^{N-m-1}\left(x_{n+m}-\bar{x}\right)^2 \cdot \sum_{n=0}^{N-m-1}\left(y_n-\bar{y}\right)^2\right]^{1/2}} & \text{for all } m \geq 0 \\ C_{yx}(-m) & \text{for all } m \prec 0 \end{cases} \qquad (2\text{-}1)$$

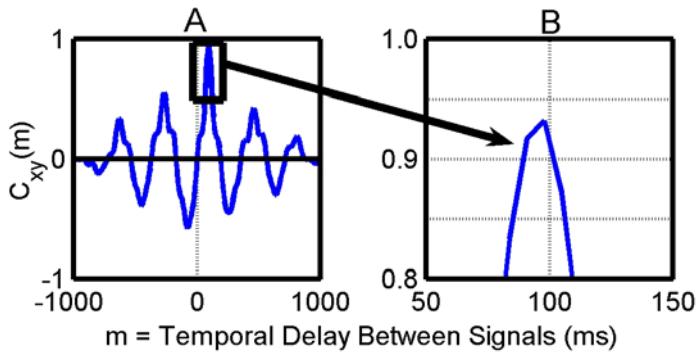

Figure 2.2: Cross-correlation analysis determines the temporal delay to be 98 ms.

where $\bar{x}$ is the mean value of x and $\bar{y}$ is the mean value of y. If we calculate the cross-correlation function for each integer multiple of Δt within the range ±0.5*(heart period), the maximum of the cross-correlation function occurs at the actual temporal delay between the two signals. Figure 2.2A shows the cross-correlation function (C_{xy}) of the two signals in Figure 2.1 as a function of the temporal delay (m) between the signals. Figure 2.2B shows only the maximum peak from Figure 2.2A, and we can see that the two signals correlate maximally at the temporal delay we initially defined between them

(98 ms). Figure 2.3 shows the same signals from Figure 2.1 now plotted with the temporal shift of 98 ms as calculated by the cross-correlation function. After temporal correction using the cross-correlation function, the two signals are synchronous in time.

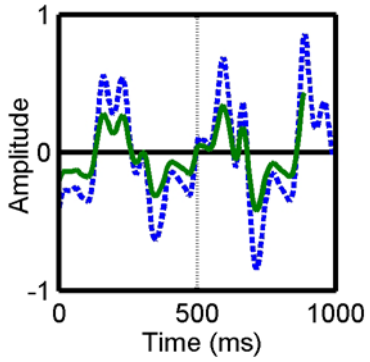

Figure 2.3 The signals match in time after plotting them with the temporal delay determined using cross-correlation analysis.

Calculation of Systolic and Diastolic Temporal Delays

We can apply the cross-correlation function to any two velocity curves to calculate a temporal delay between them. In order to calculate systolic and diastolic temporal delays independently, we divide the myocardial velocity curves into *systole* and *diastole* using the timing of aortic and mitral valve opening and closing (Figure 2.4). This data can be obtained from pulsed Doppler images of the aortic and mitral valve outflow tracts which are routinely collected during an echocardiogram. We can use a cross-correlation function to calculate a temporal delay for the systolic portion (from aortic valve opening to aortic valve closure) and diastolic portion (from mitral valve opening to

mitral valve closure) of the myocardial velocity curves independently. We can also calculate a temporal delay for the whole velocity curve. Therefore, the output of the cross-correlation comparison of two myocardial velocity curves is:

1) Whole-cycle temporal delay,

2) Systolic temporal delay, and

3) Diastolic temporal delay.

Each of these parameters can be calculated and compared to determine which one will best quantify mechanical dyssynchrony and predict response to CRT.

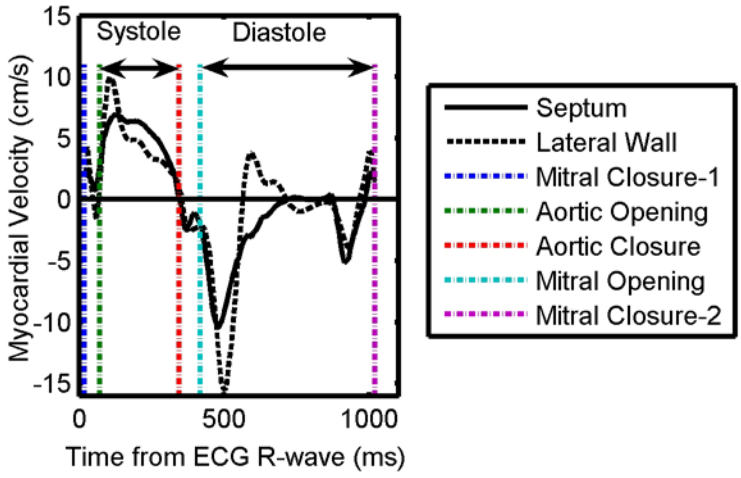

Figure 2.4: Myocardial velocity curves divided into systolic and diastolic portions.

Estimation of Global Dyssynchrony

In order to estimate global dyssynchrony, we calculate the temporal delay

between opposing basal segments in apical 2-, 3- and 4-chamber views and take a *maximum* of these values. This will be a maximum of 3 temporal delays. For example, Figure 2.5 shows an apical 4-chamber view of the LV with oval 30x6mm regions of interest (ROIs) placed in the basal segments of the septum and lateral wall. The ROI represents the area over which Doppler-derived velocity data will be averaged in order to output the myocardial velocity curve. We calculate the 4-chamber temporal delay as the cross-correlation temporal delay between the basal septum and basal lateral wall ROIs. From each apical view we obtain a temporal delay from the opposing basal segments. Therefore, using the three standard apical views, we obtain 3 temporal delays and take a maximum of these values as an estimate of *global* dyssynchrony.

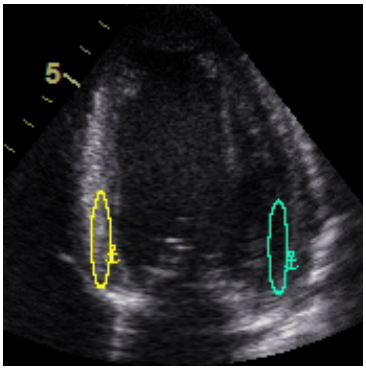

Figure 2.5: Regions of interest placed on an apical 4-chamber echocardiogram of the left ventricle.

Automated Quantitative Analysis

The quantitative data analysis described above has been programmed into a

quantitative analysis software package (MatLab version 7.40 from MathWorks, Inc., Natick, MA). We can export tissue Doppler myocardial velocity data from commercially available EchoPAC PC SW software (version 4.0.3, GE Vingmed Ultrasound, Horten, Norway). This data can then be uploaded into MatLab and processed using MatLab programs that we have written and optimized in order to automate the analysis. This automated analysis is intended to minimize human error during data processing.

Hemodynamic Quantification of Ventricular Dyssynchrony

There are two approaches to quantification of LV dyssynchrony. We have discussed methods to automate and improve upon quantification of LV dyssynchrony using TDI-based motion analysis of the myocardium. Another approach to quantifying LV dyssynchrony is to examine the dyssynchrony in blood flow created by dyssynchronous motion of the ventricular walls. This hemodynamic approach may represent a more direct physiological measure of dyssynchrony than parameters based on wall motion analysis.

Paradoxical systolic flow toward late-activated or dyssynchronous segments has been reported and quantified previously using Doppler echocardiography of blood flow in the LV[10, 41]. In addition, reversed *diastolic* flow towards the LV base has been observed in patients with anterior wall ischemia[42], presumably due to dyssynchronous contraction caused by ischemia. Thus, the underlying pathophysiology of dyssynchrony is a reduced efficiency of ventricular ejection due to blood flowing *internally* or within the LV instead of moving directly through the LV and into the aorta.

Internal flow can be quantified by conductance catheter and expressed as a percentage of the total ejected volume (referred to as the internal flow *fraction*)[11]. Steendijk *et al* demonstrated that patients with LBBB had an internal flow fraction of 78% compared to only 20% in normal controls[11]. A recent study also showed that internal flow fraction was reduced from 71% to 42% after 6 months of CRT[12]. Thus, quantification of internal flow has shown promise in identifying dyssynchrony and in demonstrating the hemodynamic benefit of CRT.

Internal flow can be calculated from regional volume versus time curves for any number of regional volumes of the LV:

$$IF(t) = \frac{\sum_i |\Delta V_i(t)| - |\Delta V_{LV}(t)|}{2} \qquad (2\text{-}2)$$

where $IF(t)$ is the internal flow at time t, $V_i(t)$ is the volume of segment i at time t, and $V_{LV}(t)$ is the volume of the entire LV at time t[11]:

$$V_{LV}(t) = \sum_i V_i(t) \qquad (2\text{-}3)$$

Note that division of equation (2) by 2 takes into account the fact that any blood which exits one regional volume must enter another regional volume if it does not leave the LV. Internal flow *fraction* (IFF) is defined as the total internal flow divided by the stroke volume. IFF can be calculated in systole ($IFF_{systole}$), diastole ($IFF_{diastole}$) and over the entire cardiac cycle (IFF_{whole}).

The clinical utility of internal flow analysis is currently limited by the invasive

catheterization procedure required for its calculation. However, we can generate regional volume versus time curves for the LV using cardiac magnetic resonance (CMR) imaging to enable *non*-invasive quantification of IFF. This will represent a significant step forward in making hemodynamic quantification of LV dyssynchrony more useful and readily available to assist in diagnosis and treatment of LV dyssynchrony.

CHAPTER 3

AIM 1: QUANTIFY THE EFFECT OF REGION OF INTEREST TRACKING ON THE DIAGNOSIS OF LEFT VENTRICULAR DYSSYNCHRONY FROM TISSUE DOPPLER IMAGES

Introduction

Left ventricular mechanical dyssynchrony can be diagnosed using tissue Doppler imaging (TDI) of the myocardium.[27] Diagnosis of dyssynchrony with TDI requires two main post-processing steps which have not been standardized. First, velocity-time curves are generated from myocardial segments by placing regions of interest (ROIs) within both the mid-ventricular and basal segments of the LV walls.[43] Manual "tracking" of the ROI throughout the cardiac cycle is performed to ensure that the ROI remains in a mid-myocardial location. Tracking is required to generate the true shape of the myocardial velocity curve, but is time consuming and typically not performed when diagnosing dyssynchrony.[44] Importantly, many authors have omitted the description of whether or not ROI tracking was employed.[6, 8, 9, 20, 28, 34-36, 45, 46]

The second post-processing step required to diagnose dyssynchrony using TDI is to compare the velocity-time curves from different myocardial walls to generate a quantitative value of dyssynchrony. Unfortunately, there is no accepted parameter for calculating dyssynchrony. Most methods utilize parameters based on a time-to-peak analysis where the time from the electrocardiogram Q-wave to the peak systolic velocity is measured in each segment of the LV. A simple difference in this time-to-peak ≥60ms

between the basal septal and lateral segments can be used to define dyssynchrony.[8] We developed systolic, diastolic and whole-cycle cross-correlation delay (XCD) parameters which utilize all velocity data points from 3 consecutive beats (~420 points) to quantify dyssynchrony.

Dyssynchrony parameters are typically calculated from velocity-time curves generated from a stationary ROI. A stationary ROI generates a slightly different velocity-time curve than a tracked ROI because the stationary ROI includes regions of the ventricular cavities (outside the myocardial segment of interest) during part of the cardiac cycle. For example, Figure 3.1 shows an ROI placed in the basal septum of a patient with heart failure. The ROI includes some of the right ventricular cavity at end-systole and some of the left ventricular cavity at end-diastole. Inclusion of data from the ventricular cavities may lead to a change in the location of the peak systolic velocity, which may affect the diagnosis of dyssynchrony. No study to date has examined the effect of manual ROI tracking on the diagnosis of dyssynchrony.

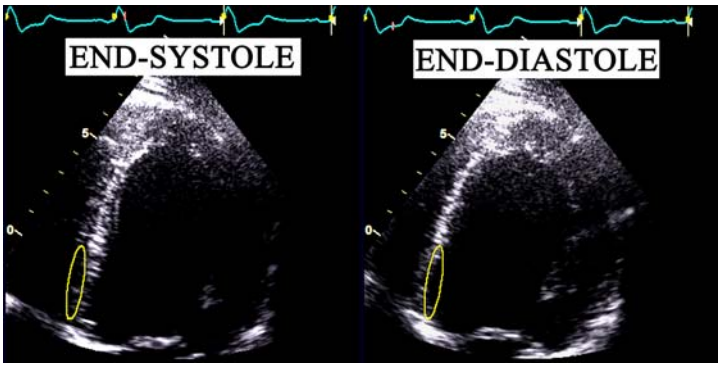

Figure 3.1: The myocardium moves into and out of a stationary region of interest during the cardiac cycle.

We *hypothesized* that using a stationary ROI to quantify dyssynchrony from TDI would affect the diagnosis of dyssynchrony in patients with heart failure. We tested our hypothesis by quantifying dyssynchrony using both tracked and stationary ROIs in 18 patients with heart failure who were being evaluated for CRT. We examined the effect of ROI tracking on 3 published time-to-peak dyssynchrony parameters and the 3 XC delay parameters.

Methods

Patient Population

Consecutive patients referred to Emory University Crawford Long Hospital for potential treatment with CRT were evaluated for inclusion. Inclusion criteria were: 1) left ventricular ejection fraction <35%, 2) QRS duration > 120ms, and 3) New York Heart Association (NYHA) class III or IV heart failure. Twenty patients satisfied criteria and were enrolled initially. However, subsequent testing revealed that one patient had a QRS duration of 96 ms and another had an ejection fraction of 57%. These two patients were excluded. Characteristics of the final 18 patients are shown in Table 3.1. All patients gave informed consent under guidelines established by the institutional review board.

Table 3-1: Characteristics of the patient population.

Variable (units)	Value (mean ± SD, *n* = 18)
Age (years)	58 ± 16
Male gender (%)	9 (50%)
LV end systolic volume (ml)	115 ± 51
LV end diastolic volume (ml)	165 ± 64
LV ejection fraction (%)	31 ± 10
QRS duration (ms)	183 ± 36

Tissue Doppler Data Acquisition

Apical 2-, 3- and 4-chamber TDI of the myocardium were acquired with the patient lying in the lateral decubitus position using a commercial system (Vivid 7, GE Vingmed, Horten, Norway). The myocardial walls were aligned as parallel to the Doppler beam as possible to minimize the angle of insonation, and frame rate was optimized from 100 to 140 Hertz. Pulsed Doppler spectral recordings of the aortic outflow tract were acquired for definition of systole.

Tissue Doppler Post-processing

EchoPAC PC SW post-processing software (version 4.0.3, GE Vingmed, Horten, Norway) was used to export velocity data from the 12 basal and mid-wall segments of the 6 standard LV walls (septum and lateral walls in 4-chamber view, anteroseptal and posterior walls in 3-chamber view, and anterior and inferior walls in 2-chamber

view). The curves were processed with the default averaging filter (30ms) within the EchoPAC software prior to export. Velocity data was exported using two methods for comparison:

(1) Tracked ROIs: A 30x6-millimeter ROI was located over the mid-wall of the myocardium and was moved manually throughout the cardiac cycle to maintain this mid-wall location within the ventricular segment of interest.

(2) Stationary ROIs: A 30x6-millimeter ROI was placed at the center of motion of the ventricular segment of interest.

Six dyssynchrony parameters were calculated from the exported velocity curves:

(1) basal septal-to-lateral delay in time-to-peak systolic velocity (SLD)[8]

(2) maximum difference in times-to-peak systolic velocity between any 2 of the basal septal, lateral, anterior and inferior LV segments (MaxDiff)[33]

(3) the standard deviation of times-to-peak systolic velocity in the 12 basal and mid-wall segments of the LV (Ts-SD)[19]

(4) Systolic XCD - The *maximum* cross-correlation temporal delay between the systolic portion of the myocardial velocity curves from opposing basal sections in apical 2-, 3- and 4-chamber views. Systole was defined to include the isovolumic contraction period from mitral valve closure to aortic valve closure.

(5) Diastolic XCD - Diastolic XCD was calculated similarly to systolic XCD, except the diastolic portion of the velocity curve was used. Diastole was

defined to include the isovolumic relaxation period from aortic valve closure to mitral valve closure.

(6) Whole-cycle XCD - The *maximum* cross-correlation temporal delay between myocardial velocity curves from opposing basal sections in apical 2-, 3- and 4-chamber views.

Prior to cross-correlation processing, the velocity curves were bilinearly interpolated so that there was a constant time step between data points for each subject.

Each dyssynchrony parameter was calculated twice for each patient: first using velocity curves from the tracked ROIs and second using velocity curves from the stationary ROIs. An average velocity curve was generated from three cardiac cycles of velocity data prior to measuring dyssynchrony parameters. Pulsed Doppler of the aortic outflow tract was used to define systole for identification of the peak systolic velocity for calculation of time-to-peak parameters.

Correction for Heart Rate

Dyssynchrony parameters were normalized by the square root of the R-R interval in seconds to normalize for differences in heart rate.

Statistics

Bland-Altman plots were generated to demonstrate the agreement between calculating dyssynchrony using tracked versus stationary ROIs for each of the 6

dyssynchrony parameters. Paired student's t-tests were used to compare dyssynchrony derived from tracked versus stationary ROIs for each of the 6 dyssynchrony parameters. A value of $p<0.05$ was defined as statistically significant. Threshold values to diagnose dyssynchrony were used to determine whether use of a stationary ROI changed the diagnosis of dyssynchrony for any patients.

Results

Bland-Altman Agreement Between Tracked and Stationary ROIs

Results for each patient are shown (Tables 3.2 and 3.3). There was no significant difference in mean values for tracked versus stationary ROI analysis for any dyssynchrony parameter (Table 3.4).

Bland-Altman analysis (Figure 3.2) demonstrated excellent agreement between stationary and tracked ROIs for the XCD parameters (2*SD of the mean difference = 11ms, 11ms and 10 ms, respectively for whole-cycle, systolic and diastolic XCD). The agreement was poor for the time-to-peak dyssynchrony parameters (2*SD of the mean difference = 74, 71, 18 ms, respectively, for SLD, MaxDiff and Ts-SD).

Table 3-2: Dyssynchrony values for time-to-peak parameters using tracked versus stationary regions of interest.

Patient Number	SLD (threshold = 60ms)		MaxDiff (threshold = 65 ms)		Ts-SD (threshold = 34.4 ms)	
	Tracked	Stationary	Tracked	Stationary	Tracked	Stationary
1	94	94	110	110	46	48
2§	30	30	80	176	30	63
3	68	76	107	107	61	62
4	66	66	83	76	50	50
5	109	109	116	116	62	64
6	77	77	116	116	51	54
7	0	0	15	15	45	45
8*	105	16	119	111	68	65
9	122	114	168	152	78	77
10*†§	0	134	17	135	31	55
11	73	73	94	102	47	46
12	0	0	44	44	24	24
13	6	6	20	20	34	34
14	21	21	57	57	45	44
15	15	15	25	25	27	27
16	7	7	36	36	35	37
17	16	16	16	16	27	27
18	7	0	16	9	31	30

Threshold values for diagnosing dyssynchrony are given in the column headers for each parameter. *Use of a stationary region of interest changed the diagnosis of dyssynchrony according to SLD. †Use of a stationary region of interest changed the diagnosis according to MaxDiff. §Use of a stationary region of interest changed the diagnosis according to Ts-SD.

Table 3-3: Dyssynchrony values for the XC delay parameters using tracked versus stationary regions of interest.

Patient Number	Whole-XCD (threshold = 25 ms)		Systolic-XCD (threshold = 53 ms)		Diastolic-XCD (threshold = 22 ms)	
	Tracked	Stationary	Tracked	Stationary	Tracked	Stationary
1	23	23	38	46	15	15
2	10	10	91	91	29	29
3	150	150	32	39	158	158
4	45	45	110	81	36	36
5	90	90	90	90	90	90
6	5	5	58	58	5	5
7	45	45	133	133	37	37
8*	23	23	93	93	23	16
9	92	100	146	146	69	69
10	60	40	0	7	60	60
11	171	171	139	139	170	170
12	67	67	15	15	99	82
13	64	71	28	28	92	99
14	21	21	85	85	28	21
15	44	44	51	51	44	44
16	21	21	36	43	7	7
17	49	57	16	16	227	219
18	300	300	0	0	30	30

Threshold values for diagnosing dyssynchrony are given in the column headers for each parameter. *Use of a stationary region of interest changed the diagnosis of dyssynchrony according to diastolic XCD.

Table 3-4: Comparison of dyssynchrony values using tracked versus stationary regions of interest.

Parameter	Tracked (ms)*	Stationary (ms)*	p†	Dyssynchrony Threshold (ms)	Disagreement on Diagnosis between Tracked and Stationary
SLD	40 ± 37	43 ± 42	0.76	60	11 %
MaxDiff	62 ± 40	73 ± 49	0.23	65	6 %
Ts-SD	40 ± 12	43 ± 13	0.14	34.4	11 %
Whole-XCD	65 ± 67	65 ± 67	0.99	25	0 %
Systolic-XCD	59 ± 42	59 ± 41	0.82	53	0 %
Diastolic-XCD	62 ± 55	60 ± 54	0.17	22	6 %

*Values are means ± SD, $n = 18$. †Paired t-test comparing tracked and stationary values.

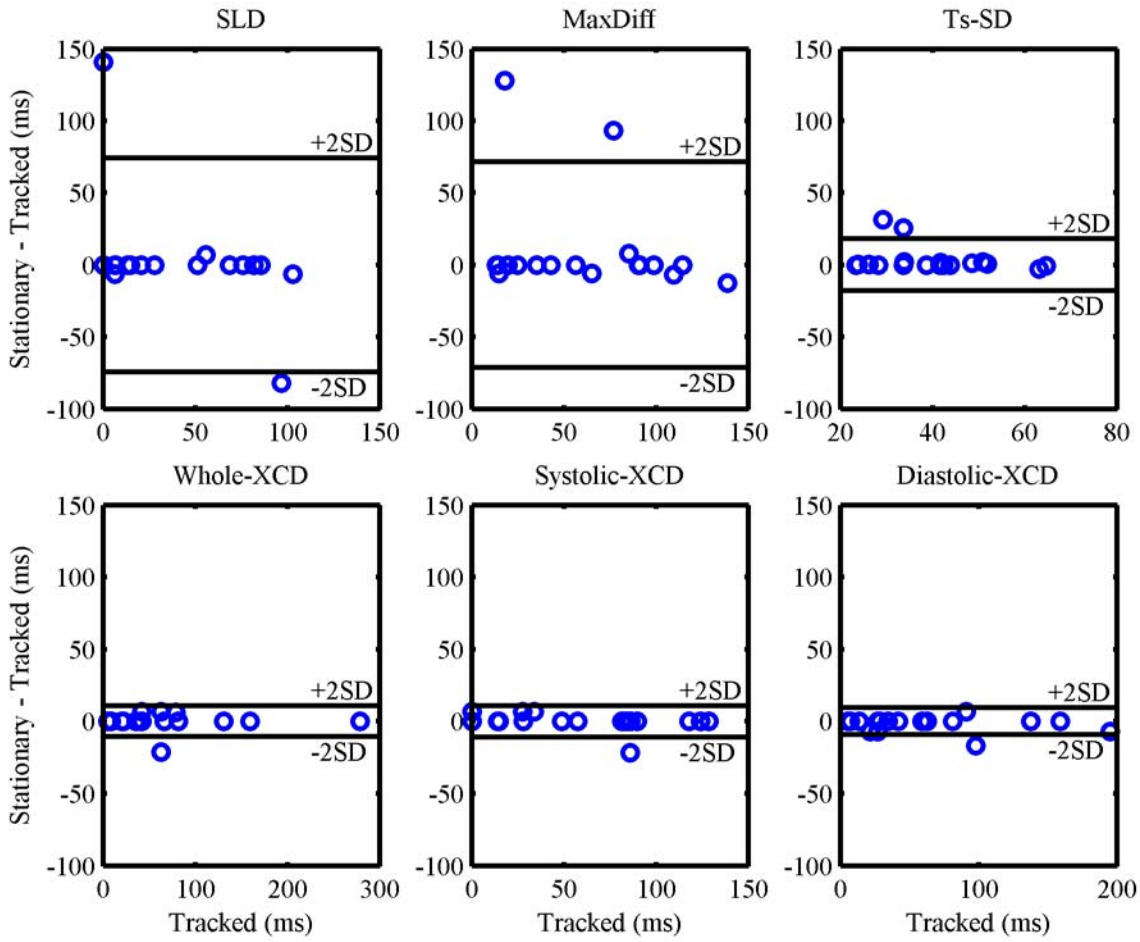

Figure 3.2: XCD shows the closest agreement between tracked and stationary ROIs

Effects of Tracking on the Diagnosis of Dyssynchrony

ROI tracking did *not* affect the diagnosis of dyssynchrony in any patients when using whole-cycle or systolic XCD (Table 3.4). ROI tracking changed the diagnosis of dyssynchrony in only one patient when using diastolic XCD. However, ROI tracking changed the diagnosis of dyssynchrony in 2, 1 and 2 of the patients when using SLD,

MaxDiff and Ts-SD, respectively (Table 3.4). For example, Figure 3.3A shows velocity curves from the basal septum and lateral wall of patient number 10 using tracked ROIs. Figure 3.3B shows velocity curves from the same patient using stationary ROIs placed in the same segment as the tracked ROIs. The patient had a SLD of 0 ms using tracked ROIs compared to a SLD of 141 ms using stationary ROIs. Since the threshold value for diagnosing dyssynchrony with SLD is 60 ms, the stationary ROI suggested that the patient had dyssynchrony while the tracked ROI demonstrated that the patient did not have dyssynchrony.

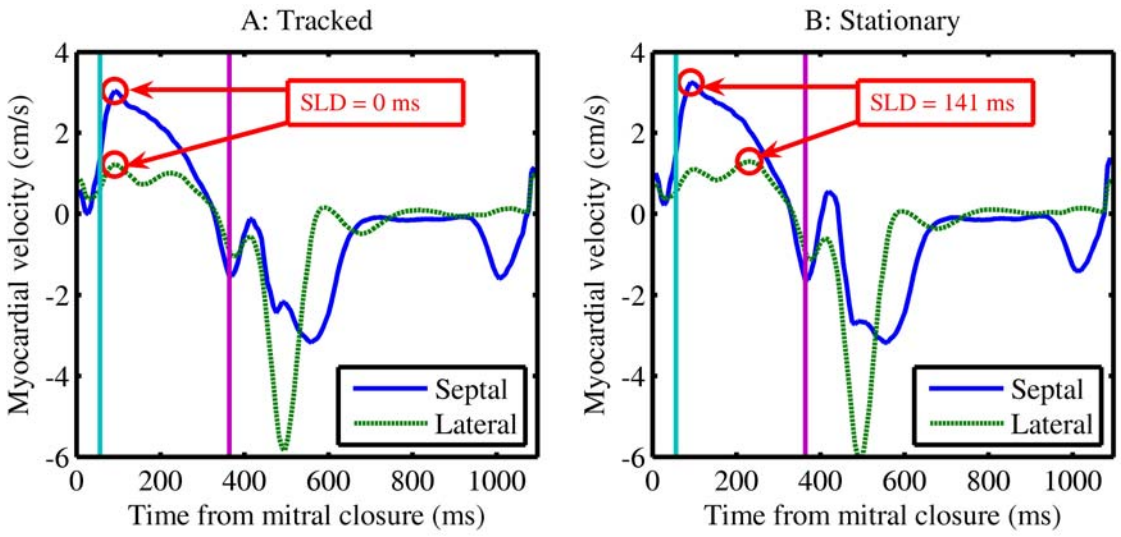

Figure 3.3: Stationary ROI versus tracked ROI shows a different diagnosis using SLD

Discussion

Tissue Doppler imaging (TDI) of the myocardium is a powerful tool to diagnose LV mechanical dyssynchrony.[27] Dyssynchrony is diagnosed by placing sample volumes, or regions of interest (ROIs), in several ventricular segments and comparing the velocity tracings from these segments. Manual tracking of the ROIs needs to be performed to maintain the location of the ROI within the segment of interest as the heart moves. However, the process of manual tracking is time-consuming and not typically done.[44] We showed that using a *stationary* ROI changed the diagnosis of dyssynchrony in 6-11% of patients with advanced heart failure using time-to-peak dyssynchrony parameters while use of a stationary ROI did *not* affect the diagnosis using whole-cycle and systolic cross-correlation delay analysis. This is the first study to report the effects of ROI tracking on the diagnosis of dyssynchrony.

Region of Interest Tracking in Other TDI Dyssynchrony Studies

The significance of ROI tracking on dyssynchrony indices has been largely ignored in the literature. Ten of the most commonly cited studies using color TDI to measure ventricular dyssynchrony[6, 8, 9, 20, 28, 34-36, 45, 46] failed to specify whether the authors used a tracked or stationary ROI. (However, in a correspondence letter, Yu et al stated that their group always uses a tracked ROI.[47]) Studies using pulsed TDI to quantify dyssynchrony[33, 48-50] all use stationary ROIs as software has not been developed to reconstitute velocity tracings with a tracked pulsed Doppler ROI. Our study suggests that

ROI tracking is important and should be addressed in future TDI dyssynchrony studies.

The predictors of response to CRT (PROSPECT) trial is the first international, multi-center study using TDI dyssynchrony measures to predict response to CRT.[38] The PROSPECT trial showed that no TDI dyssynchrony parameter predicted response to CRT[39]. However, the PROSPECT echocardiography core labs used a stationary ROI to quantify dyssynchrony. We have shown that quantification of dyssynchrony using stationary ROIs is suboptimal when using time-to-peak parameters, and this may partially account for the negative results of the trial.

Studies using strain rate imaging to quantify dyssynchrony have reported using a tracked ROI for analysis.[51, 52] Since Doppler-derived strain rate is calculated with a velocity gradient, velocity must be measured accurately in two places within the myocardium. Thus, we expect that strain rate imaging will be *more* susceptible to ROI tracking than velocity-based measures of dyssynchrony.

Correction for Heart Rate

We corrected for heart rate by dividing dyssynchrony values by the square root of the R-R interval for each patient. We chose to do this to facilitate comparison of dyssynchrony values across the different chapters in this thesis (the pediatric patients in Chapter 5 had heart rates that were much higher than the typical adult patients from Chapters 3, 4 and 6). However, published threshold values used to diagnose dyssynchrony with the time-to-peak parameters were *not* developed from datasets that were corrected for heart rate. Using *un*-corrected dyssynchrony values, the diagnosis of

dyssynchrony changed due to use of a stationary ROI in 17, 11 and 17% of the patients according to SLD, MaxDiff and Ts-SD (compared to 11, 6 and 11% using *corrected* values). Values from the *un*-corrected data may represent a more clinically relevant estimation of the error due to use of a stationary ROI in time-to-peak diagnosis of dyssynchrony from tissue Doppler images.

Comparison to Existing Studies

The mean values of dyssynchrony in our study compare well with previous reports. Yu et al[19] reported a Ts-SD of 38 ± 11 ms in a group of 25 patients undergoing CRT compared to 40 ± 12 ms in our group of 18 patients. Bax et al[34] reported a value of 73 ± 49 ms for MaxDiff in a group of 85 patients receiving CRT, which was identical to that seen in our study. SLD shows variability in the literature as Bax et al reported a value of 71 ± 38 ms in 25 patients with heart failure[8] and 97 ± 35 ms in a different group of 22 patients.[9] In another study, Yu et al[20] reported a mean SLD of 36 ms in a group of 30 heart failure patients, which compares well with the value of 40 ± 37 ms in our group of patients.

Cross-correlation Delay versus Time-to-peak Parameters for Quantification of Dyssynchrony

The majority of techniques to assess LV dyssynchrony utilize "time-to-peak" analysis where the time from the QRS onset to the peak velocity of a ventricular wall is

compared to that of a different ventricular wall.[8] Using TDI, it is possible to obtain velocity curves from two ventricular walls simultaneously at frame rates over 140 Hertz. Therefore, when analysis is limited to time-to-peak systolic myocardial velocity, only one of approximately 140 data points per heart cycle is utilized. XCD analysis overcomes this limitation by utilizing all data (~420 points from 3 consecutive heart beats) from the myocardial velocity curves to quantify dyssynchrony as opposed to just peak values. Therefore it is not surprising that XCD is less vulnerable to the slight errors caused by the myocardium being outside of the stationary ROI for brief periods during the cardiac cycle.

The results of this study demonstrate a significant advantage of XCD while at the same time highlighting a weakness in conventional time-to-peak parameters. XCD dyssynchrony can be diagnosed with a stationary ROI while a tracked ROI should be used to measure conventional time-to-peak parameters. Thus, XCD can be calculated approximately 30 minutes faster per patient than time-to-peak parameters when using current commercially-available software platforms.

Automation of Region Tracking

The main deterrent from performing ROI tracking is the prolonged time required to complete the analysis. Manual ROI tracking added approximately 30 minutes of post-processing time per patient in our study. However, new speckle tracking technology which enables manual tracking of the myocardium in 2 dimensions[53] could be utilized to perform automated ROI tracking in future TDI post-processing software platforms. A

recent study implemented this technique and showed its feasibility.[54]

Study Limitations

Since there is no gold standard for diagnosing dyssynchrony, a limitation of our study is that it was unknown whether or not each patient in this study did or did not have dyssynchrony. Thus, we could not compare the performance of the 4 dyssynchrony parameters in diagnosing dyssynchrony. However, a comparison of the accuracy of each parameter in diagnosing dyssynchrony was performed in Aim 2 which is reported in Chapter 4 of this thesis.

The true impact of ROI tracking on dyssynchrony assessment may be underestimated in this study as we only included patients with severe heart failure. These patients may have different or less myocardial motion than patients with either normal hearts or less severe disease. Further studies are needed to determine whether the amplitude of myocardial motion causes differing errors when stationary ROIs are used to diagnose dyssynchrony.

Five patients in our study had a left ventricular ejection fraction less than 35% quantified by short-axis M-mode but between 35 and 41% as quantified by a Simpson's bi-plane analysis. We chose *not* to exclude these patients since inclusion criteria for CRT include ejection fraction < 35% typically quantified by M-mode. However, we reported ejection fractions in Table 3.1 using Simpson's method since this is usually done in the research setting.

Conclusions

Use of a stationary region of interest (ROI) changes the diagnosis of dyssynchrony in 6-11% of patients when using conventional Doppler tissue imaging time-to-peak parameters such as septal-to-lateral delay. Cross-correlation delay (XCD) diagnosis of dyssynchrony is minimally affected by use of a stationary region of interest. These data demonstrate that using a stationary region of interest may be inaccurate approximately 11-17% of the time when using time-to-peak parameters to quantify dyssynchrony. However, cross-correlation delay dyssynchrony can be diagnosed accurately using stationary regions of interest, which saves post-processing time.

CHAPTER 4

AIM 2: EVALUATE THE ABILITY OF XCD TO DISCRIMINATE BETWEEN POSITIVE AND NEGATIVE CONTROL GROUPS COMPARED TO PREVIOUSLY PUBLISHED DYSSYNCHRONY PARAMETERS

Introduction

As mentioned in Chapter 3, there are two main steps required to quantify dyssynchrony from tissue Doppler images that have not been standardized. First, velocity-time curves are generated from myocardial segments by placing regions of interest (ROIs) within the different myocardial segments.[43] Manual "tracking" of the ROI needs to be performed to ensure that the ROI remains in a mid-myocardial location, but is rarely performed since it is very time-consuming. The results of Chapter 3 showed that the XC delay parameters can be accurately quantified without tracking the ROI.

The second post-processing step required to diagnose dyssynchrony using TDI is to compare the velocity-time curves from different myocardial walls to generate a quantitative value of dyssynchrony. This Chapter will compare the diagnostic accuracy of several published dyssynchrony parameters to the XC delay parameters in order to standardize this second post-processing step.

The majority of techniques to assess LV dyssynchrony utilize tissue Doppler

velocity imaging (TDI) of the myocardium and are based on a "time-to-peak" analysis.[7] A recent study showed that the most commonly used dyssynchrony parameters agree on the diagnosis of dyssynchrony only half the time.[37] This lack of agreement may be due to the quantitative simplicity of "time-to-peak" parameters. In "time-to-peak" analysis, the time from the electrocardiogram Q-wave to the peak velocity of a ventricular wall is compared to that of a different ventricular wall, or walls.[8] Using TDI, it is possible to obtain the time-dependent velocity of two ventricular walls simultaneously at frame rates over 140 Hertz (one data point every 7 milliseconds). Therefore, when analysis is limited to time-to-peak systolic myocardial velocity, only one of approximately 140 data points per heart cycle is utilized.

To overcome this limitation, we developed a new mathematical method to calculate a temporal delay between two myocardial velocity curves. Our method utilizes a cross-correlation (XC) function to quantify either *systolic*, *diastolic* or *whole-cycle* cross-correlation delay (XCD) using TDI data collected *throughout* the cardiac cycle (not just peak values). We ***hypothesized*** that XC delays would provide a more accurate measure of dyssynchrony than methods based on "time-to-peak" analysis and will ultimately assist in the refinement of CRT selection criteria. We tested this hypothesis by comparing the ability of XC delays and other published dyssynchrony parameters to quantify dyssynchrony in groups of positive controls with known dyssynchrony and negative controls with normal synchrony.

Methods

Positive Controls (Responders to CRT)

Eleven positive controls were identified retrospectively from a database of patients who have received CRT at Emory University Crawford Long Hospital. Inclusion criteria were: 1) TDI and 2-dimensional echocardiogram at baseline and 3 months after CRT, 2) clinical evaluation at baseline and 3 months after CRT including 6-minute hall walk, quality of life score according to the Minnesota Living with Heart Failure questionnaire, and NYHA classification, 3) a positive response to CRT defined as a decrease in LV end-systolic volume of at least 15% 3 months after pacemaker implantation. All patients fit standard CRT selection criteria of ejection fraction <35%, QRS duration ≥120ms, and NYHA class III or IV heart failure. Patients with atrial fibrillation or chronic RV pacing were *not* excluded. Patients had a mean age of 68±14 years and 8/11 were male. Five patients had ischemic etiology, 4 had a right-ventricular pacemaker at baseline and one patient had atrial fibrillation. Implantation and programming of the CRT device followed standard procedures previously described.[40]

Negative Controls

Twelve adult volunteers (mean age 29±7 years) with no known history of cardiac disease, a normal 2-D echocardiogram and normal 12-lead electrocardiogram were identified as negative controls. All subjects gave informed consent under guidelines established by the Institutional Review Board.

Echocardiographic Post-processing

Ejection fraction was quantified using the modified Simpson's rule. End-systolic and end-diastolic dimensions were measured from M-mode parasternal short axis mid-papillary images. Mitral regurgitation was quantified as the average area of the jet on color flow Doppler from apical 2- and 4-chamber views and also as the ratio of the jet to left atrial area in both views.

Tissue Doppler Data Acquisition

Apical 2-, 3-, and 4-chamber tissue Doppler images of the myocardium were acquired with a Vivid 7 system (GE Vingmed, Horten, Norway). The myocardial walls were aligned parallel to the Doppler beam to minimize the angle of insonation, and frame rate was optimized from 100 to 140 Hertz. Pulsed Doppler images of the aortic outflow tract were acquired for post-processing.

Tissue Doppler Post-processing

All studies were confirmed to be technically adequate by an independent cardiologist. EchoPAC PC post-processing software (version 4.0.3, GE Vingmed, Horten, Norway) was used to export velocity curves from the TDI data. An average velocity curve was generated from three cardiac cycles of velocity data prior to measuring times-to-peak. Pulsed Doppler of the aortic outflow tract was used to define

systole. Myocardial velocity data was exported from the 12 basal and mid-wall segments of the LV using a stationary, 30x6mm oval region of interest.

Times-to-peak systolic velocities were automatically identified by a computer program written in MatLab quantitative analysis software (version 7.10, MathWorks, Inc., Natick, MA). This program imported velocity curves and aortic valve opening and closure from the EchoPAC software and exported the time from the Q-wave to the maximum velocity in the ejection phase. This was done to eliminate any error due to observer bias in selection of peak velocities.

Three published dyssynchrony parameters were calculated from these times-to-peak values: 1) basal septal-to-lateral delay in time-to-peak systolic velocity (SLD)[8], 2) maximum difference in times-to-peak systolic velocity between any 2 of the basal septal, lateral, anterior and inferior LV segments (MaxDiff)[33], and the standard deviation of times-to-peak systolic velocity in the 12 basal and mid-wall segments of the LV (Ts-SD).[19]

Estimation of Global Dyssynchrony Using Cross-correlation

Three contiguous cycles of velocity data were exported from the basal segments of the 6 standard LV walls (septum and lateral walls in 4-chamber view, anteroseptal and posterior walls in 3-chamber view, and anterior and inferior walls in 2-chamber view). Velocity curves were imported into MatLab. Prior to cross-correlation processing, the velocity curves were bilinearly interpolated so that there was a constant time step between data points for each subject. The normalized cross-correlation spectrum was

computed between two velocity curves by shifting one curve in time relative to the other curve and computing the normalized correlation between the curves for each time shift. A normalized correlation value of 1 therefore meant the two curves were perfectly synchronous in time while a value of –1 meant the two curves were completely dyssynchronous. The time shift between the two curves that resulted in the maximum correlation value was defined as the temporal delay between the two curves. This temporal delay was calculated from opposing basal ventricular segments in each apical view (i.e. the temporal delay derived from the cross-correlation spectrum was calculated for the septal versus lateral basal velocity curves, the anterior versus inferior basal velocity curves, and the anteroseptal versus inferolateral basal velocity curves). Global dyssynchrony was defined as the *maximum* absolute value of these three temporal delays. This maximum delay is referred to as the cross-correlation delay (XCD) and was calculated with three different datasets:

1. Whole-cycle XCD – The *maximum* cross-correlation temporal delay between myocardial velocity curves from opposing basal sections in apical 2-, 3- and 4-chamber views. This represents a maximum of three cross-correlation temporal delays (one delay between the velocity curves from the two opposing basal segments in each of the three apical views).

2. Systolic XCD – The *maximum* cross-correlation temporal delay between the systolic portion of the myocardial velocity curves from opposing basal sections in apical 2-, 3- and 4-chamber views. Systole was defined to include the isovolumic contraction period from mitral valve closure to aortic valve closure.

3. Diastolic XCD – Diastolic XCD was calculated similarly to systolic XCD, except the diastolic portion of the velocity curve was used. Diastole was defined to include the isovolumic relaxation period from mitral valve closure to aortic valve closure.

Comparison to Existing TDI Dyssynchrony Parameters

It is important to note that SLD, MaxDiff and Ts-SD were calculated with the same velocity curves used to calculate XCD. Dyssynchrony parameters were compared by their ability to discriminate between the positive and negative control groups with a numerical threshold. In addition, dyssynchrony was assessed in the positive control group 3 months after pacemaker implantation to determine whether each dyssynchrony parameter was reduced after CRT.

Correction for Heart Rate

Dyssynchrony parameters were normalized by the square root of the R-R interval in seconds to normalize for differences in heart rate.

Statistics

SPSS version 15.0 (SPSS Inc., Chicago, IL) was used to calculate the area under the ROC curve as a measure of a parameter's ability to discriminate between the positive

and negative controls. Areas under the ROC curve were statistically compared using the method described by Hanley and McNeil.[55] The mean values of each parameter in the positive and negative controls were compared with an un-paired t-test. Baseline and 3-month post-CRT values of dyssynchrony were compared for each parameter using a paired t-test. A value of $p<0.05$ was defined as statistically significant.

Results

Negative Control Group

Table 4.1 shows the mean dyssynchrony and percentage of negative controls exhibiting dyssynchrony according to each parameter. SLD, MaxDiff and Ts-SD showed dyssynchrony in 5, 6 and 7 out of the 12 negative controls, respectively. Whole-cycle XCD showed dyssynchrony in zero subjects. Systolic and diastolic XCD showed dyssynchrony in 3 and 1 subject, respectively. Figure 4.1 shows an example of a representative negative control who exhibited dyssynchrony according to all the time-to-peak parameters and none of the XCD parameters.

Table 4-1: Dyssynchrony parameters in the negative control group.

Parameter	Value* (ms)	Dyssynchrony Threshold (ms)†	Negative controls with Dyssynchrony
SLD	48 ± 41	60	42 %
MaxDiff	56 ± 43	65	50 %
Ts-SD	28 ± 16	34.4	58 %
Whole-XCD	9 ± 5	25	0 %
Systolic-XCD	29 ± 27	53	25 %
Diastolic-XCD	14 ± 7	22	8 %

*Values are means ± SD, n = 12. †Determined from ROC analysis in Figure 4.7 for XCD parameters, taken from[8,34,36] for the other parameters.

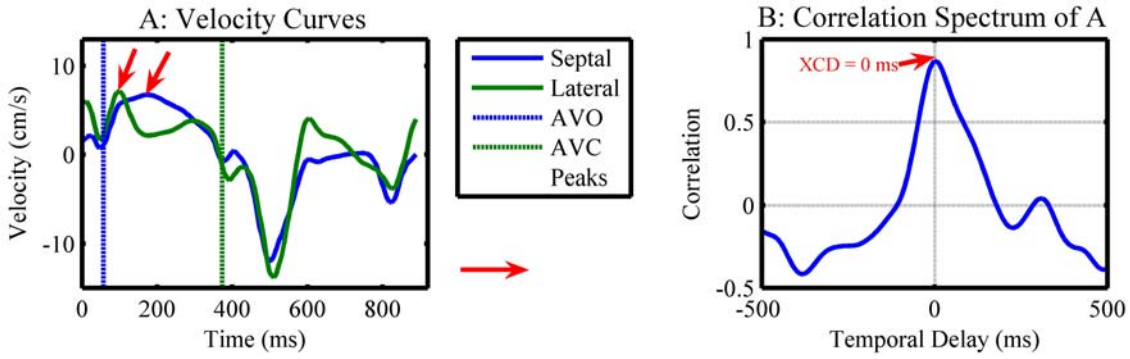

Figure 4.1: A negative control subject shows dyssynchrony according to all parameters except XCD. Red arrows show the location of the peak systolic velocities.

Table 4-2: Patient characteristics before and after CRT.

Variable	Pre-CRT	Post-CRT	p Value*
Dyssynchrony parameters			
SLD (ms)	49 ± 41	81 ± 49	0.182
MaxDiff (ms)	85 ± 42	111 ± 45	0.127
Ts-SD (ms)	70 ± 18	64 ± 18	0.531
Whole-XCD (ms)	160 ± 113	119 ± 30	0.442
Systolic-XCD (ms)	110 ± 75	106 ± 47	0.809
Diastolic-XCD (ms)	124 ± 105	55 ± 43	0.028
Echocardiographic measurements			
LV end-systolic volume (ml)	145 ± 76	88 ± 38	0.002
LV end-diastolic volume (ml)	188 ± 84	139 ± 47	0.004
LV end-systolic dimension (cm)	5.9 ± 1.1	4.9 ± 1.7	0.01
LV end-diastolic dimension (cm)	6.6 ± 1.1	6.0 ± 1.7	0.161
LV ejection fraction (%)	24 ± 7	37 ± 10	< 0.001
Mitral regurgitation area (cm^2)	7.4 ± 4.5	5.2 ± 3.8	0.082
Ratio of mitral regurgitation area to left atrial area (%)	34 ± 17	23 ± 15	0.06
QRS Duration (ms)	175 ± 23	160 ± 27	0.18
NYHA Class	3.1 ± 0.3	1.8 ± 0.8	< 0.001
Quality of life score†	54 ± 27	26 ± 29	0.007
6 minute hall walk (m)	227 ± 127	327 ± 103	0.055

Values are means ± SD, *n* = 11. *p value from paired t-test. †according to the Minnesota Living with Heart questionnaire. Post-CRT values are 3 months after implantation of a biventricular pacemaker.

Positive Control Group

Table 4.2 reports the mean dyssynchrony, echocardiographic, and clinical characteristics of the positive control group both before and 3 months after CRT. Patients showed a significant ($p<0.05$) decline in LV end-systolic volume, LV end-diastolic volume, and NYHA functional class. Patients also showed a significant ($p<0.05$) increase in LV ejection fraction and quality of life. The mean mitral regurgitation decreased, but the decline was not significant. Similarly, the mean six-minute hall walk distance

increased but was not significant.

Diastolic XCD was the *only* dyssynchrony parameter which showed a significant reduction (56%) from baseline to 3 months after biventricular pacemaker implantation. Nine, 7 and 8 of the 11 positive controls showed a decrease in whole-cycle, systolic and diastolic XCD, respectively, 3 months after CRT compared with only 3, 3, and 5 for SLD, MaxDiff and Ts-SD, respectively. Figure 4.2 shows an example of a representative positive control who exhibited a decrease in whole-cycle XCD following CRT.

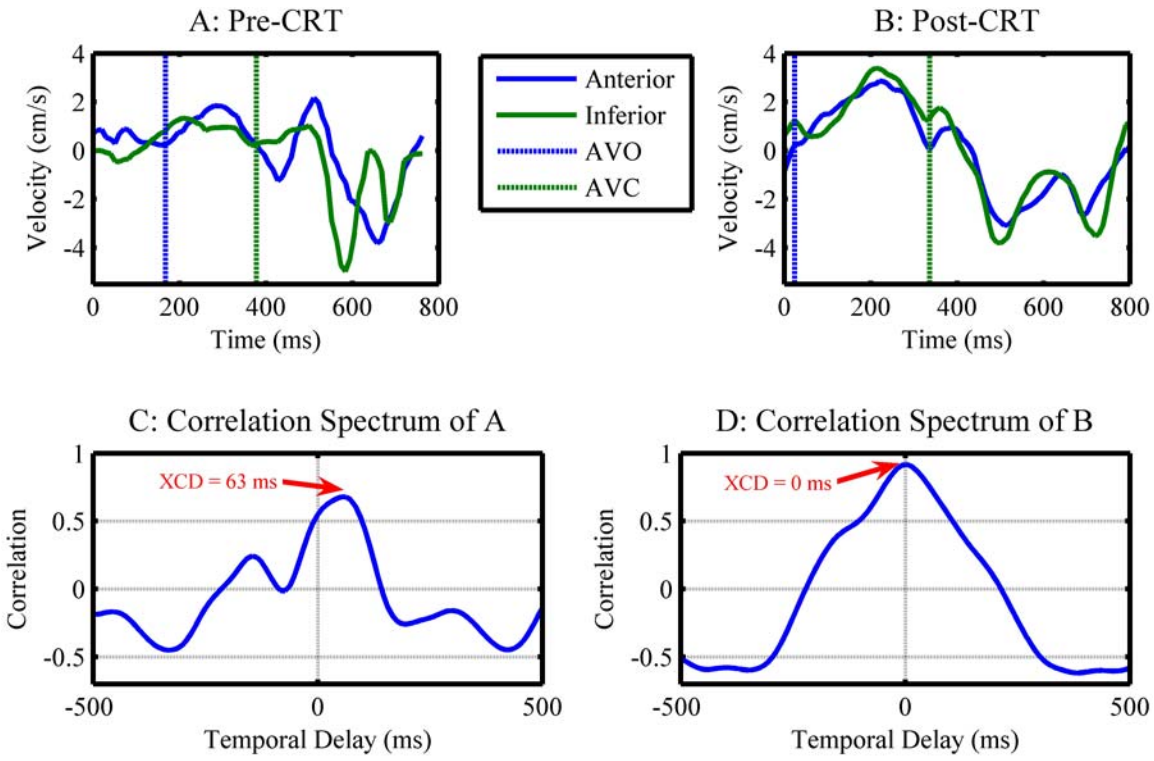

Figure 4.2: A positive control subject shows a decrease in whole-cycle XCD 3 months after CRT.

Figures 4.3 and 4.4 show values of each dyssynchrony parameter for all the positive controls (both before and 3 months after CRT). Four, 6, and 11 of the 11 positive controls showed dyssynchrony according to published threshold values (reported in table 4.1) for SLD, MaxDiff and Ts-SD, respectively. Eleven, 8, and 10 of the 11 positive controls showed dyssynchrony according to whole-cycle, systolic and diastolic-XCD, respectively.

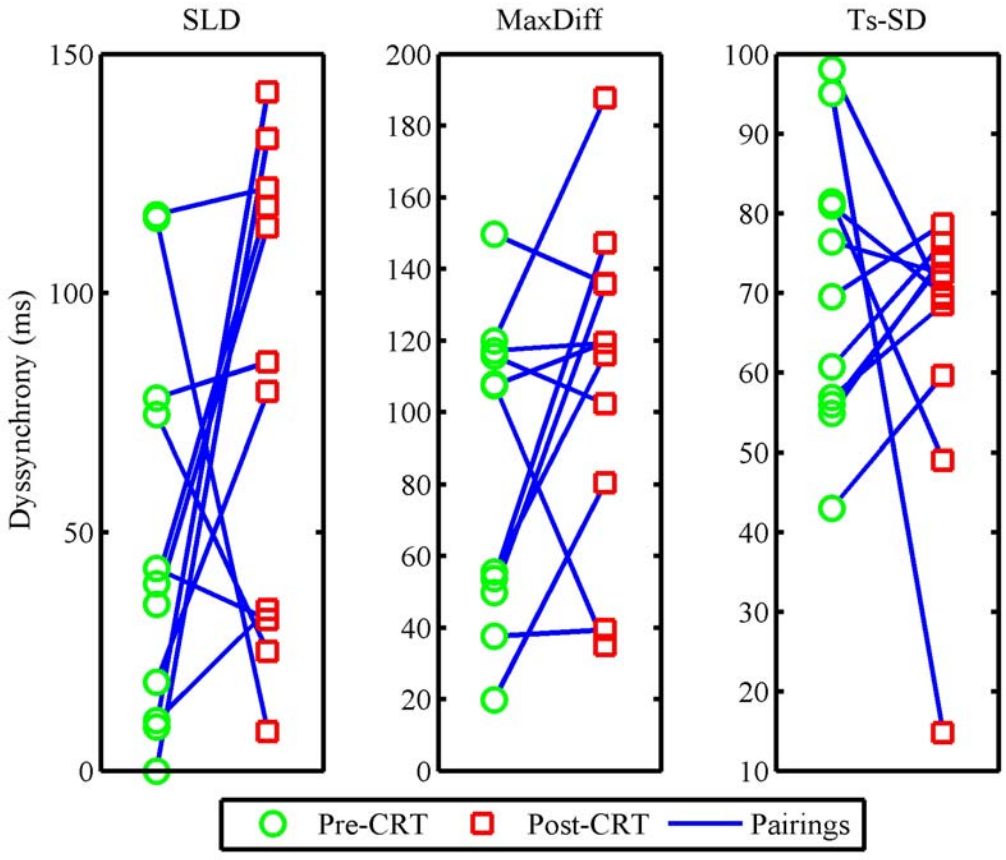

Figure 4.3: None of the time-to-peak parameters decline 3 months after CRT.

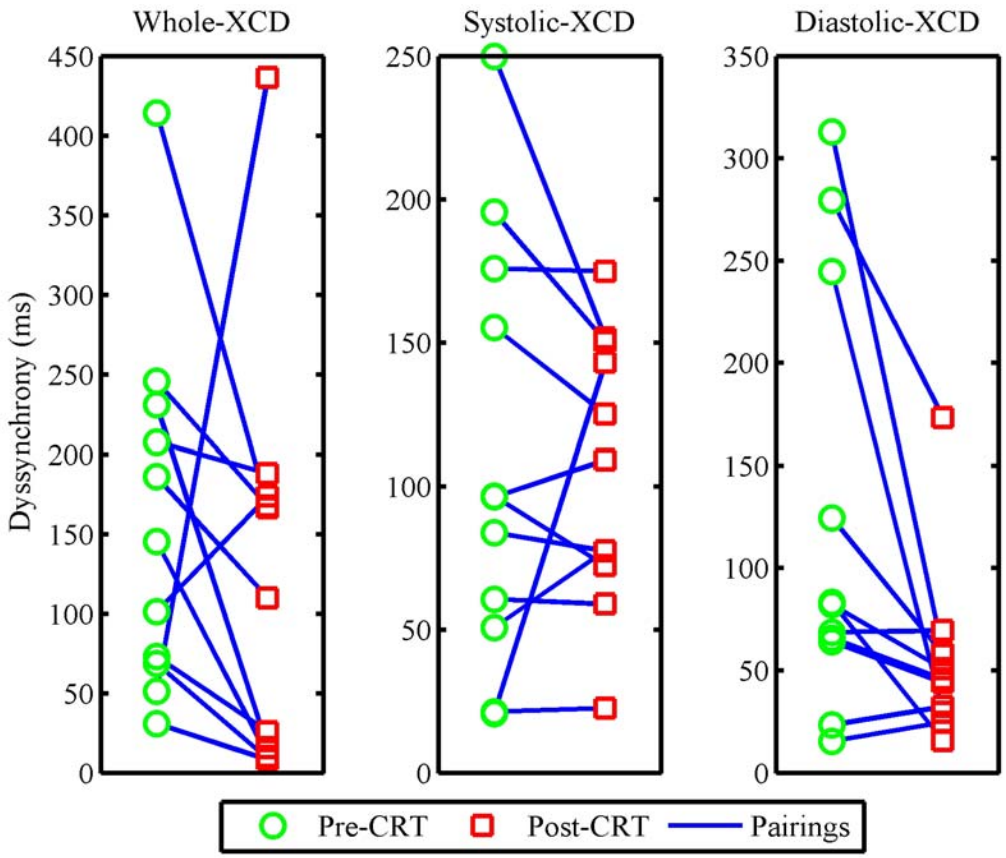

Figure 4.4: Most patients show a reduction in XCD 3 months after CRT.

Discrimination Between Positive and Negative Control Groups

All the cross-correlation delay parameters and Ts-SD showed a significant difference between the positive and negative control groups ($p<0.01$ for all comparisons). SLD and MaxDiff did *not* show a significant difference between the positive and negative control groups ($p=0.930$ and $p=0.091$, respectively). Figures 4.5 and 4.6 show values of each dyssynchrony parameter for all the positive and negative control subjects along with threshold values used to diagnose dyssynchrony.

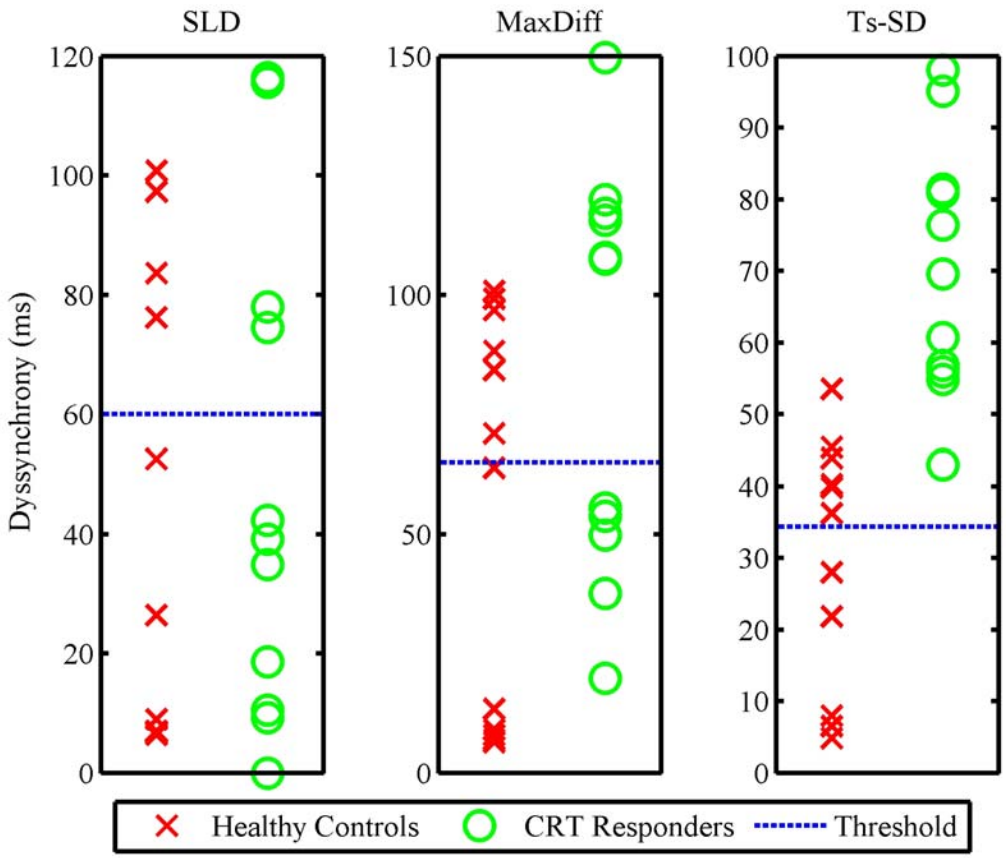

Figure 4.5: Time-to-peak parameters show poor discrimination between the positive and negative control groups.

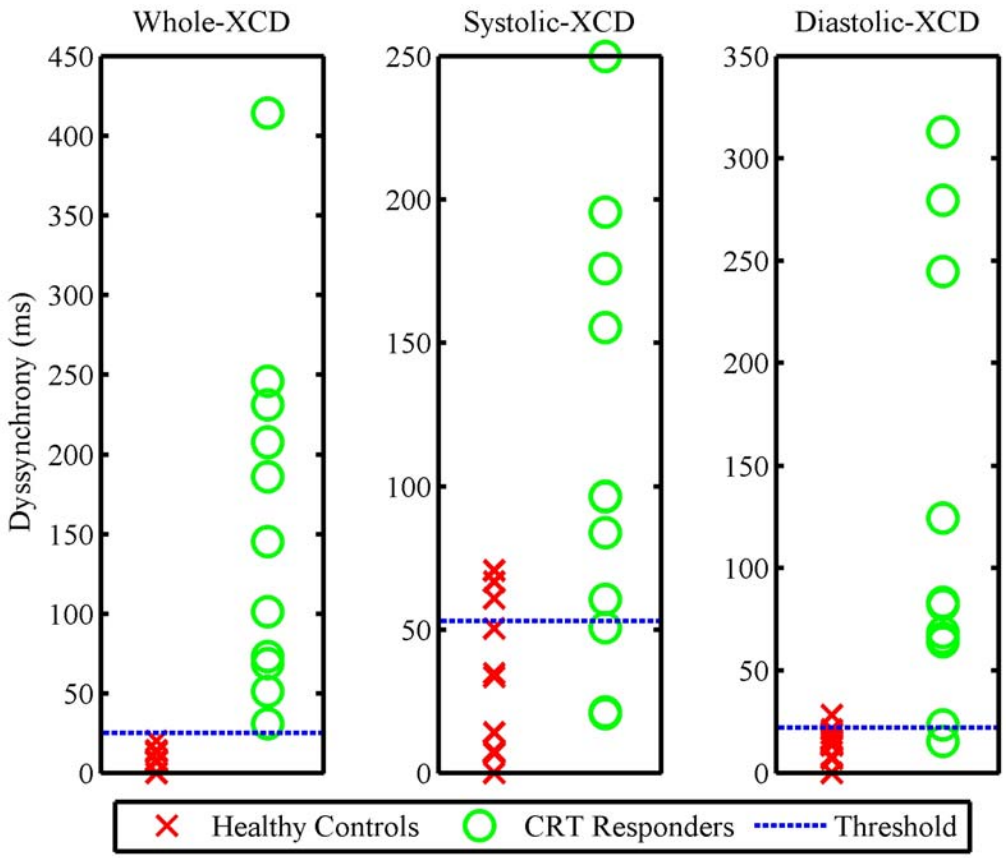

Figure 4.6: XCD parameters show excellent discrimination between the positive and negative control groups.

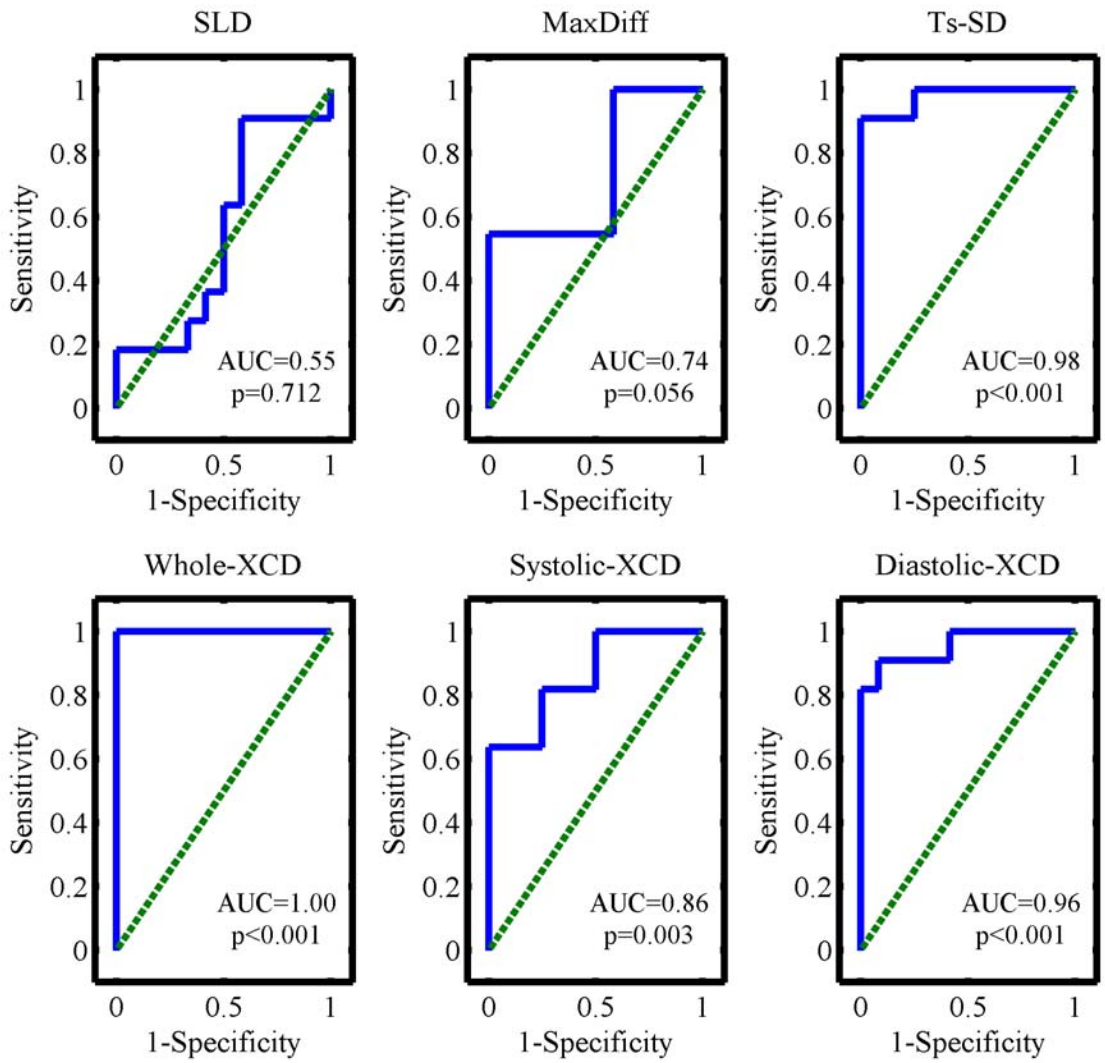

Figure 4.7: XCD parameters show significant discrimination by ROC analysis.

Figure 4.7 shows the ROC curves for each dyssynchrony parameter. All the cross-correlation delay parameters demonstrated significant discrimination between the positive and negative control groups (all $p<0.01$, Table 4.3). Ts-SD was the only time-to-peak parameter which showed significant discrimination between positive and negative controls ($p<0.01$). Whole-cycle XCD had an area under the ROC curve that was

significantly greater than SLD (p<0.001) and MaxDiff (p=0.017). Systolic-XCD had an area under the ROC curve that was significantly greater than SLD (p=0.044). Diastolic-XCD had an area under the ROC curve that was significantly greater than SLD (p=0.001) and MaxDiff (p=0.042). ROC analysis determined that a threshold XCD of 25ms had the highest sensitivity and specificity of all dyssynchrony parameters (100 and 100%, respectively) (Table 4.3).

Table 4-3: ROC comparison of dyssynchrony parameters.

Variable	Area Under the ROC Curve*	Standard Error†	Asymptotic Significance‡	Sensitivity§	Specificity§
SLD	0.55 (0.30, 0.79)	0.127	0.712	36 %	58 %
MaxDiff	0.74 (0.52, 0.95)	0.111	0.056	55 %	50 %
Ts-SD	0.98 (0.93, 1.03)	0.027	<0.001	100 %	42 %
Whole-XCD	1.00 (1.00, 1.00)[a,b]	<0.001	<0.001	100 %	100 %
Systolic-XCD	0.864 (0.71, 1.01)[a]	0.076	0.003	73 %	75 %
Diastolic-XCD	0.955 (0.87, 1.04)[a,b]	0.042	<0.001	91 %	92 %

*Asymptotic 95% confidence interval given in parentheses. †Under the nonparametric assumption. hypothesis: area under the ROC curve = 0.5 (no discriminatory value). §For discriminating between posit negative controls. [a]p<0.05 versus SLD. [b]p<0.01 versus MaxDiff.

Discussion

Quantification of LV dyssynchrony using tissue Doppler imaging (TDI) may improve selection of patients who will benefit from cardiac resynchronization therapy.[7] However, most TDI-based dyssynchrony parameters are quantitatively simplistic and rely on a "time-to-peak" analysis that utilizes only one of approximately 140 data points of

the myocardial velocity curve collected for each heart beat. Based on this limitation, we developed 3 new dyssynchrony parameters that utilize all velocity data from 3 consecutive beats (~420 points). XCD quantifies dyssynchrony *throughout* the cardiac cycle. XCD performed better than published dyssynchrony parameters in: 1) demonstrating minimal dyssynchrony in normal negative control subjects, 2) discriminating between positive and negative control subjects.

Dyssynchrony in Normal Subjects

SLD, MaxDiff and Ts-SD showed dyssynchrony in 42, 50 and 58% of negative controls, respectively. Given that many studies have suggested a need to expand CRT selection criteria to include TDI assessment of LV dyssynchrony[7], this number of false positives is far from ideal. In contrast, whole-cycle XCD showed dyssynchrony in 0 of the 12 negative controls.

Three studies have quantified dyssynchrony in normal subjects for comparison to our results: 1) Yu *et al* reported a mean Ts-SD of 17±8ms in 88 normal controls[6], 2) Lafitte *et al* reported a mean Ts-SD of 16±9ms in 50 normal controls[37], and 3) Poerner *et al* reported a standard deviation of 40±27ms in 47 normal controls.[56] Note that Poerner *et al* calculated the standard deviation of the 12 segments (including the apex) visible on 2- and 4-chamber apical views, which differs slightly from Ts-SD. The mean level of Ts-SD in our 12 negative controls was 28±16ms, which falls between the results of these previous studies. SLD and MaxDiff have not been measured in normal controls for

comparison to our results.

Discrimination Between Positive and Negative Control Groups

Our results suggest that XCD and Ts-SD can differentiate positive control subjects (patients with known dyssynchrony) from negative control subjects (patients with no dyssynchrony) more accurately than SLD and MaxDiff. This is consistent with 2 previous studies that showed Ts-SD was superior to SLD by ROC analysis.[35, 57] However, the published threshold value for Ts-SD of 34.4ms[36] to diagnose dyssynchrony resulted in a specificity of only 50%. XCD discriminated between the positive and negative control groups with a sensitivity and specificity of 100%.

Two studies have compared dyssynchrony parameters with a ROC analysis.[35, 36] Both reported Ts-SD having an area under the ROC curve similar to that seen in our study (0.96 versus 0.94 and 0.90). Yu *et al* reported an area under the ROC curve for SLD of 0.80[35], which is somewhat higher than the value of 0.55 in our study. Future studies will be needed to investigate this discrepancy.

Dyssynchrony in Responders to Cardiac Resynchronization Therapy

Diastolic XCD was the only parameter which decreased after 3 months of biventricular pacing within our group of 11 responders to CRT. Previous studies have shown a decline in SLD[8, 9], MaxDiff[34], and Ts-SD[19, 20] after CRT. However, a recent study reported results similar to ours, with no reduction in Ts-SD following CRT in a

group of responders.[58] This highlights a problem with current dyssynchrony parameters – many are highly non-specific for assessing dyssynchrony and results are not reproducible between centers.

It is important to note that whole-cycle XCD also declined in 9 out of the 11 positive controls 3 months after CRT. However, one patient had an increase in whole-cycle XCD from 51 ms to 436 ms, which caused the reduction to be non-significant ($p = 0.44$). The high whole-cycle XCD for this patient 3 months after CRT was likely due to a failure of cross-correlation analysis (Figures 4.8 and 4.9). The peak correlations for each apical view are shown as red circles. The peak correlation between the apical 2-chamber view basal anterior and inferior wall velocity curves occurred at a time delay nearly equal to half of the R-R interval (the maximum possible delay) and had a low correlation value (0.33). The actual delay may have been at the location of the red arrow. Suggestions to improve upon this problem are discussed in Chapter 7. Exclusion of this patient shows a significant reduction in whole-cycle XCD 3 months after CRT ($p = 0.02$).

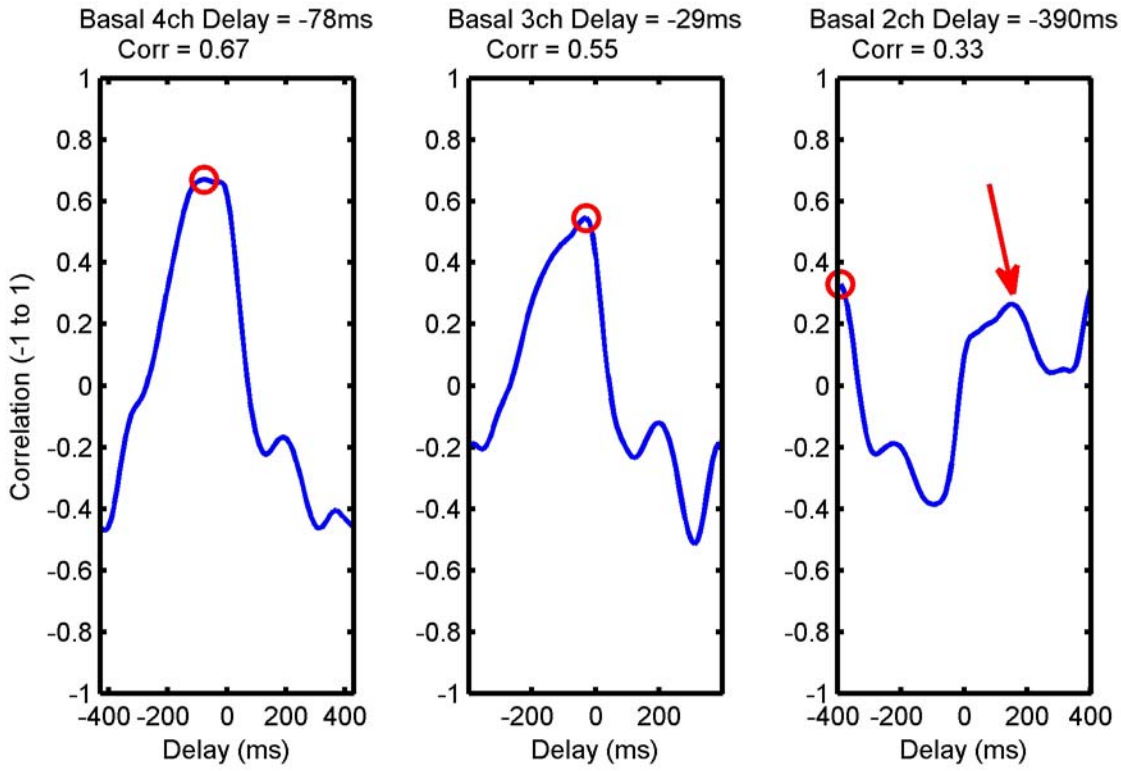

Figure 4.8: Whole-cycle XCD may have been calculated erroneously in this patient 3 months after CRT.

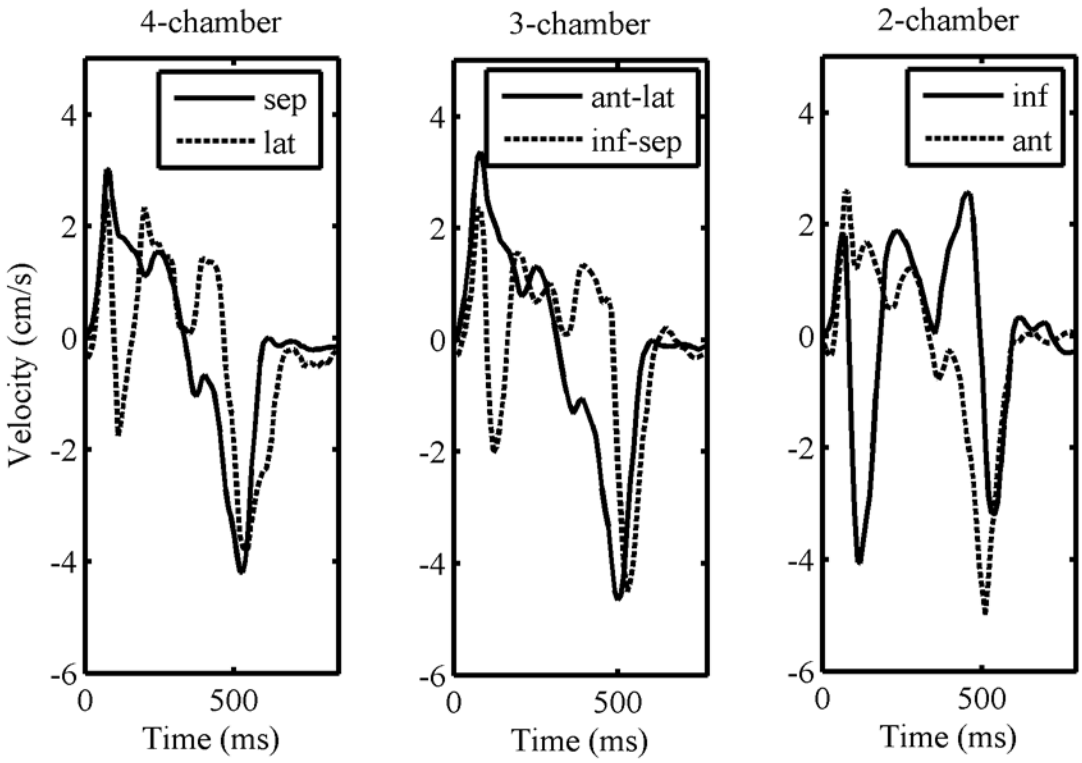

Figure 4.9: Velocity curves used to calculate the cross-correlations in Figure 4.8.

Advantages of XCD

It is important to note that the myocardial velocity curves used to calculate all dyssynchrony parameters in this study were taken from *identical* regions of interest and the same heart beats. The difference between the dyssynchrony parameters can be attributed to a difference in the post-processing of velocity curves *after* placement of the regions of interest. Therefore, our results suggest that XCD is a more robust *processing* technique to identify dyssynchrony between two myocardial velocity curves.

Whole-cycle XCD does not require identification of systole or manual selection of peak velocities. Most existing TDI dyssynchrony parameters require identification of systole so that the peak systolic velocity can be located and not confused with the

isovolumic contraction peak. Systole is typically identified by collecting pulsed Doppler of the aortic outflow tract or M-mode through the aortic valve.[36] However, these measurements of aortic valve opening and closure are collected at different times (and potentially different heart rates and loading conditions) from when the TDI data is collected so that the marking of systole adds a source of potential error to the quantification of dyssynchrony. In addition to this, clinicians typically select the systolic peaks manually to calculate dyssynchrony parameters, adding yet another source of potential error. Whole-cycle XCD eliminates both of these sources of error, and its calculation is fully automatable and could be easily incorporated into any TDI post-processing software.

All three of the XC delay parameters can be calculated from any velocity curves from the 6 basal segments of the LV and are *not* specific to the Vivid 7 GE ultrasound system used in this study. Calculation of XCD adds less than 1 minute to the post-processing time required to calculate existing TDI dyssynchrony parameters.

We focused on global dyssynchrony in this study. However, our methodology is easily translated into assessment of regional dyssynchrony to aid in determining the area of latest activation and assist in optimal lead placement for CRT. The methodology can be used to calculate a temporal delay between any two waveforms, and could also be applied to strain, strain rate, or displacement curves.

We used normalized cross-correlation analysis to calculate a temporal delay between velocity curves as a measure of dyssynchrony. However, cross-correlation methodology can also be used to derive a correlation value at that temporal delay. The

correlation value is a measure of the similarity in shape between the two velocity curves, and this value could prove useful in future studies. For example, in the current study, the positive control group showed a significant difference in the correlation value when compared to the negative controls ($p<0.0001$). Further studies are needed to elicit the utility of the normalized correlation value.

Study Limitations

The positive controls were retrospectively identified from a database of patients who received CRT at a single center. While retrospective analysis is not ideal, this study serves the purpose to introduce the XCD parameters and demonstrate their potential. Prospective, multi-center studies are needed to further explore the utility of XCD in diagnosing dyssynchrony.

As opposed to several previous studies that have introduced new techniques to quantify LV dyssynchrony, we chose not to base the initial evaluation of XCD parameters on their ability to discriminate responders from non-responders. There are many causes for a non-response to CRT in addition to the absence of baseline dyssynchrony.[7] We strongly believe that in order to rigorously investigate the phenomena of a "non-response to CRT", we must be sure that our measurement of baseline dyssynchrony does in fact quantify dyssynchrony as accurately as possible. Only then will we be able to improve selection criteria by identification of all factors that affect the outcome of CRT. Therefore, we felt it was important to establish the rigor of the XCD parameters in a positive and negative control study prior to exploring their ability to

discriminate responders from non-responders.

We did not use age-matched controls in our study. However, this is *not* a case-control study. We wanted the negative controls to be entirely free of dyssynchrony. Since LV dyssynchrony may increase with age[56], the young negative controls in our study are less likely to have dyssynchrony than a group of age-matched controls.

This study is limited by a small sample size. However, the sample size was large enough to show statistical differences between XCD and the other dyssynchrony parameters. Future studies with larger sample sizes will be required to further characterize the utility of the XCD parameters.

Temporal delay calculated from a normalized cross-correlation analysis may not be accurate when the correlation value is low (i.e. less than 0.5, for example). This issue may become important when using XCD to discriminate responders to CRT from non-responders. However, XCD worked very well in the subjects in this study, and a larger sample size would be needed to investigate this potential limitation.

The effect of frame rate on the calculation of XCD was not investigated in this study and is a potentially important issue to investigate in the future.

Conclusions

Cross-correlation delay (XCD) is a new, highly automatable method for quantifying left ventricular dyssynchrony that is superior to existing parameters at discriminating patients with known dyssynchrony from those with normal LV function.

In the patients we examined, a threshold whole-cycle XCD of 25 ms discriminated positive and negative control groups with 100% accuracy.

CHAPTER 5

AIM 3: EVALUATE THE ABILITY OF XCD TO DIAGNOSE ACUTE "PACING-INDUCED DYSSYNCHRONY"

Introduction

Accurate diagnosis of mechanical dyssynchrony in the heart is becoming increasingly important for two reasons. First, the presence of mechanical dyssynchrony has been shown to be a predictor of cardiac events in heart failure patients[33]. Second, dyssynchrony can be treated successfully with cardiac resynchronization therapy (CRT) utilizing biventricular pacemaker implantation[5].

The results of Chapter 4 demonstrated that the XC delay parameters had a superior ability to diagnose dyssynchrony in patients with heart failure compared to normal, healthy controls. This chapter will further investigate the ability of XC delays to quantify mechanical dyssynchrony in the heart. We will utilize a model of dyssynchrony to verify whether XC delays are able to diagnose dyssynchrony.

A recent study showed that the most commonly used dyssynchrony parameters agree on the diagnosis of dyssynchrony only half the time[37]. Thus, while many parameters to quantify dyssynchrony have been proposed, no single methodology has emerged as a standard. This lack of consensus on a single parameter may be due to two limitations of current parameters.

First, many dyssynchrony parameters are based on an approach that examines the "time-to-peak" systolic velocity of a ventricular wall using tissue Doppler imaging (TDI)[7]. This analysis assumes that the peak systolic velocity is the most clinically important component criterion of ventricular synchrony. Furthermore, it is quantitatively simplistic in that it utilizes only 1 data point from the 140 points typically collected per heart beat. This peak may also be difficult to identify. For example, it is often located near the isovolumic contraction peak.

To overcome the first limitation, we developed a new mathematical method to calculate a temporal delay between two myocardial velocity curves. Our method utilizes a cross-correlation function to quantify systolic, diastolic or whole-cycle cross-correlation delay (XCD) using TDI data collected *throughout* the cardiac cycle. By using all data points on the velocity curves, XCD *does not rely on peak values* like "time-to-peak" analyses.

The second limitation of current dyssynchrony parameters is that they were all developed solely to identify patients who will benefit from CRT[7]. No parameter has been evaluated in a model system of dyssynchrony such as "pacing-induced dyssynchrony." Thus, it is unclear whether existing dyssynchrony parameters are in fact quantifying dyssynchrony accurately. Pacing from the right ventricular apex (RVA) creates a model of dyssynchrony[59] that can be compared to synchronous, atrial pacing at the same rate as a negative control. This has been performed in dogs[60, 61] and in humans[62]. Based on similarities between electrocardiogram patterns in RVA pacing and left bundle branch block, this model is often referred to as "pacing-induced left bundle branch block" or

"experimental left bundle branch block"[60, 62, 63].

To overcome the second limitation, we evaluated the ability of the three XCD parameters to identify pacing-induced dyssynchrony in patients who received catheter ablation for non-preexcited supraventricular tachycardia. We compared the XCD parameters to three standard dyssynchrony parameters. We *hypothesized* that XCD parameters would perform better at diagnosing ventricular dyssynchrony than existing "time-to-peak" dyssynchrony parameters.

Methods

Subjects

Inclusion criteria were referral for catheter ablation of non-preexcited reentrant supraventricular tachycardia (i.e., atrioventricular nodal re-entrant tachycardia or atrioventricular re-entrant tachycardia) and normal cardiac structure and function documented on 2-dimensional echocardiography. Patients were excluded if they exhibited manifest preexcitation on baseline sinus 12-lead electrocardiogram. Fourteen patients (age 12.9 $\pm$ 3.6 years, 9 male) fit the criteria and were included. The study was approved by the Children's Healthcare of Atlanta institutional review board and all subjects gave informed consent prior to enrollment.

Electrophysiology

Studies and ablations were performed with the patient under general anesthesia

with continuous propofol infusion, which is standard at our institution. All cardiac medications were discontinued 5 days before the procedure. Quadrapolar catheters were placed in the RVA, right atrial appendage and adjacent to the His bundle, and a decapolar catheter was advanced into the coronary sinus. Tachycardia mechanism was confirmed with standard electrophysiologic testing.

The decision to ablate the arrhythmia substrate was based upon clinical indications. Catheter ablation was performed either with radiofrequency energy or cryotherapy at the discretion of the attending electrophysiologist. Subsequent electrophysiologic testing confirmed elimination of tachycardia substrate in all patients.

The pacing and TDI data collection were performed during the post-ablation waiting interval so as not to increase the duration of the patient's procedure. Cardiac pacing was performed at identical rates with the following configurations: atrial pacing from the right atrial appendage (AAI) and ventricular VVI pacing from the right ventricular apex (RVA). The sequence of pacing modes was random for each patient and a washout time of 3 minutes was used between pacing modes. QRS morphology was used to exclude fusion and capture beats from analysis. The pacing rate was set to 25% over normal sinus rhythm to a minimum of 100 beats per minute to ensure intrinsic ventricular conduction did not occur.

Echocardiographic Acquisition

Apical 2-, 3- and 4-chamber tissue Doppler color velocity images were collected during each pacing mode (AAI and RVA) and during normal sinus rhythm (NSR) with a

5MHz GE (Horten, Norway) Vivid 7 system. This enabled evaluation of dyssynchrony parameters in a state of dyssynchrony (RVA) compared to normal synchrony (AAI and NSR). Patients were paced for at least one minute prior to image acquisition. Tissue Doppler was acquired at a minimum frame rate of 140 Hz, and the ventricular walls were aligned to within 20^0 from parallel with the Doppler beam. Pulsed Doppler of the aortic outflow tract was acquired during each pacing mode to identify systole for measurement of systolic dyssynchrony parameters. A minimum of 3 beats of velocity data were collected during a breath-hold.

Tissue Doppler Post-processing

EchoPAC PC SW post-processing software (version 4.0.3, GE Vingmed, Horten, Norway) was used to generate 3-beat average curves of longitudinal velocity versus time from the 12 basal and mid-wall segments of the left ventricle. Each velocity curve was exported from a stationary 30x6 mm oval region of interest. The curves were processed with the default averaging filter (30ms) within the EchoPAC software prior to export. Systole was defined using the pulsed Doppler data from the aortic outflow tract so that the peak systolic velocities could be identified.

Cross-correlation Analysis

Prior to cross-correlation processing, the velocity curves were bilinearly interpolated so that there was a constant time step between data points for each subject.

Cross-correlation post-processing of velocity curves was performed in MatLab quantitative analysis software (version 7.10, MathWorks, Inc., Natick, MA). A cross-correlation function was used to calculate the time delay which resulted in maximum correlation between velocity curves from opposing ventricular segments. One velocity curve was shifted relative to the other curve, and the cross-correlation value was computed for each time shift using a normalized scale. A value of 1 meant the two curves were perfectly synchronous in time while a value of –1 meant the two curves were dyssynchronous. A value of 1 is achieved when "auto-correlating" a velocity curve with itself while a value of –1 is achieved when correlating a velocity curve with its own negative. The time shift between the two curves that resulted in the maximum correlation value was defined as the cross-correlation delay (XCD) between the two curves.

Three dyssynchrony parameters were calculated with a cross-correlation function:

(1) Whole-cycle XCD – The *maximum* cross-correlation temporal delay between myocardial velocity curves from opposing basal sections in apical 2-, 3- and 4-chamber views. This represents a maximum of three cross-correlation temporal delays (one delay between the velocity curves from the two opposing basal segments in each of the three apical views).

(2) Systolic XCD – The *maximum* cross-correlation temporal delay between the systolic portion of the myocardial velocity curves from opposing basal sections in apical 2-, 3- and 4-chamber views. Systole was defined to include the isovolumic contraction period as mitral valve closure to aortic valve closure.

(3) Diastolic XCD – Diastolic XCD was calculated similarly to systolic XCD, except the diastolic portion of the velocity curve was used. Diastole was defined as aortic valve closure to mitral valve closure.

Calculation of Time-to-Peak Dyssynchrony Parameters

Three time-to-peak dyssynchrony parameters were calculated for comparison to the cross-correlation dyssynchrony parameters:

(1) SLD – Basal septal-to-lateral delay in time-to-peak systolic velocity[8]

(2) MaxDiff – maximum difference in time-to-peak systolic velocity between any 2 of the basal septal, lateral, anterior and inferior left ventricular segments[34]

(3) Ts-SD – the standard deviation of times-to-peak systolic velocity in the 12 basal and mid-wall segments of the left ventricle[36]

It is important to note that these time-to-peak dyssynchrony parameters were calculated with the same velocity curves from the same regions of interest used in the XCD analysis.

Correction for Heart Rate

To facilitate comparison of dyssynchrony parameters at different heart rates (paced heart rates were 25% higher than NSR and heart rates differed significantly between patients), all dyssynchrony parameters were normalized by the square root of the

R-R interval.

Statistics

Statistical calculations were performed in SPSS version 14.0 (SPSS Inc., Chicago, IL). A value of $p<0.05$ was defined as statistically significant. Dyssynchrony parameters were compared by their ability to:

(1) Detect the pacing-induced dyssynchrony caused by RVA pacing: Mean values of each parameter for the different pacing modes (NSR, AAI, RVA) were compared using a repeated-measures ANOVA with a Huynh-Feldt correction followed by a Bonferroni multiple comparison post-hoc test.

(2) Diagnose dyssynchrony using a numerical threshold: ROC curves were generated for each parameter by plotting sensitivity versus 1-specificity for multiple threshold values. The area under the ROC curve was used to rank the ability of the dyssynchrony parameters to discriminate between AAI pacing (no dyssynchrony) and RVA pacing (dyssynchrony). Threshold values to diagnose dyssynchrony were then determined for each parameter by locating the point on the ROC curves where sensitivity was equal to specificity[34].

Results

Raw data from each subject is available in Tables 5.1 and 5.2.

Table 5-1: Dyssynchrony values for the time-to-peak parameters during each pacing mode.

	SLD			MaxDiff			Ts-SD		
Patient Number	NSR	AAI	RVA	NSR	AAI	RVA	NSR	AAI	RVA
1	24	34	110	23	34	118	27	30	89
2	14	18	30	17	18	92	6	11	51
3	107	74	39	109	90	138	60	38	86
4	96	132	9	96	152	172	74	62	68
5	10	21	87	61	73	98	94	43	47
6	66	111	90	138	115	92	63	48	53
7	156	70	77	176	126	90	62	54	88
8	97	91	126	131	99	178	72	57	86
9	54	113	18	54	120	209	46	59	65
10	104	127	113	112	127	153	51	73	96
11	69	73	96	122	101	96	56	64	42
12	29	22	158	29	22	164	53	25	84
13	119	110	0	222	110	6	80	72	101
14	18	23	145	21	39	146	16	25	76

All values are dyssynchrony in milliseconds.

Table 5-2: Dyssynchrony values for the XCD parameters during each pacing mode.

	Whole-XCD			Systolic-XCD			Diastolic-XCD		
Patient Number	NSR	AAI	RVA	NSR	AAI	RVA	NSR	AAI	RVA
1	6	7	7	58	41	136	6	14	7
2	14	17	87	7	17	122	15	26	19
3	8	17	9	99	109	85	8	17	9
4	8	13	9	55	78	0	8	0	9
5	10	11	0	20	84	137	10	0	0
6	7	9	9	103	82	127	7	9	0
7	8	17	9	62	69	120	8	17	9
8	14	10	29	78	87	155	7	10	0
9	9	18	11	9	166	190	11	18	11
10	7	16	33	57	25	190	7	8	0
11	71	98	224	85	71	128	71	98	150
12	19	20	26	38	10	180	19	20	26
13	13	16	32	88	40	199	14	16	32
14	0	22	36	20	51	7	0	22	14

All values are dyssynchrony in milliseconds. *AAI* = right atrial appendage pacing; *NSR* = normal sinus rhythm with no pacing; *RVA* = right ventricular apex pacing; *XCD* = cross-correlation delay.

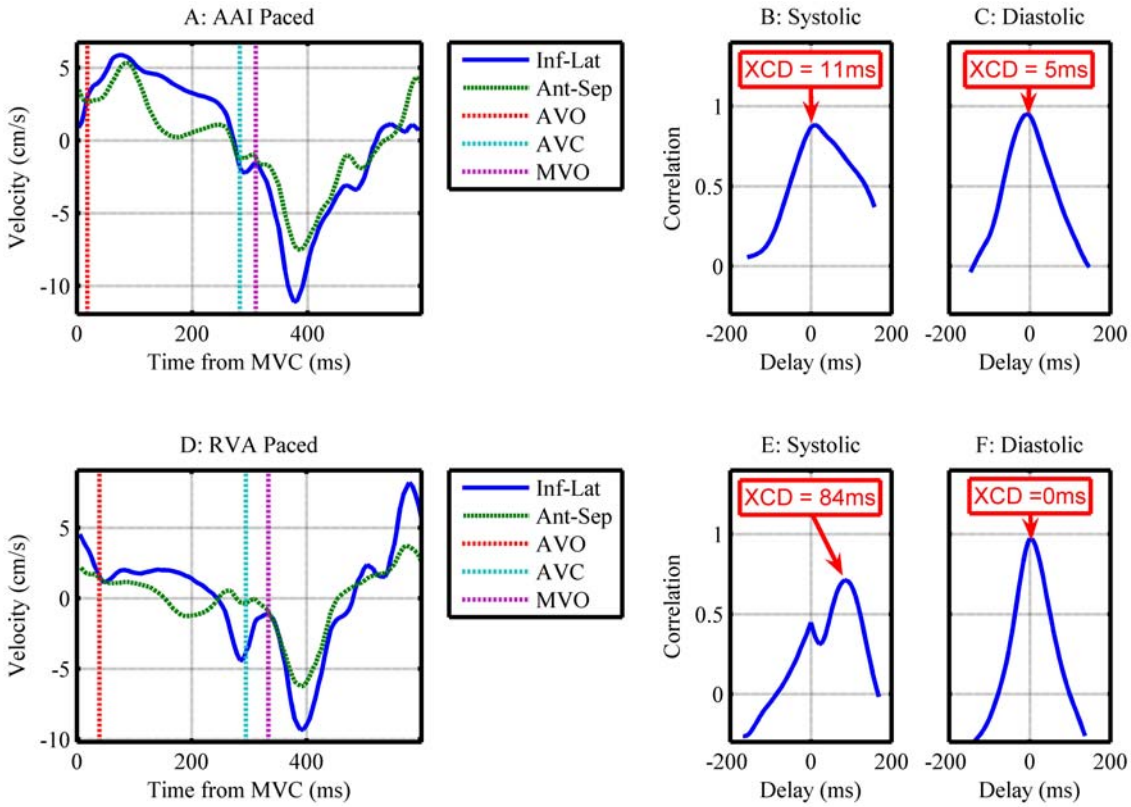

Figure 5.1: Acute RVA pacing creates systolic dyssynchrony with preserved diastolic synchrony.

Figure 5.1 shows velocity curves from the septal and lateral wall of a representative patient. The systolic and diastolic cross-correlation plots for this patient are also shown to illustrate how the XCD parameters were calculated. This patient showed a large increase in systolic dyssynchrony due to acute RVA pacing with no change in diastolic synchrony.

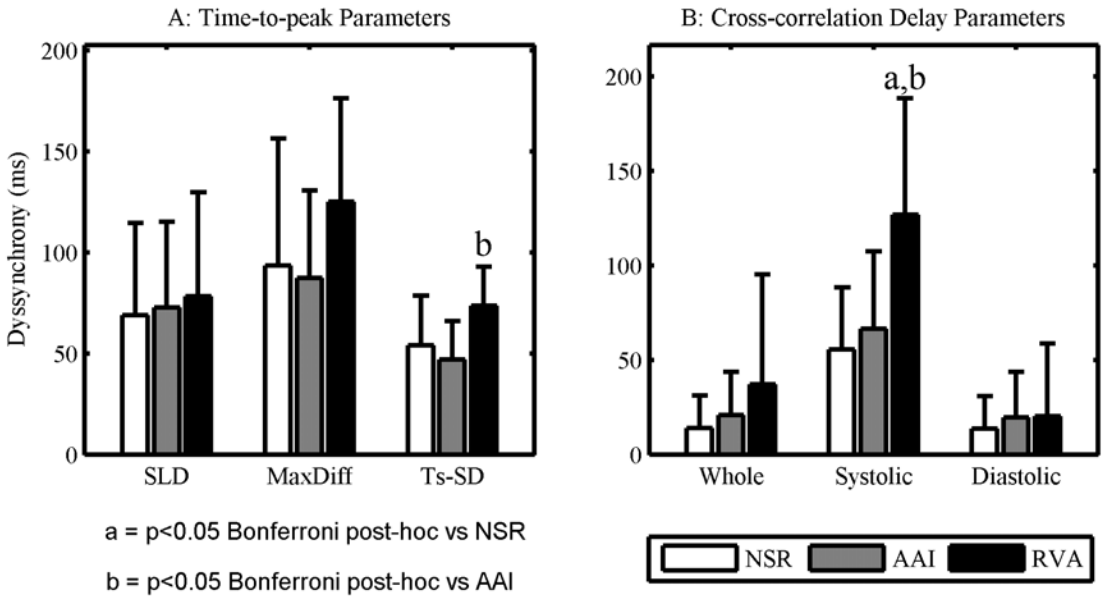

Figure 5.2: Systolic XCD is the only parameter that is increased due to RVA pacing compared to AAI and NSR.

Table 5-3: Dyssynchrony parameters for each pacing mode.

Parameter	NSR	AAI	RVA	p*
Dyssynchrony Parameters				
SLD	69 ± 46	73 ± 43	78 ± 51	0.794
MaxDiff	94 ± 63	87 ± 43	125 ± 51	0.160
Ts-SD	54 ± 24	47 ± 19	74 ± 19 †	0.002
Whole-XCD	14 ± 17	21 ± 23	37 ± 58	0.079
Systolic-XCD	56 ± 33	66 ± 41	127 ± 62 †,§	0.001
Diastolic-XCD	14 ± 17	20 ± 24	20 ± 38	0.285
QRS Duration (ms)	80 ± 15	78 ± 16	140 ± 15†,§	<0.001
Heart Rate (bpm)	86 ± 19	109 ± 15§	109 ± 15§	<0.001

Data are mean ± SD. n = 14 for all pacing modes. *repeated-measures ANOVA for comparing the mean values between pacing modes, †p<0.05 versus AAI by Bonferroni post-hoc multiple comparison. §p<0.05 versus NSR by Bonferroni post-hoc multiple comparison.

AAI versus NSR

No parameter showed a difference in dyssynchrony between AAI and NSR (Figure 5.2 and Table 5.3). Thus, acute atrial pacing *did not* change the level of dyssynchrony from that present at baseline during NSR.

Systolic Dyssynchrony

AAI versus RVA

Acute RVA pacing created systolic dyssynchrony. Ts-SD and systolic XCD showed a significant increase from AAI to RVA pacing (p=0.003 and p=0.005, respectively) (Figure 5.2). SLD and MaxDiff were *not* significantly different between the AAI and RVA pacing modes. Systolic XCD had the greatest percent increase from AAI to RVA pacing (91% increase versus 57% for Ts-SD).

NSR versus RVA

Systolic XCD was the only parameter that was significantly different between NSR and RVA pacing modes (Figure 5.2 and Table 5.3).

Diastolic Dyssynchrony

Acute RVA pacing *did not* create diastolic dyssynchrony. Diastolic XCD did not change between the three pacing modes (p = 0.285) (Figure 5.2 and Table 5.3).

Whole-cycle Dyssynchrony

Whole-cycle XCD was not significantly different between any of the pacing modes (p = 0.079).

ROC Analysis

Ts-SD and systolic XCD were the only dyssynchrony parameters that showed significant discrimination between AAI and RVA pacing modes (Table 5.4 and Figure 5.3). Systolic XCD had an area under the ROC curve that was significantly greater than SLD. Systolic XCD had the highest sensitivity and specificity of 79% to diagnose dyssynchrony, compared with 57%, 57% and 71% SLD, MaxDiff and Ts-SD, respectively (Table 5.4).

Table 5-4: ROC comparison of dyssynchrony parameters.

Parameter	p*	Area under the ROC curve†	Standard error‡	ROC Threshold	Sensitivity§	Specificity§|
SLD	0.783	0.53 (0.31, 0.75)	0.11	82 ms	57%	57%
MaxDiff	0.081	0.69 (0.49, 0.90)	0.10	106 ms	57%	57%
Ts-SD	0.004	0.82 (0.67, 0.98)	0.08	60 ms	71%	71%
Whole-cycle XCD	0.854	0.52 (0.28, 0.76)	0.12	17 ms	50%	57%
Systolic XCD	0.006	0.81 (0.61, 1.00)	0.10	86 ms	79%	79%
Diastolic XCD	0.112	0.39 (0.17, 0.61)	0.11	12 ms	36%	36%

*Null hypothesis: area under the ROC curve = 0.5 (no discriminatory value). †Asymptotic 95% confidence interval given in parentheses. ‡Under the nonparametric assumption. §For diagnosing dyssynchrony due to right ventricular apex pacing.

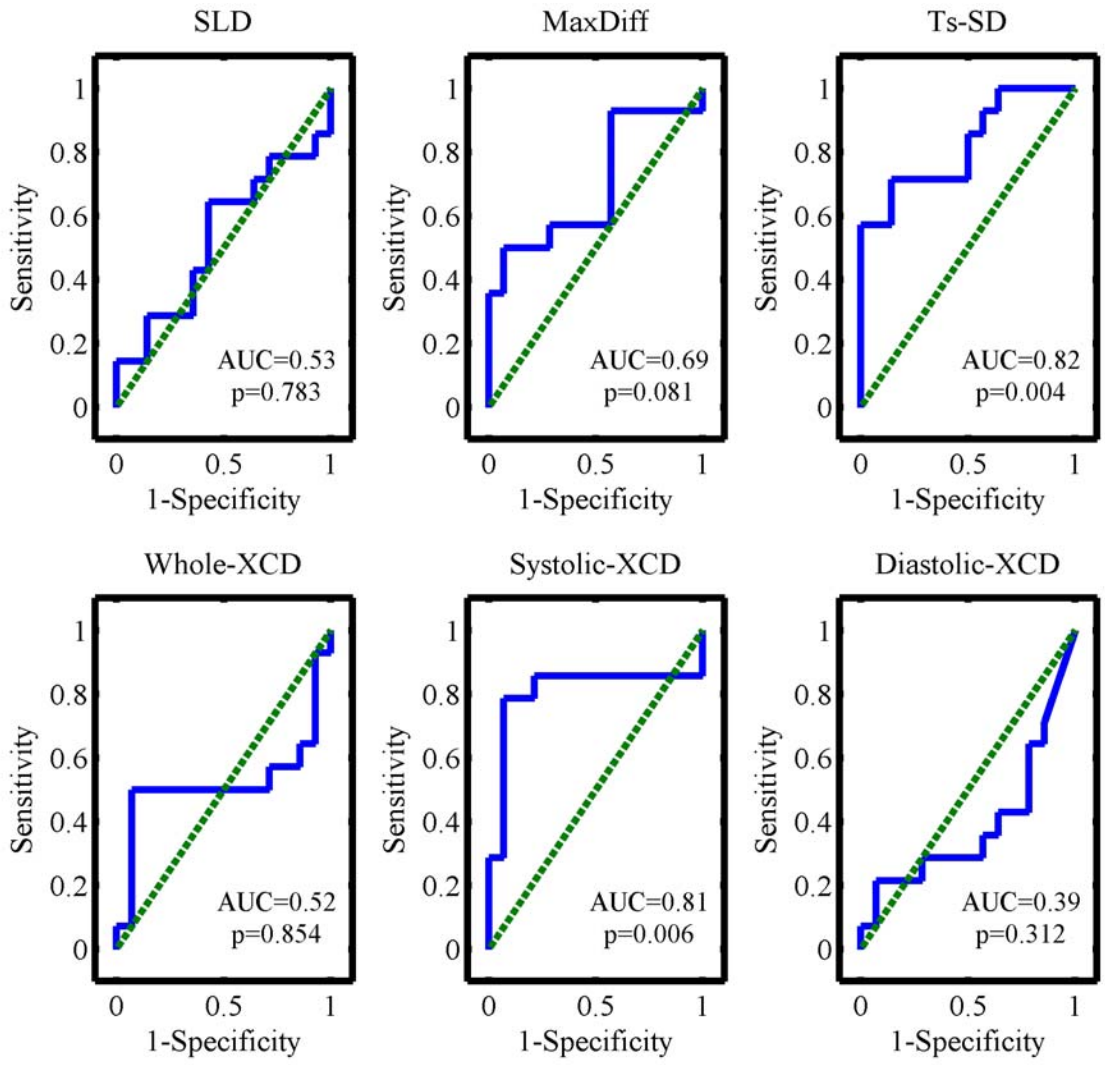

Figure 5.3: Systolic XCD shows significant discrimination between AAI and RVA.

Discussion

We sought to develop and test a new parameter to quantify dyssynchrony in the heart that does not rely on identification of peak myocardial velocities. We developed three parameters which all utilize a cross-correlation function and calculated the systolic, diastolic or whole-cycle dyssynchrony between velocity curves from opposing ventricular walls. We demonstrated two important results:

(1) Cross-correlation delay analysis of myocardial velocity curves is superior to existing parameters for quantitatively assessing dyssynchrony in this model of pacing-induced dyssynchrony in the human heart. Systolic XCD showed the largest increase from normal synchrony (AAI) to pacing-induced dyssynchrony (RVA) and had the highest sensitivity and specificity for discriminating between AAI and RVA.

(2) Acute right ventricular apex pacing creates systolic dyssynchrony with preserved diastolic synchrony.

Dyssynchrony Assessment to Identify Responders to CRT

The most widely-used application of dyssynchrony parameters is selection of patients who respond favorably to CRT[7]. Identification of these "responders" to CRT is important, as one-third of patients selected for CRT show no improvement[5]. Several studies have shown that responders to CRT have a high degree of mechanical dyssynchrony while non-responders do not[7].

However, the discrimination of responders from non-responders is complicated by additional factors such as heart failure etiology, scar burden, lead placement, gender and mitral regurgitation[64, 65]. Accurate quantification of dyssynchrony is essential for quantifying the influence of these additional factors in predicting response to CRT. We developed a new, more quantitatively sophisticated dyssynchrony parameter and showed its superiority to existing parameters in diagnosing dyssynchrony in a pacing-induced model of dyssynchrony.

Pacing-induced Dyssynchrony

Patients with non-preexcited supraventricular tachycardia represent a unique population with structurally normal hearts in which it is possible to conduct well-controlled acute dyssynchrony experiments in humans. We acutely paced the right ventricular apex at rates slightly above the intrinsic heart rates in order to create a "pacing-induced dyssynchrony."

Wyman *et al* used tagged MRI to prove that RVA pacing in a canine model creates a mechanical dyssynchrony in the left ventricle[59]. The authors determined that the inter-ventricular septum is rapidly activated during RVA pacing, perhaps due to limited, local activation of the Purkinje system. Purkinje activation did not spread beyond the septum, as the rapid septal activation was followed by a slower spread of mechanical activation towards the left ventricular free wall at a rate similar to values reported for electrical conduction through the myocardium[59]. This provides evidence that RVA pacing creates a dyssynchrony that should be quantifiable using standard echocardiographic

dyssynchrony parameters. We documented this dyssynchrony in RVA pacing using existing parameters and our new XCD parameters. Systolic XCD showed better discrimination between synchronous and dyssynchronous activation than the standard dyssynchrony parameters.

Diastolic Function During Ventricular Pacing

Ventricular pacing acutely impairs diastolic function by increasing the time constant of relaxation,[66-68] decreasing the peak lengthening rate[68] and decreasing peak negative dP/dt.[68, 69] Thus, one might hypothesize that acute RVA pacing would cause diastolic dyssynchrony. However, our results show that acute RVA pacing does *not* affect diastolic synchrony.

Our results can be explained by a discussion of the predominant factors which control relaxation in the heart. Diastolic relaxation is controlled both by the sensitivity of the contractile system to the prevailing load (load dependence) and the decaying activation (inactivation dependence).[70] Several energy-dependent processes (such as the detachment of actin from myosin and sequestering of calcium into the sarcoplasmic reticulum) determine the inactivation dependence of the ventricle.[71] This inactivation-dependent control mechanism modulates the load-dependent control, which is dominant during early diastolic relaxation.[72] This early-diastolic load dependence enables the fibers to elongate instantaneously in unison during early diastole *despite* potentially inhomogeneous, or dyssynchronous, activation.[72] Thus, dyssynchronous activation of healthy myocardium where the load dependence of relaxation is maintained leads to

systolic dyssynchrony with preserved diastolic synchrony.

Diastolic Dyssynchrony

While most studies on dyssynchrony have focused on systole, diastolic dyssynchrony is more frequent than systolic dyssynchrony in dilated cardiomyopathy.[73, 74] In addition, diastolic dyssynchrony has been reported in other cardiovascular diseases such as hypertrophic cardiomyopathy.[75] Thus, evaluation of diastolic synchrony may be important, and few studies have investigated this phenomenon.

This is the first study to demonstrate the effect of acute RVA pacing on *diastolic* synchrony in structurally normal human hearts. We demonstrated that acute RVA pacing does *not* affect diastolic synchrony despite the large increase in systolic dyssynchrony. Our results suggest that systolic and diastolic dyssynchrony develop through separate mechanisms. This finding is corroborated by a recent study on 373 patients with congestive heart failure in which isolated diastolic dyssynchrony was present in 18% of patients and isolated systolic dyssynchrony was present in 30% of patients.[76] Other studies have also shown a lack of correlation between systolic and diastolic dyssynchrony.[77] Thus, systolic and diastolic dyssynchrony do not appear to be tightly coupled and potentially develop through separate mechanisms.

In contrast to systolic dyssynchrony, diastolic dyssynchrony in heart failure may develop over a longer duration. A recent study by Kang *et al* compared patients with acquired LBBB to patients with RV pacemakers and normal function.[77] The RV-paced patients had a low amount of diastolic dyssynchrony that was comparable to that of the

patients with acquired LBBB and normal EF. However, patients with LBBB and low EF (<35%) had nearly three times the level of diastolic dyssynchrony compared to patients with LBBB and normal EF. The authors concluded that conduction system disease alone cannot induce diastolic dyssynchrony, and pathology of the myocardium may be the cause of both diastolic dyssynchrony and LV systolic dysfunction.[77] Our results further support the hypothesis that conduction system disease alone cannot induce diastolic dyssynchrony by showing that diastolic dyssynchrony does not develop during acute dyssynchronous activation of the LV (which is a model for LBBB conduction system disease).

Dyssynchronous electrical activation of the LV leads to pathological changes in the myocardium,[78] which may be the cause of diastolic dyssynchrony. Dyssynchronous activation induces hypertrophy of the LV wall in late activated regions both in dogs[79] and in humans with congenital complete heart block and pacing-induced dyssynchrony.[80] LV mass index correlates with diastolic dyssynchrony in patients with heart failure and normal ejection fraction.[74] Therefore, the hypertrophy due to long-term dyssynchronous activation in the LV may play an important role in causing diastolic dyssynchrony in heart failure.

The process of calcium binding and uptake is also disturbed in the failing myocardium.[81, 82] This may alter the load sensitivity following the isovolumic relaxation period since efficient calcium sequestering in the sarcoplasmic reticulum is required to generate the early diastolic load dependence.[72] Thus, regional inhomogeneities in the failing heart may lead to diastolic dyssynchrony due to the changes in early diastolic load

dependence.

Conflicting Studies

There are two studies that conflict with our results. First, Betocchi *et al* found that acute ventricular pacing increases diastolic dyssynchrony relative to atrial pacing in patients with coronary artery disease.[83] However, in this patient group, early onset of lengthening may occur in hypoxic muscle supplied by partially occluded coronary arteries.[84, 85] In addition, hypoxia suppresses the load dependence of relaxation,[72] suggesting that patients with coronary artery disease may have a different response to acute pacing relative to the healthy patients in our study.

Aoyagi *et al* reported that diastolic dyssynchrony increased from 12 ± 4 during right atrial pacing to 27 ± 6 during RVA sequential pacing in 7 open-chest dogs.[66] This study only examined dyssynchrony between 3 segments on the anterior wall as opposed to our study in which we examined dyssynchrony from all 6 walls of the LV. Also, we quantified dyssynchrony using cross-correlation methodology which is potentially more accurate in identifying dyssynchrony than time to peak analysis[86] such as that employed by Aoyagi *et al*.

Systolic Dyssynchrony

Systolic dyssynchrony appears to be an acute effect of dyssynchronous activation. Our study and previous studies[59, 87, 88] have shown that systolic dyssynchrony is acutely

created by RVA pacing. Conduction system disease in patients with congestive heart failure can also lead to systolic dyssynchrony and worsened LV function which can be treated with cardiac resynchronization therapy (CRT) utilizing biventricular pacemakers.[7] CRT acutely reduces systolic dyssynchrony,[8,9] and the reduction can be reversed immediately when the pacemaker is turned off.[9] Thus, LV systolic dyssynchrony is an acutely-induced, reversible consequence of dyssynchronous activation.

ROC Thresholds Relative to Previously Determined Thresholds for SLD, MaxDiff and Ts-SD

We defined threshold levels of dyssynchrony to discriminate between AAI pacing and RVA pacing at the same heart rate. Our results are different from published threshold values for SLD, MaxDiff and Ts-SD in adults (82 versus 60ms[8], 106 versus 65ms[34], and 60 versus 34.4ms[36], respectively). This difference may in part be due to heart rate as we normalized by the square root of the R-R interval while studies in adults typically do not do this (un-normalized threshold values would be approximately 67, 86, and 49 ms for SLD, MaxDiff and Ts-SD, respectively). However, heart rates in adults are typically close to 60 bpm while heart rates in the children in this study ranged from 60 to nearly 150 bpm, so we thought it was important to normalize. This is the first study to determine these thresholds in pediatric patients.

CRT in Pediatrics

CRT is now being used in a limited number of pediatric patients with dilated cardiomyopathy[90]. While CRT has shown extremely promising results in adults, the translation of this success into the pediatric population is complicated by the heterogeneity of the underlying cardiac defects. To date, there is little or no evidence-based medicine to prove the benefit of CRT in pediatric patients. Existing evidence is in the form of case reports and case series[90] with no prospective multi-center trials completed or ongoing.

A critical first step in translation of CRT into pediatrics is identifying a population of patients who have a high likelihood of responding to the treatment. The current study provides a noninvasive measure to diagnose dyssynchrony in pediatric patients that is superior to similar measures used in adults. This may help identify pediatric patients who will respond favorably to CRT.

The absence of diastolic dyssynchrony in this acute pacing model also has implications for the young patient who requires life-long ventricular pacing. If diastolic dyssynchrony is indeed a long-term sequela of dyssynchronous ventricular activation, then young patients who receive life-long RVA pacing may develop a "pacing-induced diastolic dyssynchrony." Further investigation into this area may have implications for choosing biventricular pacing over RVA pacing to treat these young patients.

Limitations

The patients in this study underwent an invasive cardiac procedure involving catheter ablation, which may have an unknown effect on structure and/or function. However, we documented normal cardiac structure and function with 2-dimensional echocardiography and 12-lead electrocardiography following ablation of the arrhythmia substrate. The patients also served as their own controls, which should minimize any effect the procedure had on the data.

We paced patients for 1 minute before acquiring tissue Doppler images to assess dyssynchrony. We did not pace patients for a longer duration in order to minimize the length of the catheterization procedure. Diastolic dyssynchrony may develop after a longer duration of pacing. However, multiple studies have documented the acute decline in systolic and diastolic *function* due to RVA pacing after only 15-30 seconds.[66, 68] Thus, we felt it was important to also document the effect of ventricular pacing on diastolic dyssynchrony after a similar duration of 1 minute prior to exploring the longer-term effects.

This study is limited by a small sample size (14 patients). However, the sample size was large enough to show statistical differences in systolic dyssynchrony between pacing modes.

RVA pacing was performed in VVI mode, which de-synchronizes the atria and ventricles. We chose VVI over AV synchronous pacing to ensure that conduction from the atria through the AV node did not occur during RVA pacing. This atrio-ventricular de-synchronization may affect LV diastolic synchrony. However, we found no difference

in LV diastolic synchrony between AAI and VVI-RVA pacing modes. Thus, if atrio-ventricular de-synchronization does affect diastolic synchrony, the effect is very small.

Conclusions

We developed a new parameter (XCD), which utilizes a cross-correlation function to analyze data from the entire cardiac cycle for quantifying systolic, diastolic or whole-cycle mechanical dyssynchrony in the heart. We compared XCD to existing dyssynchrony parameters in a model system of pacing-induced dyssynchrony in structurally normal human pediatric hearts. Our results demonstrated that XCD analysis of myocardial velocity curves is a more robust method for quantifying dyssynchrony than "time-to-peak" analyses used in the calculation of existing parameters. Using both our new parameters and existing dyssynchrony parameters, we showed that acute right ventricular apex pacing creates systolic dyssynchrony with preserved diastolic synchrony.

CHAPTER 6

AIM 4: DEVELOP AND EVALUATE A NEW METHOD FOR QUANTIFYING LEFT VENTRICULAR INTERNAL FLOW FROM STANDARD CINE CARDIAC MAGNETIC RESONANCE IMAGES

Introduction

Specific Aim 4 focuses on achieving the 2nd objective of this dissertation (develop a non-invasive method to quantify internal flow within the LV as a measure of dyssynchrony). The development and validation of cross-correlation methodology in Specific Aims 1-3 focused on improving the quantification of dyssynchrony using tissue Doppler data that is routinely available. However, Aim 4 focuses on a different approach to quantification of dyssynchrony based on the dyssynchrony in blood flow.

The presence of left ventricular (LV) dyssynchrony increases mortality[91], and dyssynchrony can be effectively treated with cardiac resynchronization therapy (CRT) utilizing a biventricular pacemaker[5]. Surface electrocardiogram QRS duration remains the only accepted clinical measure of LV dyssynchrony for identifying patients who need CRT, but sensitivity[92] and specificity[7] are low (~50-60%). Thus, better methods to quantify LV dyssynchrony are needed.

Mechanical dyssynchrony creates abnormal displacement of blood *within* the LV, between early-activated regions and late-activated regions[10, 11]. This internal flow, or "sloshing," represents wasted energy due to dyssynchronous motion of the LV walls.

Quantification of internal flow may represent a better method to diagnose the presence and physiologic severity of dyssynchrony that could be used to identify patients who need treatment with CRT.

LV internal flow has been quantified from regional volume measurements made with a conductance catheter[11]. However, catheter-based quantification of internal flow is an invasive and expensive procedure. We *hypothesized* that: 1) LV internal flow can be quantified *non*-invasively using standard cine cardiac magnetic resonance (CMR) images and 2) CMR-based internal flow will be significantly increased in patients undergoing CRT compared to healthy, normal controls.

Materials and Methods

CMR images were obtained from 10 patients (age 64 ± 14 years, 6 Male) being evaluated for treatment with CRT. Inclusion criteria were New York Heart Association class III or IV heart failure, LV ejection fraction <35%, and QRS >150ms. CMR images were also obtained from 10 healthy volunteers (age 30 ± 7 years, 9 Male) with no history of cardiac disease, normal 12-lead electrocardiography and normal CMR. The study was approved by the institutional review board, and all subjects gave informed consent prior to enrollment.

Image Acquisition

Steady-state free procession short-axis cine images were acquired during 10-15

second breath-holds with a 1.5T Philips Intera scanner using a 5-element phased array cardiac coil (Philips Medical Systems, Best, Netherlands). Contiguous 8-10mm short axis slices were acquired at 20 frames per cardiac cycle. Acquisition parameters were as follows: acquired matrix size = 192 x 256, reconstructed matrix size = 256 x 256, field of view = 370 mm, flip angle = 65^0, TR = 4 msec, and TE = 2 msec. Two-chamber and four-chamber SSFP long-axis cine images were also acquired.

Quantification of Internal Flow

Calculation of internal flow required three main steps: 1) three-dimensional reconstruction of the LV cavity from the two-dimensional CMR images (Figure 6.1A), 2) segmentation of the LV cavity into regional volumes (Figures 6.1B and 6.2), and 3) quantification of internal flow from the regional volume versus time curves. These steps are described in separate sections below.

Three-dimensional Reconstruction of the Left Ventricular Cavity

Image processing was performed in MatLab (version 7.40, The MathWorks, Natick, MA). The endocardial surface was detected in each image with a semi-automated level set approach[93]. The short-axis images were registered to the 2-chamber long-axis images to correct for differences in the level of the diaphragm during end-expiration breath-hold acquisitions. A three-dimensional LV endocardial surface was created from the endocardial border points identified on the CMR images (Figure 6.1A). The aortic

outflow tract was excluded from analysis.

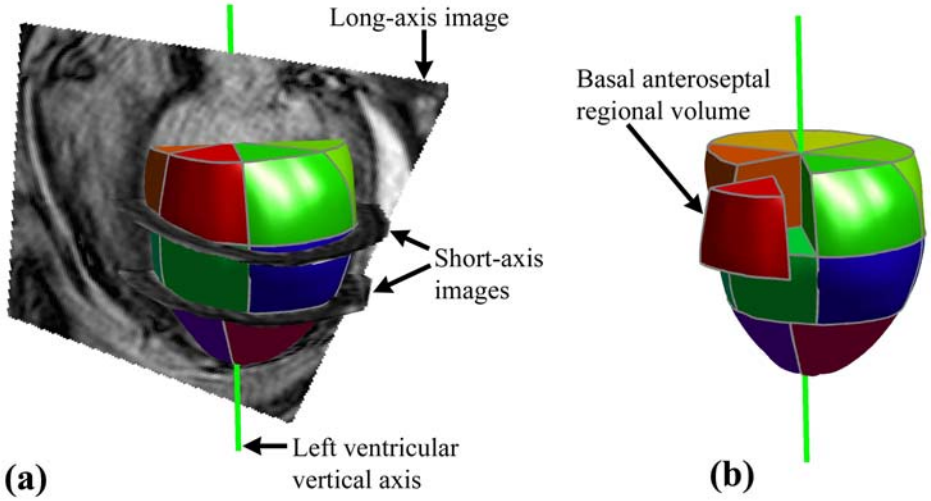

Figure 6.1: 3-D endocardial surface of the LV divided into 16 regional volumes.

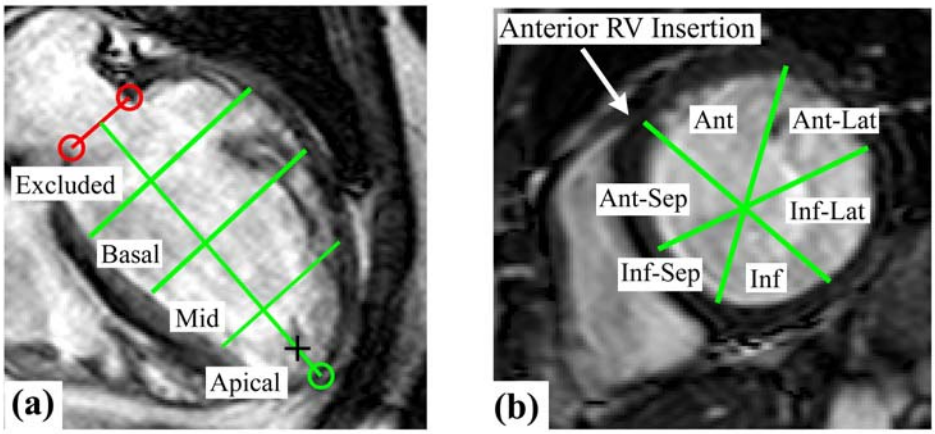

Figure 6.2: Segmentation of the LV cavity into 16 regional volumes.

Segmentation into Regional Volumes

The three-dimensional LV endocardial surface was divided into 16 wedge-shaped regional volumes according to the American Heart Association standardized segmentation model for the left ventricle[43] (Figures 6.1 and 6.2). This standardized segmentation model consists of 6 wedge-shaped 60^0 regional volumes at the basal and mid-wall levels and 4 wedge-shaped 90^0 regional volumes at the apex.

A vertical axis from the center of the mitral annulus to the apex was defined on both the 2-chamber and 4-chamber long-axis images. The center of the mitral annulus was defined as the midpoint of the 2 manually identified leaflet insertion points (shown as red circles in Figure 6.2A). To define the apex, a line was drawn from the center of the mitral annulus through the center of the bottom 15% of the endocardial border points on each long-axis image (shown as a black "+" sign in Figure 6.2A). This line was extended beyond the endocardial border and its intersection with the endocardium was defined as the apex (shown as a green circle in Figure 6.2A). This vertical axis was defined for each time frame in the cardiac cycle. The LV vertical axis was defined as an average of the 2-chamber and 4-chamber vertical axes for each time frame. The vertical axis was then used to define basal, mid-wall, and apical longitudinal locations after excluding the outflow tract as shown in Figure 6.2A.

The anterior right ventricular insertion point was defined on an end-diastolic basal short-axis image (Figure 6.2B). A plane passing through this right ventricular insertion point and the mean vertical axis (the mean of the vertical axes from each time frame) was defined. This plane was rotated 60^0 around the vertical axis and again rotated 120^0 to

define the 6 wedge-shaped regional volumes at each of the basal and mid-wall locations. The same plane was rotated 15^0 and 105^0 to define the 4 wedge-shaped regional volumes at the apex.

Internal Flow Calculation

The volume of each wedge-shaped region was calculated for each time step to generate the 16 regional volume versus time curves. The regional volume curves were smoothed with a Gaussian kernel (length = 5, standard deviation = 1). Internal flow was calculated from these 16 regional volume curves.

Internal flow within the LV decreases volume in one region of the ventricle while simultaneously increasing volume in an adjacent region. This flow results in *no net change* in the global LV volume. Thus, for each time step in the cardiac cycle, the sum of the absolute value of the changes in the regional volumes is *not* equal to the absolute value of the change in the global volume if internal flow has occurred during that time step. Therefore, we defined internal flow as[11]:

$$IF(t) = \frac{\sum_i |\Delta V_i(t)| - |\Delta V_{LV}(t)|}{2} \tag{6-1}$$

where $IF(t)$ is the volume of internal flow at time t, $V_i(t)$ is the volume of segment i at time t, and $V_{LV}(t)$ is the volume of the entire LV at time t:

$$V_{LV}(t) = \sum_i V_i(t) \tag{6-2}$$

Note that division by 2 in equation (1) accounts for the fact that any blood which exits one regional volume must enter another regional volume if it does not leave the LV. Internal flow *fraction* (IFF) was defined as the total internal flow divided by the stroke volume. IFF was calculated in systole ($IFF_{systole}$), diastole ($IFF_{diastole}$) and over the entire cardiac cycle (IFF_{whole}). End-systole and end-diastole were defined as the times when the LV volume reached a minimum and maximum, respectively. Stroke volume was defined as the difference between end-diastolic volume and end-systolic volume.

Statistics and Data Analysis

$IFF_{systole}$, $IFF_{diastole}$ and IFF_{whole} were compared between the normal controls and the patients using an unpaired student's t-test. A value of $p < 0.05$ was defined as statistically significant. A threshold value of IFF to discriminate between patients and controls was defined as the value which gave a maximum sum of sensitivity and specificity.

Relationship with Tissue Doppler Dyssynchrony Parameters

Cross-correlation delays and time-to-peak dyssynchrony parameters were quantified in the patients and normal controls as described in Aim 1 (with a stationary, 30x6 oval region of interest). Each internal flow fraction parameter (whole, systolic and diastolic) was plotted against the corresponding cross-correlation delay for each patient and normal control. In addition, $IFF_{systole}$ and IFF_{whole} were plotted against each of the

time-to-peak parameters to determine whether they correlated.

Inter-observer Reproducibility

To assess inter-observer reproducibility, two independent observers each performed complete internal flow analysis including endocardial border detection and identification of mitral leaflet insertion points on 5 randomly selected patients and 5 randomly selected normal controls.

Table 6-1: Cardiac function in the patients and normal controls.

Variable	Patients	Normal Controls	p Value*
QRS Duration (ms)	193 ± 28	92 ± 10	<0.001
Volumes			
Left ventricular end-systolic volume (ml)	195 ± 97	48 ± 12	<0.001
Left ventricular end-diastolic volume (ml)	263 ± 101	128 ± 26	<0.001
Left ventricular ejection fraction (%)	29 ± 11	63 ± 5	<0.001

Values are means ± standard deviation, n = 10 for each group. *p value from unpaired t-test.

Results

The patients had prolonged QRS durations, increased ventricular volumes, and reduced ejection fractions compared to the normal controls (Table 6.1). IFF_{whole}, $IFF_{systole}$ and $IFF_{diastole}$ were significantly increased in the patients ($p<0.001$ versus the normal controls for all comparisons) (Figure 6.3). IFF_{whole} values for each patient and normal control are shown in Figure 6.4. An IFF_{whole} threshold of 4% discriminated between

patients and normal controls with 90% sensitivity and 100% specificity (Table 6.2). Threshold values of $IFF_{systole}$ and $IFF_{diastole}$ to discriminate between patients and controls are reported in Table 6.2.

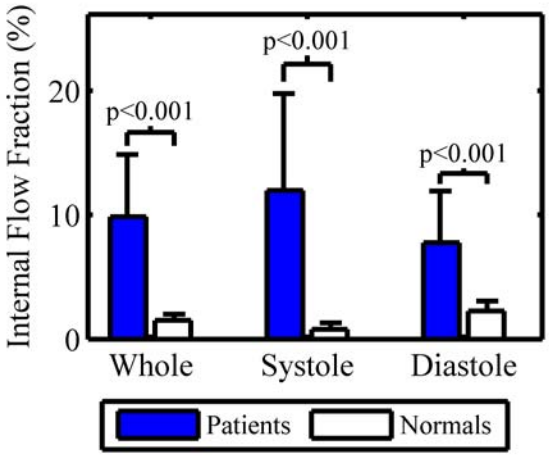

Figure 6.3: Internal flow is significantly increased in patients with dyssynchronous heart failure.

Table 6-2: Discrimination between the patients and normal controls using IFF.

Variable	Threshold*	Sensitivity	Specificity
IFF_{whole}	4%	90%	100%
$IFF_{systole}$	2%	100%	100%
$IFF_{diastole}$	4%	90%	100%

Values are means ± standard deviation, n = 10 for each group. *Threshold values determined as the level where the sum of sensitivity and specificity was maximal.

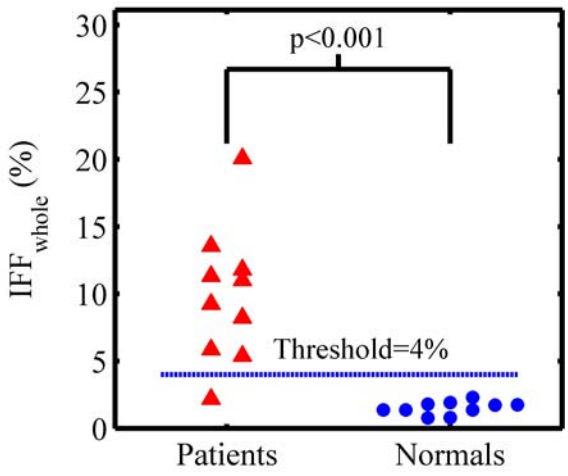

Figure 6.4: IFF_{whole} discriminates patients from normal controls with 95% accuracy.

Figure 6.5 shows regional volume curves from a representative patient and a normal control. The volume curves are highly uniform in the normal control, representing synchronous motion with all segments reaching minimum volume at approximately the same time. In contrast, the regional volume curves from the patient are highly non-uniform due to the dyssynchronous motion of the LV walls.

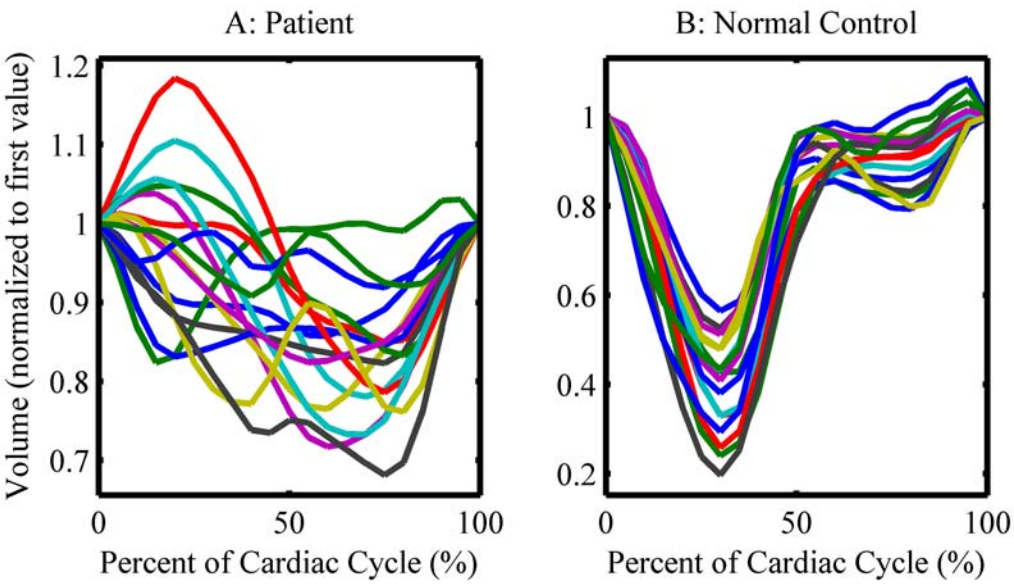

Figure 6.5: LV regional volume curves are significantly more dyssynchronous in the patients compared to the normal controls.

Internal Flow Over the Cardiac Cycle

Internal flow between the septum and lateral wall of a patient is shown in Figure 6.6. The regional volume curves from the 5 regions adjacent to the septum (basal and mid antero- and infero-septal regions and apical septal region) and the 5 regions adjacent to the lateral wall (basal and mid antero- and infero-lateral regions and apical lateral region) were summed to simplify the display. Note that internal flow is occurring when the volume curves in Figure 6.6 slope in opposite directions (marked by the 2 shaded rectangles). In early systole, the volume of blood adjacent to the septum decreases as the septum contracts. Simultaneously, the lateral wall volume is increasing. This volume change represented by curves moving in opposite directions (shaded rectangle on the left) shows internal flow from the early-activated septum towards the lateral wall. In late

systole the opposite occurs as the late-activated lateral wall displaces blood volume back towards the septum. This internal flow does not occur in the normal heart shown in Figure 6.6B.

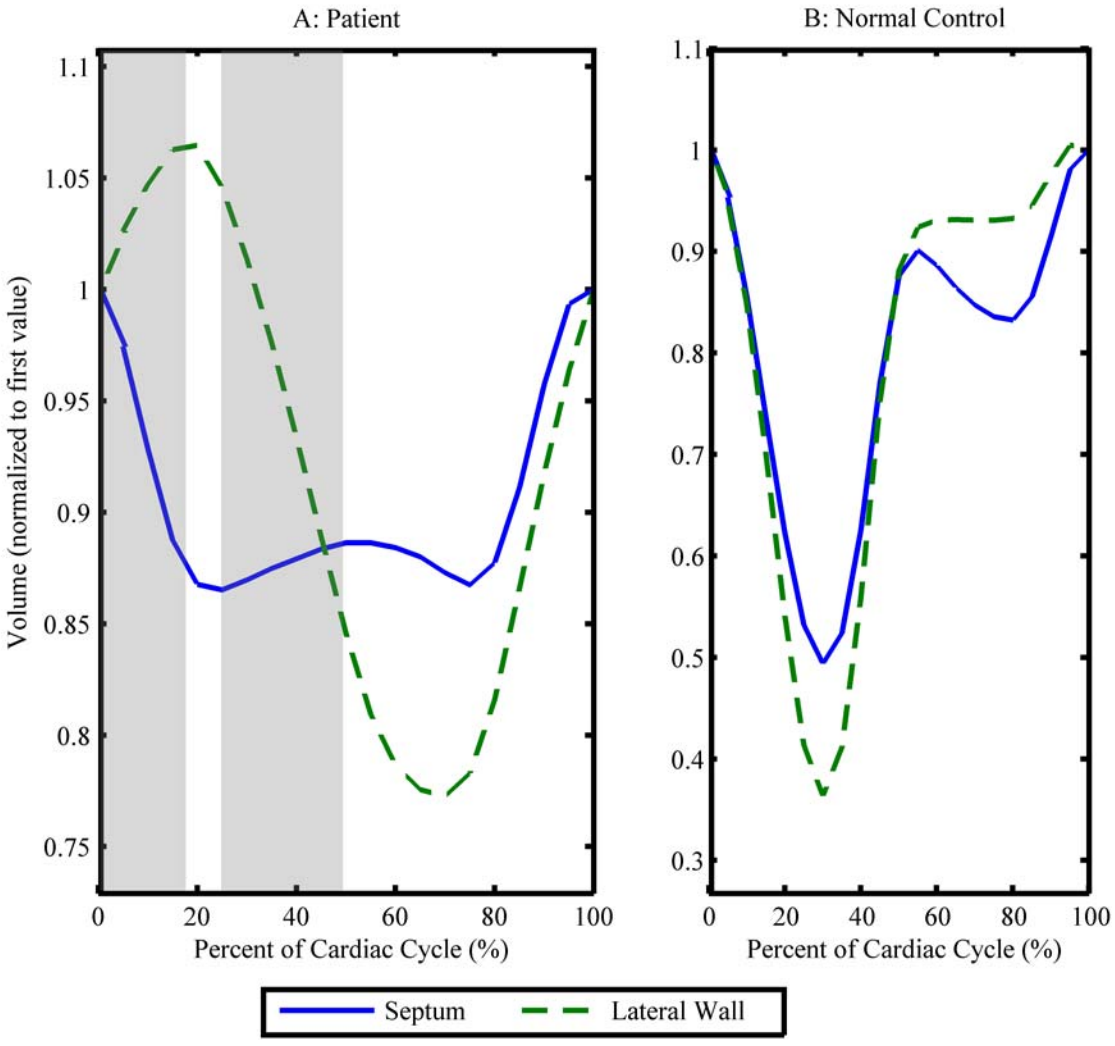

Figure 6.6: Regional volume analysis shows early and late systolic internal flow in a patient that is not present in the normal control.

Systolic and Diastolic Internal Flow

Figure 6.7 shows the mean internal flow in the patients and controls throughout the cardiac cycle. The normal control group had three peaks in internal flow which occurred during isovolumic contraction, isovolumic relaxation, and diastolic filling.

Internal flow in the normals was nearly 3 times greater during diastole ($IFF_{diastole}$ = 2.3 ± 0.8% compared to $IFF_{systole}$ = 0.8 ± 0.5%, $p<0.001$). However, this was not the case in the patients as $IFF_{diastole}$ and $IFF_{systole}$ were not different (7.8% versus 12.0%, p = 0.11).

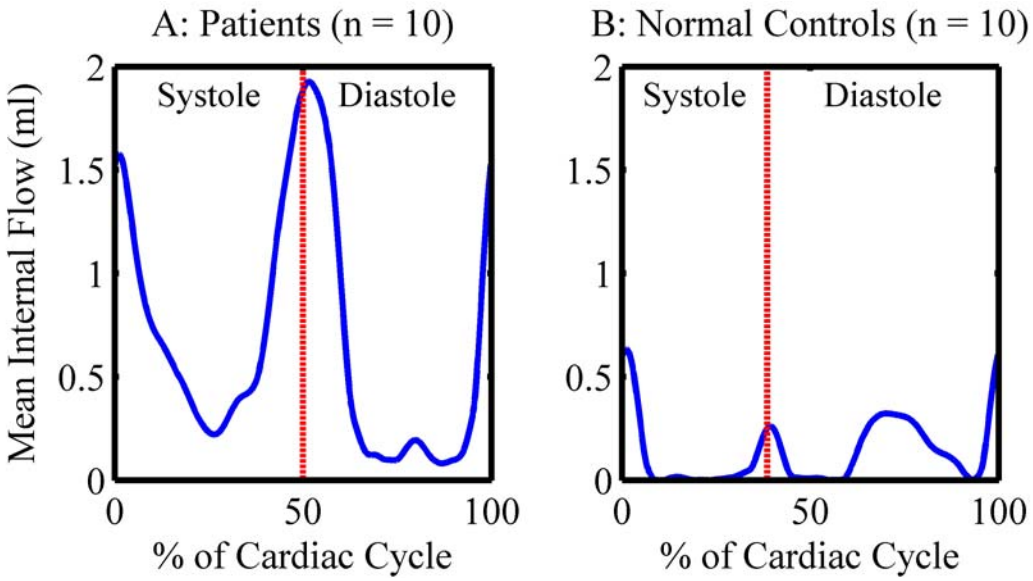

Figure 6.7: Internal flow occurs predominately during diastole in normal controls and during both systole and diastole in patients with dyssynchronous heart failure.

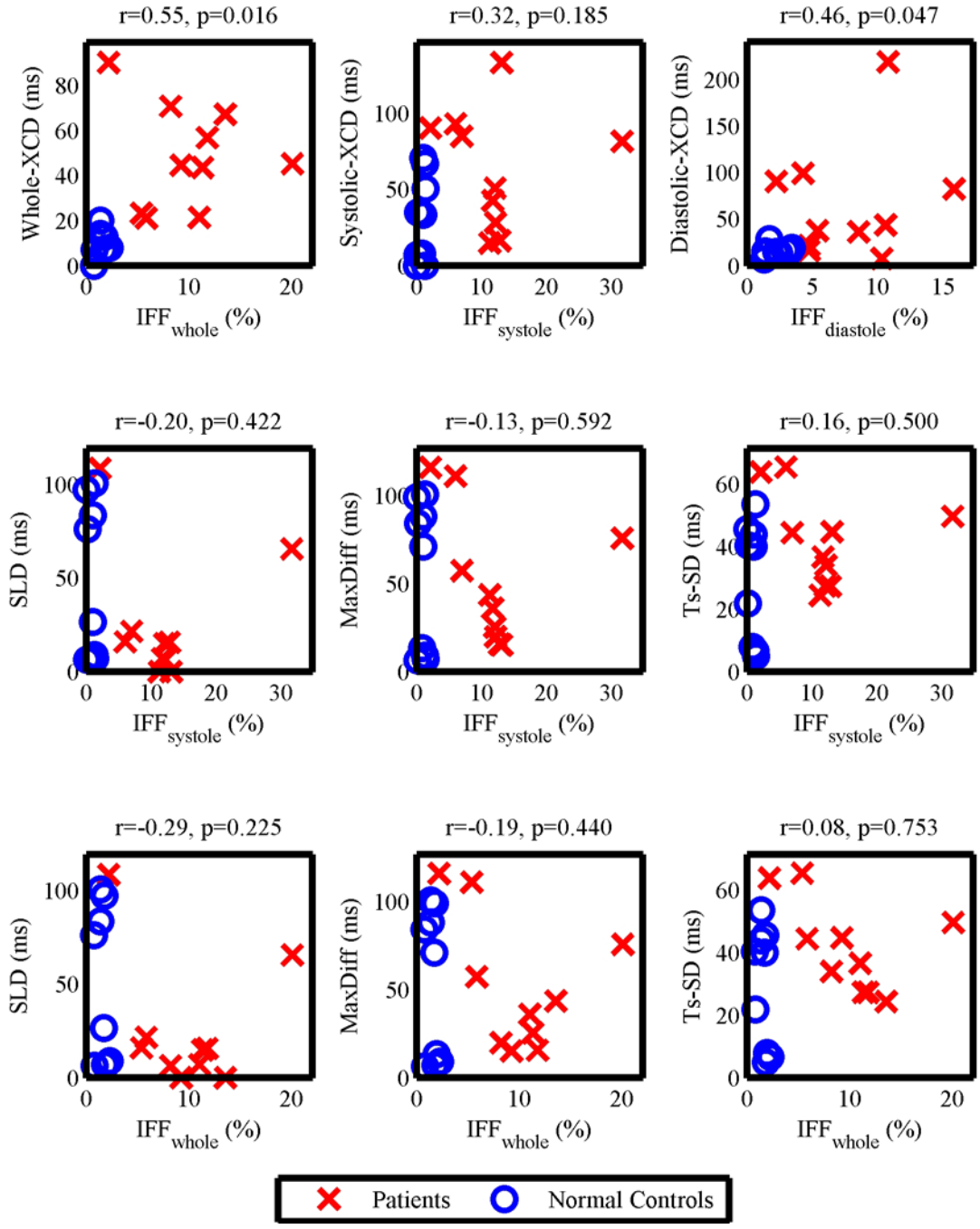

Figure 6.8: XCD correlates weakly with IFF while time-to-peak parameters do not.

Relationship with Tissue Doppler Dyssynchrony Parameters

Correlations between IFF and tissue Doppler dyssynchrony parameters in both the patients and normal controls are shown in Figure 6.8. Whole-cycle XCD correlated weakly with IFF_{whole} ($p = 0.016$). Similarly, diastolic-XCD correlated weakly with $IFF_{diastole}$ ($p = 0.047$). However, systolic-XCD did not correlate with $IFF_{systole}$ ($p = 0.185$). None of the time-to-peak dyssynchrony parameters correlated with either IFF_{whole} or $IFF_{systole}$.

Inter-observer Reproducibility

The mean inter-observer difference ± 2 standard deviations (in units of internal flow fraction i.e. *not* divided by mean values) was 0.7 ± 1.7% for IFF_{whole}, 1.2 ± 2.2% for $IFF_{systole}$ and 0.2 ± 2.5% for $IFF_{diastole}$.

Discussion

This study introduces a new method to quantify internal flow due to left ventricular dyssynchrony *non*-invasively using standard cine cardiac magnetic resonance images. The major findings are: 1) LV internal flow is 6 times greater in patients with dyssynchronous heart failure compared to normal controls, 2) a threshold internal flow fraction of 4% discriminates between patients and controls, and 3) internal flow occurs predominately during diastole in normal controls while it occurs equally during systole and diastole in patients with dyssynchronous heart failure. This is the first study to

quantify LV internal flow non-invasively.

Diagnosing Dyssynchrony in Heart Failure

Ventricular dyssynchrony in heart failure leads to increased morbidity and mortality, which can be reduced with cardiac resynchronization therapy (CRT)[94]. The duration of the QRS on surface electrocardiogram is the only clinically accepted measure for quantifying dyssynchrony, but it has low sensitivity and specificity for identifying patients who will respond to the treatment[7, 92]. Tissue Doppler imaging has shown promise in improving the selection of responders to CRT in small, single-center studies[8, 9, 19, 34, 35]. However, the first multicenter trial using tissue Doppler imaging to predict response to CRT (the PROSPECT study[38]) showed that no echocardiographic parameters could discriminate responders from non-responders[39]. Because of this, new parameters to quantify dyssynchrony are needed. This study demonstrates that CMR-based quantification of internal flow fraction may be a powerful tool in the diagnosis of dyssynchrony, and may be useful in selection of responders to CRT.

Internal flow may represent a more direct measure of cardiac dyssynchrony than existing methods used to quantify dyssynchrony. Steendijk *et al* reported that patients with left bundle branch block had an IFF_{whole} of 78% compared to only 20% in normal controls[11]. This represents a 4-fold difference in patient and normal control values, which is similar to the 6-fold difference seen in our study. However, the values from our study in both patients and normal controls were smaller than the values reported in the study by Steendijk *et al* in which internal flow was quantified from regional volume measurements

made with a conductance catheter. The differences between IFF_{whole} seen in our study and the catheter-based study may be due to the 10-fold higher temporal resolution of the conductance catheter or the more complete volume coverage by CMR. CMR-based quantification of internal flow has the advantage of being entirely non-invasive, while use of a conductance catheter is invasive and expensive.

Internal Flow in Normal Controls

The normal controls in our study showed three peaks in internal flow during: 1) isovolumic contraction, 2) isovolumic relaxation and 3) diastolic filling. The peaks during the isovolumic periods are consistent with normal physiology since the ventricle undergoes shape changes with no global volume change while the valves are closed. Internal flow during the isovolumic periods has also been documented in a previous study[11]. The peak in internal flow during diastole caused $IFF_{diastole}$ to be 3 times greater than $IFF_{systole}$ in the normal controls. Thus, internal flow is a normal component of diastolic filling. Steendijk *et al* found similar results in patients with coronary artery disease and preserved LV function[11].

Methodological Considerations

Nesser *et al* quantified regional ejection fractions with CMR and showed its utility in semi-automated detection of regional wall motion abnormalities[95]. In that study, six long-axis images of the LV rotated in 30^0 steps were used to reconstruct the 3-

dimensional endocardial surface of the LV, which results in gaps between the imaging planes where the endocardial border cannot be defined. We utilized short-axis images to cover the entire LV volume and overcome this limitation. In addition, our methodology utilizes CMR images collected during routine CMR protocols whereas collection of 6 long-axis images is not a standard acquisition protocol.

The methodology used to quantify internal flow in this study could theoretically be applied to 3-dimensional echocardiographic data[96]. However, a recent study showed that 9 out of the 16 standardized regional volumes had significantly different regional ejection fractions by 3-dimensional echocardiography in comparison to CMR[95]. Thus, the endocardial border definition from 3-dimensional echocardiography may not be accurate enough for internal flow quantification.

Other CMR-based methods for imaging myocardial motion and evaluating dyssynchrony include: 1) tagging methods[97-99], 2) displacement imaging methods[100, 101], and 3) velocity mapping methods[102]. However, each of these methods requires a specialized MR pulse sequence and complex post-processing, which limits their widespread use in *clinical* diagnosis of dyssynchrony. The advantage of IFF methodology over these techniques is that it is based on standard cine imaging which is acquired in virtually all CMR exams.

Internal Flow versus Tissue Doppler Dyssynchrony Parameters

We found a weak correlation between IFF and XCD for the whole-cycle and diastolic parameters. However, the systolic parameters did not correlate. In particular,

one patient had nearly zero internal flow with a high whole-cycle XCD (see top left "x" on top left axis in Figure 6.8). This could be explained by an artifact in the images from this patient, which made endocardial border definition extremely difficult and potentially resulted in an incorrect IFF (Figure 6.9).

There are several potential explanations for the lack of correlation between $IFF_{systole}$ and systolic XCD. First, valve timings were used to define the systolic phase for XCD analysis while volume minima and maxima were used to define the systolic phase for IFF analysis. Differences between these timings may have affected the correlation between $IFF_{systole}$ and systolic XCD. In addition, XCD is based entirely on 1-dimensional velocity tracings from three different images of the left ventricle, and may be highly affected by tethering. However, IFF is based on a stack of at least 10 images used to define the precise location of the endocardium at all phases in the cardiac cycle over all locations (not just 3 image planes) and probably represents a more complete, accurate depiction of myocardial contraction.

None of the time-to-peak parameters correlated with either IFF_{whole} or $IFF_{systole}$. However, Steendijk *et al* reported a correlation between SLD and IFF_{whole} in 12 patients with heart failure and intraventricular conduction delay ($p = 0.002$, $r = 0.79$). Further studies with larger numbers of patients will be needed to resolve this discrepancy.

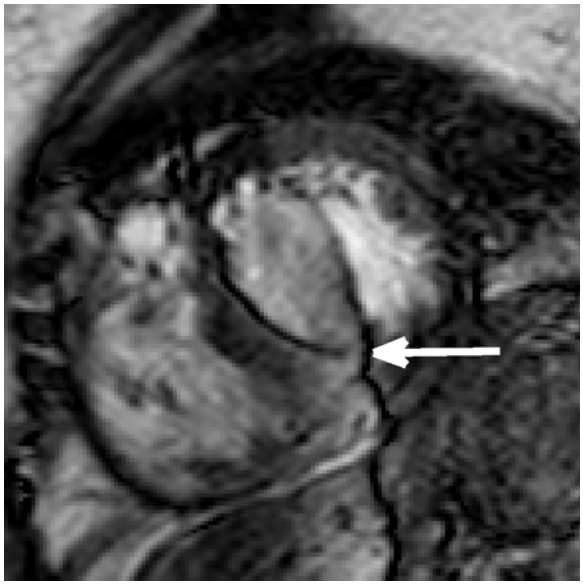

Figure 6.9: An artifact in the images from a patient may have caused inaccurate quantification of internal flow fractions.

Limitations

This study has limitations. The methodology used to calculate IFF is time-consuming, mostly due to the need for accurate LV endocardial border definition. This limits the clinical utility of IFF. However, if IFF continues to show clinical value in future studies, analysis time could be reduced by focusing on automation of the methodology.

This study is limited by a small sample size. However, the sample size was large enough to show statistical differences in IFF between the patients and normal controls. Future studies with larger sample sizes will be required to further characterize the utility of IFF.

Differences in IFF between the patients and normal controls may have been confounded by co-factors such as age, heart rate, stroke volume and LV end-systolic volume. To investigate this, we employed a backwards selection process starting from a complete linear multiple regression model with all potential predictors. Marginally insignificant terms were dropped and the model was refit. IFF_{whole} ($p = 0.04$) and $IFF_{diastole}$ ($p = 0.001$) remained significantly different between the patients and control groups in the model while $IFF_{systole}$ ($p = 0.096$) was confounded by LV end-systolic volume.

We acquired 20 images per cardiac cycle to calculate internal flow. Our methodology assumes that the rate of internal flow was constant between phases, which may not be true. Increasing the number of images acquired per cardiac cycle can only increase the amount of internal flow quantified. Future studies will be needed to determine whether more than 20 images per cardiac cycle are needed to accurately quantify internal flow. However, we have shown that 20 images per cycle is enough to document a large difference in internal flow between the patient and normal control groups.

Conclusions

In conclusion, internal flow in the left ventricle can be quantified *non*-invasively from standard cine cardiac magnetic resonance images. An internal flow fraction of 4% of stroke volume discriminates between patients with dyssynchronous heart failure and normal controls with 95% accuracy. Quantification of left ventricular internal flow from

cardiac magnetic resonance images may be useful in identifying patients who will benefit from cardiac resynchronization therapy.

CHAPTER 7

CONCLUSIONS

Project Summary

The overall goal of this project was to develop better methods to diagnose dyssynchrony in the left ventricle (LV). We developed and evaluated two new methods based on different approaches with different imaging modalities. The first method improved upon existing tissue-Doppler based diagnosis of dyssynchrony by utilizing a cross-correlation (XC) function to quantify dyssynchrony during post-processing as opposed to the quantitatively simplistic "time-to-peak" analysis that is currently utilized. The second method utilized standard cine cardiac magnetic resonance (CMR) images to quantify the dyssynchrony in the flow of blood within the left ventricle, which may represent a more direct, physiologically relevant measure of dyssynchrony.

The purpose of specific aim 1 was to quantify the effect of region of interest tracking on the diagnosis of LV dyssynchrony from tissue Doppler images. Region of interest tracking of the myocardium is rarely performed during tissue Doppler post-processing, but the effect of using a stationary region of interest had never been evaluated. The analysis was conducted in 18 patients who satisfied CRT enrollment criteria (ejection fraction < 35%, QRS > 120, class III/IV drug-refractory heart failure). The XC delay parameters were compared to 3 time-to-peak parameters: septal-to-lateral delay in time-to-peak (SLD), maximum difference in the basal 2- or 4-chamber times-to-

peak (MaxDiff) and standard deviation of the 12 basal and mid-wall times-to-peak (Ts-SD). This aim demonstrated that XC delays could be accurately quantified with a stationary region of interest while the time-to-peak parameters showed poor agreement between tracked and stationary analysis.

The purpose of specific aim 2 was to evaluate the ability of XC delays to diagnose dyssynchrony in positive and negative control groups. The analysis was conducted in 11 positive control subjects (age 68±14) and 12 normal volunteers (age 29±7). Positive controls were patients who responded to CRT (greater than a 15% reduction in LV end-systolic volume 3 months after implantation). The XC delay parameters were again compared to SLD, MaxDiff and Ts-SD. All of the XC delay parameters and Ts-SD showed significant discrimination between the positive and negative control groups by ROC analysis ($p<0.01$ for all). SLD and MaxDiff did *not* show significant discrimination between the positive and negative control groups ($p=0.712$ and $p=0.056$, respectively). Threshold values to diagnose dyssynchrony using each XC delay parameter were generated from the ROC analysis. A whole-cycle XCD of 25 ms discriminated between the positive and negative control groups with 100% sensitivity and specificity. A systolic XCD of 53 ms discriminated the groups with a sensitivity of 73% and a specificity of 75%, while a diastolic XCD of 22 ms discriminated the groups with 91% sensitivity and 92% specificity. The time-to-peak parameters showed dyssynchrony in a large percentage of the negative control group (42%, 50%, and 58%, respectively for SLD, MaxDiff and Ts-SD), while the XC delay parameters showed dyssynchrony in 0, 25 and 8% of the normal control group, respectively, for whole-cycle, systolic, and diastolic XCD. It was concluded that XC delays are superior to existing time-to-peak dyssynchrony parameters

at discriminating patients with LV dyssynchrony from subjects with normal function.

The purpose of specific aim 3 was to evaluate the ability of XC delays to diagnose acute "pacing-induced dyssynchrony" in structurally normal pediatric hearts. The analysis was conducted in 14 patients (age 13±4 years) undergoing catheter ablation for non-preexcited supraventricular tachycardia. Tissue Doppler images were acquired during normal sinus rhythm (NSR) and right atrial (AAI) and right ventricular apex (RVA) pacing. This enabled evaluation of dyssynchrony parameters in a state of dyssynchrony (RVA) compared to normal synchrony (AAI and NSR). XC delay parameters were again compared to the time-to-peak parameters SLD, MaxDiff and Ts-SD. Systolic XCD was the only parameter that showed a significant increase in dyssynchrony between RVA pacing compared to AAI ($p = 0.031$) and NSR ($p = 0.005$). Ts-SD showed a significant difference between RVA and AAI ($p = 0.003$) but not between RVA and NSR ($p = 0.095$). Threshold values to diagnose dyssynchrony in pediatric patients were developed for the time-to-peak parameters and the XC delay parameters from the ROC analysis. Systolic XCD had the highest sensitivity and specificity (79%) to discriminate between RVA and AAI pacing modes. SLD, MaxDiff and Ts-SD had a sensitivity and specificity of 57, 57, and 71%, respectively. Therefore, we concluded that systolic XCD was superior to time-to-peak parameters for diagnosing dyssynchrony in this model of acute RVA pacing. This data also demonstrated that the normal, healthy left ventricle has an inherent ability to preserve diastolic synchrony despite a large increase in systolic dyssynchrony during acute RVA pacing.

The purpose of specific aim 4 was to develop and evaluate a new method for

quantifying left ventricular internal flow using standard cine cardiac magnetic resonance images. Cardiac magnetic resonance images were obtained from 10 healthy controls and 10 patients with dyssynchronous heart failure (class III/IV, LV ejection fraction <35%, QRS>150ms). A graphical user interface was developed in MatLab which utilized a level-set technique to semi-automatically reconstruct the endocardial surface of the LV. This surface was divided into 16 regions adjacent to the standardized left ventricular segments defined by the American Heart Association. Internal flow was defined as the sum of the magnitudes of the regional volume changes minus the global volume change during each time step in the cardiac cycle. Internal flow fraction (IFF) was defined as the total internal flow as a percentage of stroke volume during systole ($IFF_{systole}$), diastole ($IFF_{diastole}$) or the whole cycle (IFF_{whole}). IFF_{whole} was significantly increased in the patients (9.9±5.0% vs 1.5±0.5% in the controls, $p<0.001$). An IFF_{whole} threshold of 4% discriminated between patients and controls with 90% sensitivity and 100% specificity. $IFF_{diastole}$ (2.3±0.8%) was greater than $IFF_{systole}$ (0.8±0.5%) in the normal controls ($p<0.001$) while the patients had similar $IFF_{diastole}$ (7.8±4.2%) and $IFF_{systole}$ (12.0±7.8%). It was concluded that left ventricular internal flow fraction can be quantified from standard cine cardiac magnetic resonance images. Left ventricular internal flow fraction discriminated patients with dyssynchronous heart failure from normal subjects with 95% accuracy.

To facilitate comparisons between XCD and IFF, XCD was quantified in all patients and normal controls from Aim 4. We found a weak correlation between IFF and XCD for the whole-cycle and diastolic parameters ($p = 0.016$ and 0.047, respectively). However, the systolic parameters did not correlate ($p = 0.185$). In addition, none of the

time-to-peak parameters correlated with either IFF_{whole} or $IFF_{systole}$. This suggests that while IFF and XCD may correlate weakly, they are not in close agreement and may provide independently useful information.

Clinical Implications

The overall goal of this project was to improve upon existing methods to diagnose dyssynchrony in the heart. This goal is particularly important as the existing methods to diagnose dyssynchrony have recently failed in the first multi-center trial attempting to predict response to CRT (PROSPECT). The work presented in this dissertation provides a new method (cross-correlation delay) for post-processing of tissue Doppler velocity curves that can be used to diagnose left ventricular dyssynchrony in a more automated, streamlined fashion with greater accuracy than existing "time-to-peak" parameters. This work also provides a new method for quantifying left ventricular internal flow *non*-invasively as a new measure of dyssynchrony. Internal flow analysis showed excellent accuracy in discriminating positive and negative control groups in a preliminary study. Both tissue Doppler-based cross-correlation delay and cardiac magnetic resonance-based internal flow analysis may help improve the poor CRT response rate. In addition, the superior ability of these methods to diagnose dyssynchrony may prove useful in risk-stratification and monitoring of other disease processes which affect the heart.

Suggestions for Future Work

Predicting Response to CRT using XCD

The next step in determining the utility of XCD for diagnosing dyssynchrony is to determine whether these parameters can predict which patients will benefit from cardiac resynchronization therapy (CRT). The predictors of response to CRT (PROSPECT) trial aimed to identify echocardiographic measures of dyssynchrony and evaluate their ability to predict response to CRT[38]. SLD, MaxDiff and Ts-SD were 3 of the parameters quantified in the patients at baseline prior to biventricular pacemaker implantation. PROSPECT enrolled 460 patients from over 30 centers world-wide and utilized two core labs to analyze all echocardiographic data. However, the preliminary results showed poor reproducibility of the echocardiographic parameters between core labs and non-significant predictive ability of all parameters studied[39]. The results of this dissertation suggest that cross-correlation delay should be evaluated in the PROSPECT study population to determine whether XCD can be used to predict response to CRT.

Correlation Value

Cross-correlation analysis produces two numerical values when comparing two velocity curves: 1) the delay between the curves and 2) the normalized correlation value *after correcting for the delay between the curves*. Correlation values less than ~0.5 may not be reliable (see Figure 4.8 for an example). Future studies determining the ability of XCD to predict response to CRT should analyze patients with correlation values above

0.5 and below 0.5 as separate groups to determine whether the predictive ability is limited for low correlation values.

Pacing-induced Diastolic Dyssynchrony

Chapter 5 demonstrated that dyssynchronous activation of the left ventricle due to right ventricular apex pacing creates systolic dyssynchrony with preserved diastolic synchrony. However, chapter 4 showed that patients with heart failure have a severely increased level of diastolic dyssynchrony compared to normal controls. Thus, diastolic dyssynchrony is not an acute effect of dyssynchronous activation and may be a long-term marker of worsening function due to pathology of the myocardium. It will be important to investigate whether patients who have had right ventricular pacemakers for prolonged periods of time have developed diastolic dyssynchrony.

Predicting Response to CRT using IFF analysis

Calculation of IFF involves significantly more post-processing and complicated analysis compared to XCD. However, its utility may lie in the fact that it is a more physiologically relevant measure of "inefficiency" in the left ventricle that can be corrected by cardiac resynchronization therapy. IFF analysis is more related to the actual increase in efficiency that CRT can provide for a patient. A trial determining the ability of IFF to predict response to CRT is definitely warranted based on the data presented in chapter 6. In addition, several centers have successfully obtained magnetic resonance

images from patients with pacemakers[103, 104]. This suggests that the primary end-point of change in LV end-systolic volume for a CRT study using IFF analysis could be quantified with MRI as opposed to echo, which would improve the power of the study nearly 10-fold due to the much higher reproducibility of calculating volumes with MRI instead of echocardiography[105].

Fusion of Multiple Modalities to Predict Response to CRT

There are several other factors that affect outcomes after CRT which can be addressed with cardiac MRI. Patients with increased scar burden have a reduced chance of responding to CRT[106, 107]. MRI delayed enhancement imaging is the gold standard for quantifying the extent and severity of myocardial scar burden, and has been used to predict response to CRT[108]. In addition, it can be difficult to access veins for placement of the left ventricular lead in the region of optimal pacing in many patients[109]. Techniques have recently been developed to visualize the coronary venous anatomy with MRI[110]. Figure 7.1 shows four slices from a 3-D, post-contrast, navigator echo-gated, whole-heart, coronary vein scan. The arrows show sections of the coronary veins in each slice that can be used to reconstruct the veins in 3 dimensions. Therefore, cardiac magnetic resonance can be used to quantify: 1) dyssynchrony using IFF analysis, 2) viability using delayed enhancement imaging and 3) coronary venous anatomy. These 3 modalities can be acquired during the same cardiac exam and could be combined in the future to provide a more complete description of a patient's chance of benefitting from CRT.

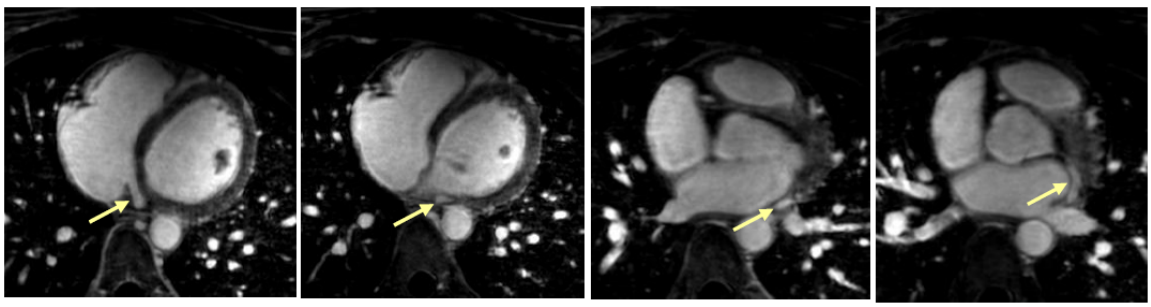

Figure 7.1: Whole-heart MRI can be used to reconstruct coronary venous anatomy.

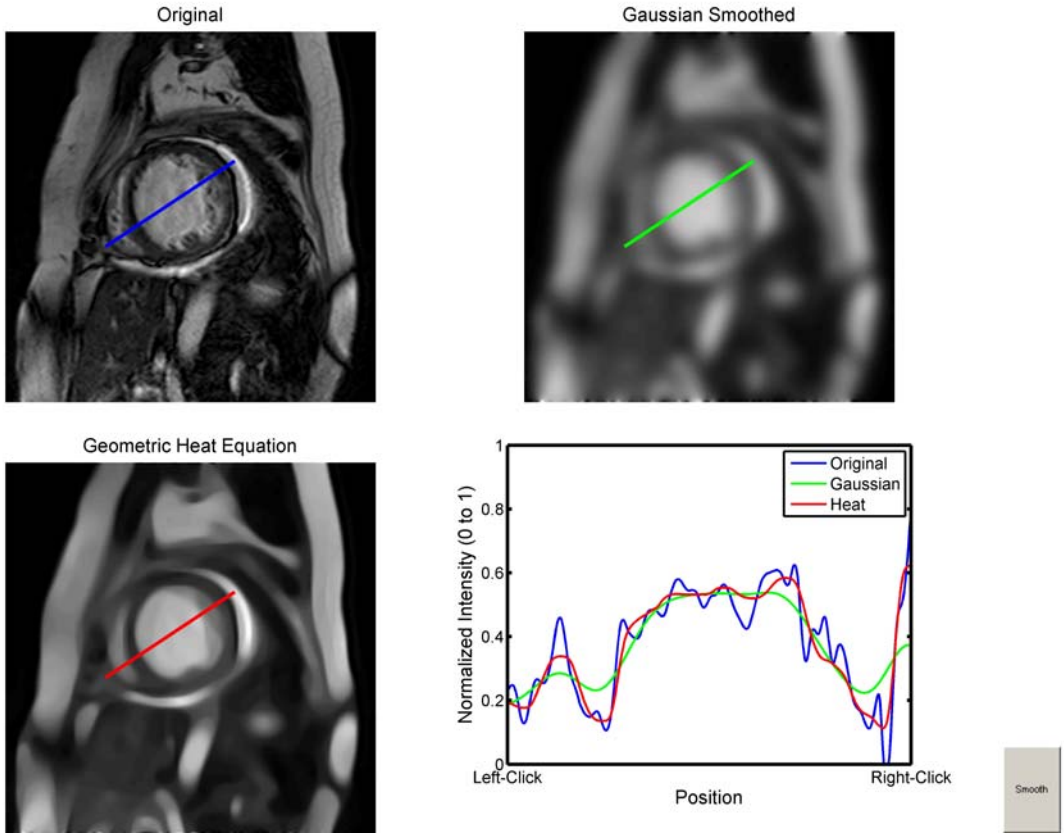

Figure 7.2: An implementation of the geometric heat equation for smoothing cardiac images with preservation of edges.

Improvement of the Post-processing Time for IFF

Calculation of IFF can require up to 6 hours to complete for one patient, mostly due to manual correction of the endocardial border identified using a level set method. Post-processing time may be reduced by implementing: 1) non-linear edge-preserving smoothing algorithms based on the geometric heat equation prior to segmentation (Figure 7.2) 2) three or four-dimensional (three spatial plus one time dimension) evolution of the level set instead of two-dimensional evolution in each image and/or 3) time evolution of the endocardial border from the first cardiac frame using optical flow (Figure 7.3). In addition, quantification of IFF may not be very sensitive to manual refinement of the endocardial borders, so it may be possible to spend less time manually correcting the borders.

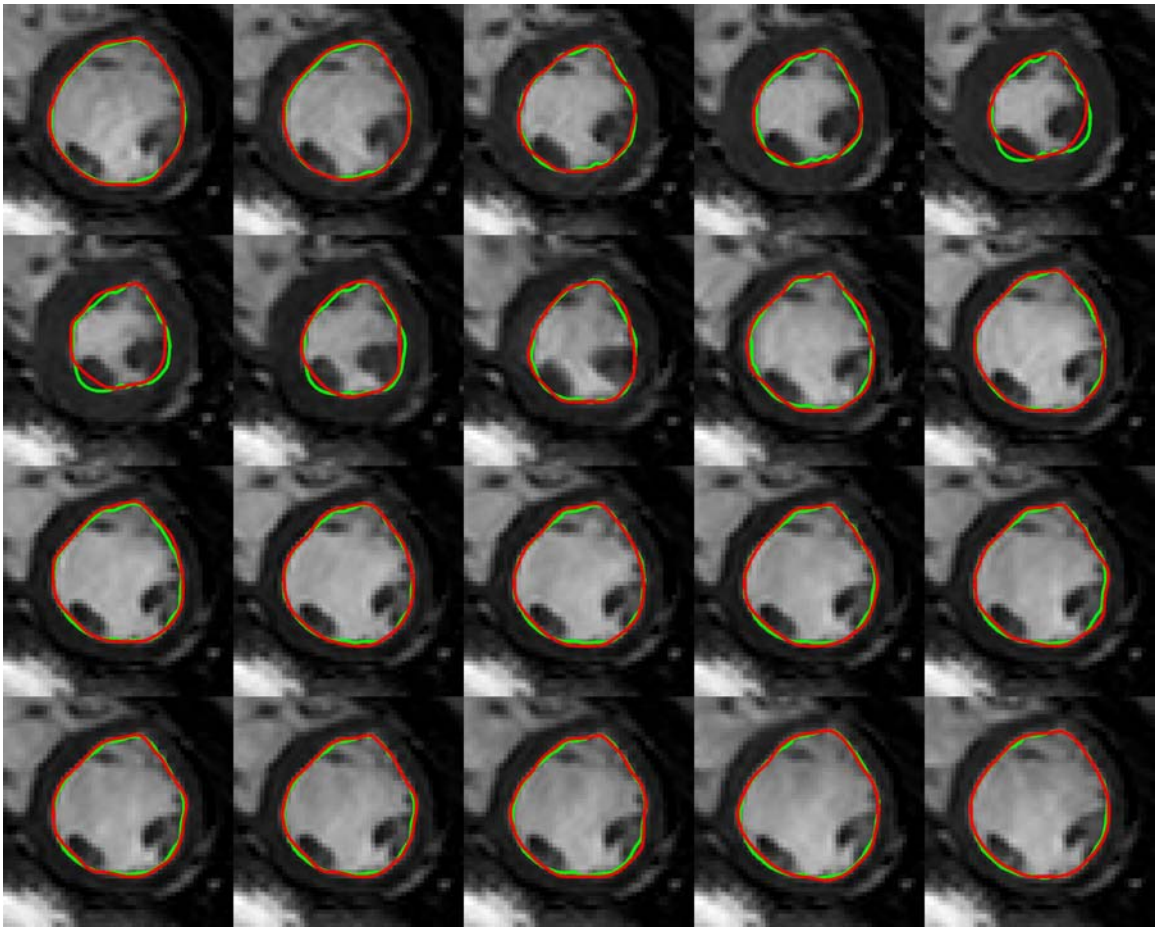

Figure 7.3 Optical flow-based propagation of the endocardial border in time using the first (top left) frame as an initial condition. Predicted borders are in green and manually-identified borders are in red.

Pronunciation of ChipoTle

Despite eating at the restaurant Chipotle nearly 20-30 times with John Oshinski throughout my graduate career, he still has yet to learn how to annunciate the word. No matter how many times we tell him that the proper phonetic spelling is "chi-poht-ley," he continues to pronounce it "chi-pollllll-teeeeeee" for reasons unknown. Potential methods for improving upon this situation are: 1) Send John to Catholic school with his kids to take speech therapy classes 2) make John take a shot of the Chipotle fire salsa every time he pronounces it incorrectly and 3) stop going to Chipotle and go to Moe's because it's easier to pronounce. However, in all of those 20-30 visits to Chipotle, I must admit I may have paid for myself a maximum of two times. If this incredible streak of free meals continues, I am fully willing to deal with John's speech problems without hesitation.

Final Thoughts

There are a multitude of methods to quantify ventricular dyssynchrony. The majority of these methods were developed within the clinical realm to predict outcomes after cardiac resynchronization therapy. Therefore, these methods never underwent rigorous scientific evaluation in positive and negative control studies. We developed two new methods to quantify dyssynchrony and showed their superiority to existing techniques in positive and negative control studies. We feel these methods will be useful in diagnosing dyssynchrony in the setting of severe, drug-refractory heart failure to help improve selection of patients who will benefit from cardiac resynchronization therapy. In

addition, it is becoming apparent that dyssynchrony may lead to worse outcomes in other populations such as children who require a pacemaker for heart rate control[80], and our methodology should be directly applicable to this and any other cardiovascular disease affecting the normal activation pattern in the heart.

REFERENCES

1. Rosenqvist M, Isaaz K, Botvinick EH, Dae MW, Cockrell J, Abbott JA, Schiller NB, Griffin JC. Relative importance of activation sequence compared to atrioventricular synchrony in left ventricular function. *Am J Cardiol.* 1991;67(2):148-156.

2. Hamby RI, Weissman RH, Prakash MN, Hoffman I. Left bundle branch block: a predictor of poor left ventricular function in coronary artery disease. *Am Heart J.* 1983;106(3):471-477.

3. Xiao HB, Roy C, Fujimoto S, Gibson DG. Natural history of abnormal conduction and its relation to prognosis in patients with dilated cardiomyopathy. *Int J Cardiol.* 1996;53(2):163-170.

4. Cazeau S, Leclercq C, Lavergne T, Walker S, Varma C, Linde C, Garrigue S, Kappenberger L, Haywood GA, Santini M, Bailleul C, Daubert JC, Multisite Stimulation in Cardiomyopathies Study I. Effects of multisite biventricular pacing in patients with heart failure and intraventricular conduction delay. *N Engl J Med.* 2001;344(12):873-880.

5. Leclercq C, Kass DA. Retiming the failing heart: principles and current clinical status of cardiac resynchronization. *J Am Coll Cardiol.* 2002;39(2):194-201.

6. Yu CM, Lin H, Zhang Q, Sanderson JE. High prevalence of left ventricular systolic and diastolic asynchrony in patients with congestive heart failure and normal QRS duration. *Heart.* 2003;89(1):54-60.

7. Bax JJ, Abraham T, Barold SS, Breithardt OA, Fung JW, Garrigue S, Gorcsan J, 3rd, Hayes DL, Kass DA, Knuuti J, Leclercq C, Linde C, Mark DB, Monaghan MJ, Nihoyannopoulos P, Schalij MJ, Stellbrink C, Yu CM. Cardiac resynchronization therapy: Part 1--issues before device implantation. *J Am Coll Cardiol.* 2005;46(12):2153-2167.

8. Bax JJ, Marwick TH, Molhoek SG, Bleeker GB, van Erven L, Boersma E, Steendijk P, van der Wall EE, Schalij MJ. Left ventricular dyssynchrony predicts benefit of cardiac resynchronization therapy in patients with end-stage heart failure before pacemaker implantation. *Am J Cardiol.* 2003;92(10):1238-1240.

9. Bax JJ, Molhoek SG, van Erven L, Voogd PJ, Somer S, Boersma E, Steendijk P,

Schalij MJ, Van der Wall EE. Usefulness of myocardial tissue Doppler echocardiography to evaluate left ventricular dyssynchrony before and after biventricular pacing in patients with idiopathic dilated cardiomyopathy. *Am J Cardiol.* 2003;91(1):94-97.

10. Garrahy PJ, Kwan OL, Booth DC, DeMaria AN. Assessment of abnormal systolic intraventricular flow patterns by Doppler imaging in patients with left ventricular dyssynergy. *Circulation.* 1990;82(1):95-104.

11. Steendijk P, Tulner SA, Schreuder JJ, Bax JJ, van Erven L, van der Wall EE, Dion RA, Schalij MJ, Baan J. Quantification of left ventricular mechanical dyssynchrony by conductance catheter in heart failure patients. *Am J Physiol Heart Circ Physiol.* 2004;286(2):H723-730.

12. Steendijk P, Tulner SA, Bax JJ, Oemrawsingh PV, Bleeker GB, van Erven L, Putter H, Verwey HF, van der Wall EE, Schalij MJ. Hemodynamic Effects of Long-Term Cardiac Resynchronization Therapy: Analysis by Pressure-Volume Loops. *Circulation.* Vol 113; 2006:1295-1304.

13. Cazeau S, Ritter P, Lazarus A, Gras D, Backdach H, Mundler O, Mugica J. Multisite pacing for end-stage heart failure: early experience. *Pacing Clin Electrophysiol.* 1996;19(11 Pt 2):1748-1757.

14. Linde C, Gadler F, Edner M, Nordlander R, Rosenqvist M, Ryden L. Results of atrioventricular synchronous pacing with optimized delay in patients with severe congestive heart failure. *Am J Cardiol.* 1995;75(14):919-923.

15. Leclercq C, Gras D, Le Helloco A, Nicol L, Mabo P, Daubert C. Hemodynamic importance of preserving the normal sequence of ventricular activation in permanent cardiac pacing. *Am Heart J.* 1995;129(6):1133-1141.

16. Brecker SJ, Xiao HB, Sparrow J, Gibson DG. Effects of dual-chamber pacing with short atrioventricular delay in dilated cardiomyopathy.[see comment][erratum appears in Lancet 1992 Dec 12;340(8833):1482]. *Lancet.* 1992;340(8831):1308-1312.

17. Stellbrink C, Breithardt OA, Franke A, Sack S, Bakker P, Auricchio A, Pochet T, Salo R, Kramer A, Spinelli J, Investigators P-C, Group CPIGCHFR. Impact of cardiac resynchronization therapy using hemodynamically optimized pacing on left ventricular remodeling in patients with congestive heart failure and ventricular conduction disturbances.[see comment]. *J Am Coll*

Cardiol. 2001;38(7):1957-1965.

18. Sogaard P, Egeblad H, Kim WY, Jensen HK, Pedersen AK, Kristensen BO, Mortensen PT. Tissue Doppler imaging predicts improved systolic performance and reversed left ventricular remodeling during long-term cardiac resynchronization therapy. *J Am Coll Cardiol.* 2002;40(4):723-730.

19. Yu CM, Chau E, Sanderson JE, Fan K, Tang MO, Fung WH, Lin H, Kong SL, Lam YM, Hill MR, Lau CP. Tissue Doppler echocardiographic evidence of reverse remodeling and improved synchronicity by simultaneously delaying regional contraction after biventricular pacing therapy in heart failure. *Circulation.* 2002;105(4):438-445.

20. Yu CM, Fung WH, Lin H, Zhang Q, Sanderson JE, Lau CP. Predictors of left ventricular reverse remodeling after cardiac resynchronization therapy for heart failure secondary to idiopathic dilated or ischemic cardiomyopathy. *Am J Cardiol.* 2003;91(6):684-688.

21. Abraham WT, Fisher WG, Smith AL, Delurgio DB, Leon AR, Loh E, Kocovic DZ, Packer M, Clavell AL, Hayes DL, Ellestad M, Trupp RJ, Underwood J, Pickering F, Truex C, McAtee P, Messenger J, Evaluation MSGMIRC. Cardiac resynchronization in chronic heart failure.[see comment]. *N Engl J Med.* 2002;346(24):1845-1853.

22. Gras D, Leclercq C, Tang AS, Bucknall C, Luttikhuis HO, Kirstein-Pedersen A. Cardiac resynchronization therapy in advanced heart failure the multicenter InSync clinical study. *Eur J Heart Fail.* 2002;4(3):311-320.

23. Rouleau F, Merheb M, Geffroy S, Berthelot J, Chaleil D, Dupuis JM, Victor J, Geslin P. Echocardiographic assessment of the interventricular delay of activation and correlation to the QRS width in dilated cardiomyopathy. *Pacing Clin Electrophysiol.* 2001;24(10):1500-1506.

24. Achilli A, Sassara M, Ficili S, Pontillo D, Achilli P, Alessi C, De Spirito S, Guerra R, Patruno N, Serra F. Long-term effectiveness of cardiac resynchronization therapy in patients with refractory heart failure and "narrow" QRS. *J Am Coll Cardiol.* 2003;42(12):2117-2124.

25. Fauchier L, Babuty D, Cosnay P, Fauchier JP. Cardiac resynchronization in chronic heart failure: some considerations about the cost-

effectiveness.[comment]. *Eur Heart J.* 2003;24(9):879; author reply 879.

26. Leclercq C, Hare JM. Ventricular resynchronization: current state of the art. *Circulation.* 2004;109(3):296-299.

27. Bax JJ, Ansalone G, Breithardt OA, Derumeaux G, Leclercq C, Schalij MJ, Sogaard P, St John Sutton M, Nihoyannopoulos P. Echocardiographic evaluation of cardiac resynchronization therapy: ready for routine clinical use? A critical appraisal. *J Am Coll Cardiol.* 2004;44(1):1-9.

28. Bleeker GB, Schalij MJ, Molhoek SG, Verwey HF, Holman ER, Boersma E, Steendijk P, Van Der Wall EE, Bax JJ. Relationship between QRS duration and left ventricular dyssynchrony in patients with end-stage heart failure. *J Cardiovasc Electrophysiol.* 2004;15(5):544-549.

29. Pitzalis MV, Iacoviello M, Romito R, Massari F, Rizzon B, Luzzi G, Guida P, Andriani A, Mastropasqua F, Rizzon P. Cardiac resynchronization therapy tailored by echocardiographic evaluation of ventricular asynchrony. *J Am Coll Cardiol.* 2002;40(9):1615-1622.

30. Breithardt OA, Stellbrink C, Kramer AP, Sinha AM, Franke A, Salo R, Schiffgens B, Huvelle E, Auricchio A, Failure P-CSGPTfCH. Echocardiographic quantification of left ventricular asynchrony predicts an acute hemodynamic benefit of cardiac resynchronization therapy. *J Am Coll Cardiol.* 2002;40(3):536-545.

31. Kawaguchi M, Murabayashi T, Fetics BJ, Nelson GS, Samejima H, Nevo E, Kass DA. Quantitation of basal dyssynchrony and acute resynchronization from left or biventricular pacing by novel echo-contrast variability imaging. *J Am Coll Cardiol.* 2002;39(12):2052-2058.

32. Kapetanakis S, Cooklin M, Monaghan MJ. Mechanical resynchronisation in biventricular pacing illustrated by real time transthoracic three dimensional echocardiography. *Heart.* 2004;90(5):482.

33. Bader H, Garrigue S, Lafitte S, Reuter S, Jais P, Haissaguerre M, Bonnet J, Clementy J, Roudaut R. Intra-left ventricular electromechanical asynchrony. A new independent predictor of severe cardiac events in heart failure patients. *J Am Coll Cardiol.* 2004;43(2):248-256.

34. Bax JJ, Bleeker GB, Marwick TH, Molhoek SG, Boersma E, Steendijk P, van der Wall EE, Schalij MJ. Left ventricular dyssynchrony predicts response and prognosis after cardiac resynchronization therapy. *J Am Coll Cardiol.* 2004;44(9):1834-1840.

35. Yu CM, Fung JW, Zhang Q, Chan CK, Chan YS, Lin H, Kum LC, Kong SL, Zhang Y, Sanderson JE. Tissue Doppler imaging is superior to strain rate imaging and postsystolic shortening on the prediction of reverse remodeling in both ischemic and nonischemic heart failure after cardiac resynchronization therapy. *Circulation.* 2004;110(1):66-73.

36. Yu CM, Zhang Q, Fung JW, Chan HC, Chan YS, Yip GW, Kong SL, Lin H, Zhang Y, Sanderson JE. A novel tool to assess systolic asynchrony and identify responders of cardiac resynchronization therapy by tissue synchronization imaging. *J Am Coll Cardiol.* 2005;45(5):677-684.

37. Lafitte S, Bordachar P, Lafitte M, Garrigue S, Reuter S, Reant P, Serri K, Lebouffos V, Berrhouet M, Jais P, Haissaguerre M, Clementy J, Roudaut R, DeMaria AN. Dynamic ventricular dyssynchrony: an exercise-echocardiography study. *J Am Coll Cardiol.* 2006;47(11):2253-2259.

38. Yu CM, Abraham WT, Bax J, Chung E, Fedewa M, Ghio S, Leclercq C, Leon AR, Merlino J, Nihoyannopoulos P, Notabartolo D, Sun JP, Tavazzi L, Investigators P. Predictors of response to cardiac resynchronization therapy (PROSPECT)--study design. *Am Heart J.* 2005;149(4):600-605.

39. Ghio S. Results of the predictors of response to CRT (PROSPECT) trial (ABSTRACT). *European Society of Cardiology Congress.* September 4, 2007:Vienna, Austria.

40. Notabartolo D, Merlino JD, Smith AL, DeLurgio DB, Vera FV, Easley KA, Martin RP, Leon AR. Usefulness of the peak velocity difference by tissue Doppler imaging technique as an effective predictor of response to cardiac resynchronization therapy. *Am J Cardiol.* 2004;94(6):817-820.

41. Jacobs LE, Kotler MN, Parry WR. Flow patterns in dilated cardiomyopathy: a pulsed-wave and color flow Doppler study. *J Am Soc Echocardiogr.* 1990;3(4):294-302.

42. Edvardsen T, Rodevand O, Aakhus S, Bjornerheim R, Ihlen H. Reversal of intraventricular flow propagation during isovolumic

relaxation: A marker of anterior wall dysfunction. *J Am Soc Echocardiogr.* 1999;12(10):801-810.

43. Cerqueira MD, Weissman NJ, Dilsizian V, Jacobs AK, Kaul S, Laskey WK, Pennell DJ, Rumberger JA, Ryan T, Verani MS, American Heart Association Writing Group on Myocardial Segmentation and Registration for Cardiac I. Standardized myocardial segmentation and nomenclature for tomographic imaging of the heart: a statement for healthcare professionals from the Cardiac Imaging Committee of the Council on Clinical Cardiology of the American Heart Association. *Circulation.* 2002;105(4):539-542.

44. Kjaergaard J, Korinek J, Belohlavek M, Oh JK, Sogaard P, Hassager C. Accuracy, reproducibility, and comparability of Doppler tissue imaging by two high-end ultrasound systems. *J Am Soc Echocardiogr.* 2006;19(3):322-328.

45. Turner MS, Bleasdale RA, Vinereanu D, Mumford CE, Paul V, Fraser AG, Frenneaux MP. Electrical and mechanical components of dyssynchrony in heart failure patients with normal QRS duration and left bundle-branch block: impact of left and biventricular pacing. *Circulation.* 2004;109(21):2544-2549.

46. Gorcsan J, 3rd, Kanzaki H, Bazaz R, Dohi K, Schwartzman D. Usefulness of echocardiographic tissue synchronization imaging to predict acute response to cardiac resynchronization therapy. *Am J Cardiol.* 2004;93(9):1178-1181.

47. Weidemann F, Bijnens B, Strotmann JM. Letter regarding article by Yu et al, "Tissue Doppler imaging is superior to strain rate imaging and postsystolic shortening on the prediction of reverse remodeling in both ischemic and nonischemic heart failure after cardiac resynchronization therapy".[comment]. *Circulation.* 2004;110(19):e498-499; author reply e498-499.

48. Penicka M, Bartunek J, De Bruyne B, Vanderheyden M, Goethals M, De Zutter M, Brugada P, Geelen P. Improvement of left ventricular function after cardiac resynchronization therapy is predicted by tissue Doppler imaging echocardiography. *Circulation.* 2004;109(8):978-983.

49. Ansalone G, Giannantoni P, Ricci R, Trambaiolo P, Laurenti A, Fedele F, Santini M. Doppler myocardial imaging in patients with heart failure receiving biventricular pacing treatment. *Am Heart J.* 2001;142(5):881-896.

50. Bordachar P, Lafitte S, Reuter S, Sanders P, Jais P, Haissaguerre M, Roudaut R, Garrigue S, Clementy J. Echocardiographic parameters of

ventricular dyssynchrony validation in patients with heart failure using sequential biventricular pacing. *J Am Coll Cardiol.* 2004;44(11):2157-2165.

51. Pislaru C, Belohlavek M, Bae RY, Abraham TP, Greenleaf JF, Seward JB. Regional asynchrony during acute myocardial ischemia quantified by ultrasound strain rate imaging. *J Am Coll Cardiol.* 2001;37(4):1141-1148.

52. Breithardt OA, Stellbrink C, Herbots L, Claus P, Sinha AM, Bijnens B, Hanrath P, Sutherland GR. Cardiac resynchronization therapy can reverse abnormal myocardial strain distribution in patients with heart failure and left bundle branch block. *J Am Coll Cardiol.* 2003;42(3):486-494.

53. Leitman M, Lysyansky P, Sidenko S, Shir V, Peleg E, Binenbaum M, Kaluski E, Krakover R, Vered Z. Two-dimensional strain-a novel software for real-time quantitative echocardiographic assessment of myocardial function. *J Am Soc Echocardiogr.* 2004;17(10):1021-1029.

54. Ingul CB, Stoylen A, Slordahl SA, Wiseth R, Burgess M, Marwick TH. Automated analysis of myocardial deformation at dobutamine stress echocardiography: an angiographic validation. *J Am Coll Cardiol.* 2007;49(15):1651-1659.

55. Hanley JA, McNeil BJ. A method of comparing the areas under receiver operating characteristic curves derived from the same cases. *Radiology.* 1983;148(3):839-843.

56. Poerner TC, Goebel B, Geiger T, Haghi D, Borggrefe M, Haase KK. Physiological range of mechanical synchronicity of the human heart: Comparison between different echocardiographic assessment modalities. *Ultrasound Med Biol.* 2005;31(9):1163-1172.

57. Yu CM, Zhang Q, Chan YS, Chan CK, Yip GWK, Kum LCC, Wu EB, Lee PW, Lam YY, Chan S, W-H Fung J. Tissue Doppler velocity is superior to displacement and strain mapping in predicting left ventricular reverse remodelling response after cardiac resynchronisation therapy. *Heart.* 2006;92(10):1452-1456.

58. Miyazaki C, Lin G, Powell BD, Espinosa RE, Miller FA, Bruce CJ, Karon BL, Oh JK. Prediction of the effect of cardiac resynchronization therapy by cardiac timing intervals and mechanical dyssynchrony by strain imaging (Abstract). *J Am*

Soc Echocardiogr. 2006;19(5):666.

59. Wyman BT, Hunter WC, Prinzen FW, McVeigh ER. Mapping propagation of mechanical activation in the paced heart with MRI tagging. *Am J Physiol.* 1999;276(3):H881-891.

60. Ono S, Nohara R, Kambara H, Okuda K, Kawai C. Regional myocardial perfusion and glucose metabolism in experimental left bundle branch block. *Circulation.* 1992;85(3):1125-1131.

61. Hirzel HO, Senn M, Nuesch K, Buettner C, Pfeiffer A, Hess OM, Krayenbuehl HP. Thallium-201 scintigraphy in complete left bundle branch block. *Am J Cardiol.* 1984;53(6):764-769.

62. Askenazi J, Alexander JH, Koenigsberg DI, Belic N, Lesch M. Alteration of left ventricular performance by left bundle branch block simulated with atrioventricular sequential pacing. *Am J Cardiol.* 1984;53(1):99-104.

63. Prinzen FW, Peschar M. Relation between the pacing induced sequence of activation and left ventricular pump function in animals. *Pacing Clin Electrophysiol.* 2002;25(4):484-498.

64. Cappola TP, Harsch MR, Jessup M, Abraham WT, Young JB, Petersen-Stejskal S, Plappert T, St John Sutton M, Cappola TP, Harsch MR, Jessup M, Abraham WT, Young JB, Petersen-Stejskal S, Plappert T, St John Sutton M. Predictors of remodeling in the CRT era: influence of mitral regurgitation, BNP, and gender. *J Card Fail.* 2006;12(3):182-188.

65. Yu CM, Wing-Hong Fung J, Zhang Q, Sanderson JE, Yu C-M, Wing-Hong Fung J, Zhang Q, Sanderson JE. Understanding nonresponders of cardiac resynchronization therapy--current and future perspectives. *J Cardiovasc Electrophysiol.* 2005;16(10):1117-1124.

66. Aoyagi T, Iizuka M, Takahashi T, Ohya T, Serizawa T, Momomura S, Sato H, Mochizuki T, Matsui H, Ikenouchi H, et al. Wall motion asynchrony prolongs time constant of left ventricular relaxation. *Am J Physiol.* 1989;257(3 Pt 2):H883-890.

67. Blaustein AS, Gaasch WH. Myocardial relaxation. VI. Effects of beta-adrenergic

tone and asynchrony on LV relaxation rate. *Am J Physiol.* 1983;244(3):H417-422.

68. Zile MR, Blaustein AS, Shimizu G, Gaasch WH. Right ventricular pacing reduces the rate of left ventricular relaxation and filling. *J Am Coll Cardiol.* 1987;10(3):702-709.

69. Bedotto JB, Grayburn PA, Black WH, Raya TE, McBride W, Hsia HH, Eichhorn EJ. Alterations in left ventricular relaxation during atrioventricular pacing in humans. *J Am Coll Cardiol.* 1990;15(3):658-664.

70. Brutsaert DL, Sys SU. Relaxation and diastole of the heart. *Physiol Rev.* 1989;69(4):1228-1315.

71. Brutsaert DL, de Clerck NM, Goethals MA, Housmans PR. Relaxation of ventricular cardiac muscle. *J Physiol.* 1978;283:469-480.

72. Brutsaert DL, Housmans PR, Goethals MA. Dual control of relaxation. Its role in the ventricular function in the mammalian heart. *Circ Res.* 1980;47(5):637-652.

73. Schuster I, Habib G, Jego C, Thuny F, Avierinos J-F, Derumeaux G, Beck L, Medail C, Franceschi F, Renard S, Ferracci A, Lefevre J, Luccioni R, Deharo J-C, Djiane P. Diastolic asynchrony is more frequent than systolic asynchrony in dilated cardiomyopathy and is less improved by cardiac resynchronization therapy. *J Am Coll Cardiol.* 2005;46(12):2250-2257.

74. Wang J, Kurrelmeyer KM, Torre-Amione G, Nagueh SF. Systolic and diastolic dyssynchrony in patients with diastolic heart failure and the effect of medical therapy. *J Am Coll Cardiol.* 2007;49(1):88-96.

75. Pacileo G, De Cristofaro M, Russo MG, Sarubbi B, Pisacane C, Calabro R. Hypertrophic cardiomyopathy in pediatric patients: effect of verapamil on regional and global left ventricular diastolic function. *Can J Cardiol.* 2000;16(2):146-152.

76. Yu CM, Zhang Q, Yip GW, Lee PW, Kum LC, Lam YY, Fung JW. Diastolic and systolic asynchrony in patients with diastolic heart failure: a common but ignored condition. *J Am Coll Cardiol.* 2007;49(1):97-105.

77. Kang SJ, Song JK, Yang HS, Song JM, Kang DH, Rhee KS, Nam GB, Choi KJ,

Kim JJ, Kim YH. Systolic and diastolic regional myocardial motion of pacing-induced versus idiopathic left bundle branch block with and without left ventricular dysfunction. *Am J Cardiol.* 2004;93(10):1243-1246.

78. Karpawich PP, Rabah R, Haas JE. Altered cardiac histology following apical right ventricular pacing in patients with congenital atrioventricular block. *Pacing Clin Electrophysiol.* 1999;22(9):1372-1377.

79. van Oosterhout MF, Prinzen FW, Arts T, Schreuder JJ, Vanagt WY, Cleutjens JP, Reneman RS. Asynchronous electrical activation induces asymmetrical hypertrophy of the left ventricular wall. *Circulation.* 1998;98(6):588-595.

80. Thambo JB, Bordachar P, Garrigue S, Lafitte S, Sanders P, Reuter S, Girardot R, Crepin D, Reant P, Roudaut R, Jais P, Haissaguerre M, Clementy J, Jimenez M, Thambo J-B, Bordachar P, Garrigue S, Lafitte S, Sanders P, Reuter S, Girardot R, Crepin D, Reant P, Roudaut R, Jais P, Haissaguerre M, Clementy J, Jimenez M. Detrimental ventricular remodeling in patients with congenital complete heart block and chronic right ventricular apical pacing.[see comment]. *Circulation.* 2004;110(25):3766-3772.

81. Harigaya S, Schwartz A. Rate of calcium binding and uptake in normal animal and failing human cardiac muscle. Membrane vesicles (relaxing system) and mitochondria. *Circ Res.* 1969;25(6):781-794.

82. Lindenmayer GE, Sordahl LA, Harigaya S, Allen JC, Besch HR, Jr., Schwartz A. Some biochemical studies on subcellular systems isolated from fresh recipient human cardiac tissue obtained during transplantation. *Am J Cardiol.* 1971;27(3):277-283.

83. Betocchi S, Piscione F, Villari B, Pace L, Ciarmiello A, Perrone-Filardi P, Salvatore C, Salvatore M, Chiariello M. Effects of induced asynchrony on left ventricular diastolic function in patients with coronary artery disease. *J Am Coll Cardiol.* 1993;21(5):1124-1131.

84. Theroux P, Ross J, Jr., Franklin D, Kemper WS, Sasyama S. Regional Myocardial function in the conscious dog during acute coronary occlusion and responses to morphine, propranolol, nitroglycerin, and lidocaine. *Circulation.* 1976;53(2):302-314.

85. Wiegner AW, Allen GJ, Bing OH. Weak and strong myocardium in series:

implications for segmental dysfunction. *Am J Physiol.* 1978;235(6):H776-783.

86. Fornwalt BK, Arita T, Bhasin M, Voulgaris G, Merlino JD, León AR, Fyfe DA, Oshinski JN. Cross-correlation quantification of dyssynchrony: a new method for quantifying the synchrony of contraction and relaxation in the heart. *J Am Soc Echocardiogr.* 2007;(In press).

87. Catanzariti D, Maines M, Cemin C, Broso G, Marotta T, Vergara G. Permanent direct his bundle pacing does not induce ventricular dyssynchrony unlike conventional right ventricular apical pacing. An intrapatient acute comparison study. *J Interv Card Electrophysiol.* 2006;16(2):81-92.

88. Cojoc A, Reeves JG, Schmarkey L, Strieper MJ, Joyner RW, Wagner MB, Campbell RM, Vinten-Johansen J, Frias PA. Effects of single-site versus biventricular epicardial pacing on myocardial performance in an immature animal model of atrioventricular block. *J Cardiovasc Electrophysiol.* 2006;17(8):884-889.

89. Yu CM, Lin H, Fung WH, Zhang Q, Kong SL, Sanderson JE. Comparison of acute changes in left ventricular volume, systolic and diastolic functions, and intraventricular synchronicity after biventricular and right ventricular pacing for heart failure. *Am Heart J.* 2003;145(5):E18.

90. Strieper M, Karpawich P, Frias P, Gooden K, Ketchum D, Fyfe D, Campbell R. Initial experience with cardiac resynchronization therapy for ventricular dysfunction in young patients with surgically operated congenital heart disease. *Am J Cardiol.* 2004;94(10):1352-1354.

91. Iuliano S, Fisher SG, Karasik PE, Fletcher RD, Singh SN. QRS duration and mortality in patients with congestive heart failure. *Am Heart J.* 2002;143(6):1085-1091.

92. Achilli A, Sassara M, Ficili S, Pontillo D, Achilli P, Alessi C, De Spirito S, Guerra R, Patruno N, Serra F. Long-term effectiveness of cardiac resynchronization therapy in patients with refractory heart failure and "narrow" QRS.[see comment]. *J Am Coll Cardiol.* 2003;42(12):2117-2124.

93. Sethian JA. *Level Set Methods and Fast Marching Methods*. Cambridge, UK: Cambridge University Press; 1999.

94. Cleland JG, Daubert JC, Erdmann E, Freemantle N, Gras D, Kappenberger L, Tavazzi L, Cardiac Resynchronization-Heart Failure Study I, Cleland JGF, Daubert J-C, Erdmann E, Freemantle N, Gras D, Kappenberger L, Tavazzi L, Cardiac Resynchronization-Heart Failure Study I. The effect of cardiac resynchronization on morbidity and mortality in heart failure.[see comment]. *N Engl J Med.* 2005;352(15):1539-1549.

95. Jaochim Nesser H, Sugeng L, Corsi C, Weinert L, Niel J, Ebner C, Steringer-Mascherbauer R, Schmidt F, Schummers G, Lang RM, Mor-Avi V. Volumetric analysis of regional left ventricular function with real-time three-dimensional echocardiography: validation by magnetic resonance and clinical utility testing. *Heart.* 2007;93(5):572-578.

96. Kapetanakis S, Kearney MT, Siva A, Gall N, Cooklin M, Monaghan MJ. Real-time three-dimensional echocardiography: a novel technique to quantify global left ventricular mechanical dyssynchrony. *Circulation.* 2005;112(7):992-1000.

97. Wyman BT, Hunter WC, Prinzen FW, Faris OP, McVeigh ER. Effects of single- and biventricular pacing on temporal and spatial dynamics of ventricular contraction. *American Journal of Physiology - Heart & Circulatory Physiology.* 2002;282(1):H372-379.

98. Wyman BT, Hunter WC, Prinzen FW, McVeigh ER. Mapping propagation of mechanical activation in the paced heart with MRI tagging. *Am J Physiol.* 1999;276(3 Pt 2):H881-891.

99. Helm RH, Leclercq C, Faris OP, Ozturk C, McVeigh E, Lardo AC, Kass DA. Cardiac dyssynchrony analysis using circumferential versus longitudinal strain: implications for assessing cardiac resynchronization. *Circulation.* 2005;111(21):2760-2767.

100. Aletras AH, Ding S, Balaban RS, Wen H. DENSE: displacement encoding with stimulated echoes in cardiac functional MRI. *J Magn Reson.* 1999;137(1):247-252.

101. Gilson WD, Yang Z, French BA, Epstein FH. Measurement of myocardial mechanics in mice before and after infarction using multislice displacement-encoded MRI with 3D motion encoding. *Am J Physiol Heart Circ Physiol.* 2005;288(3):H1491-1497.

102. Delfino JG, Bhasin M, Cole R, Eisner RL, Merlino J, Leon AR,

Oshinski JN. Comparison of myocardial velocities obtained with magnetic resonance phase velocity mapping and tissue doppler imaging in normal subjects and patients with left ventricular dyssynchrony. *J Magn Reson Imaging.* 2006;24(2):304-311.

103. Nazarian S, Roguin A, Zviman MM, Lardo AC, Dickfeld TL, Calkins H, Weiss RG, Berger RD, Bluemke DA, Halperin HR. Clinical utility and safety of a protocol for noncardiac and cardiac magnetic resonance imaging of patients with permanent pacemakers and implantable-cardioverter defibrillators at 1.5 tesla. *Circulation.* 2006;114(12):1277-1284.

104. Sommer T, Naehle CP, Yang A, Zeijlemaker V, Hackenbroch M, Schmiedel A, Meyer C, Strach K, Skowasch D, Vahlhaus C, Litt H, Schild H. Strategy for safe performance of extrathoracic magnetic resonance imaging at 1.5 tesla in the presence of cardiac pacemakers in non-pacemaker-dependent patients: a prospective study with 115 examinations. *Circulation.* 2006;114(12):1285-1292.

105. Bellenger NG, Davies LC, Francis JM, Coats AJ, Pennell DJ. Reduction in sample size for studies of remodeling in heart failure by the use of cardiovascular magnetic resonance. *J Cardiovasc Magn Reson.* 2000;2(4):271-278.

106. Adelstein EC, Saba S. Scar burden by myocardial perfusion imaging predicts echocardiographic response to cardiac resynchronization therapy in ischemic cardiomyopathy. *Am Heart J.* 2007;153(1):105-112.

107. Bleeker GB, Kaandorp TA, Lamb HJ, Boersma E, Steendijk P, de Roos A, van der Wall EE, Schalij MJ, Bax JJ. Effect of posterolateral scar tissue on clinical and echocardiographic improvement after cardiac resynchronization therapy. *Circulation.* 2006;113(7):969-976.

108. White JA, Yee R, Yuan X, Krahn A, Skanes A, Parker M, Klein G, Drangova M. Delayed Enhancement Magnetic Resonance Imaging Predicts Response to Cardiac Resynchronization Therapy in Patients With Intraventricular Dyssynchrony. 2006:j.jacc.2006.2007.2046.

109. Burkhardt JD, Wilkoff BL. Interventional electrophysiology and cardiac resynchronization therapy: delivering electrical therapies for heart failure. *Circulation.* 2007;115(16):2208-2220.

110. Chiribiri A, Kelle S, Gotze S, Kriatselis C, Thouet T, Tangcharoen T, Paetsch I, Schnackenburg B, Fleck E, Nagel E. Visualization of the cardiac

venous system using cardiac magnetic resonance. *Am J Cardiol.* 2008;101(3):407-412.